MR No. A5K16
NACA
A-2

NATIONAL ADVISORY COMMITTEE FOR AERONAUTICS

JPL LIBRARY
CALIFORNIA INSTITUTE OF TECHNOLOGY

WARTIME REPORT

ORIGINALLY ISSUED

November 1945 as
Memorandum Report A5K16

TESTS OF AN ATTACK-TYPE AIRPLANE IN THE AMES 40- BY 80-FOOT WIND TUNNEL TO IMPROVE THE HIGH-SPEED MANEUVERING CONTROL-FORCE CHARACTERISTICS

By Gerald M. McCormack

Ames Aeronautical Laboratory
Moffett Field, California

WASHINGTON

NACA WARTIME REPORTS are reprints of papers originally issued to provide rapid distribution of advance research results to an authorized group requiring them for the war effort. They were previously held under a security status but are now unclassified. Some of these reports were not technically edited. All have been reproduced without change in order to expedite general distribution.

MR No. A5K16

NATIONAL ADVISORY COMMITTEE FOR AERONAUTICS

MEMORANDUM REPORT

for the

Air Technical Service Command, U.S. Army Air Forces

TESTS OF AN ATTACK-TYPE AIRPLANE IN THE AMES 40- BY 80-FOOT WIND TUNNEL TO IMPROVE THE HIGH-SPEED MANEUVERING CONTROL-FORCE CHARACTERISTICS

By Gerald M. McCormack

SUMMARY

Wind-tunnel tests were made of a twin-engine airplane to determine modifications which would make the airplane suitable for ground-support attack operations. It was desired to reduce the high-speed elevator and aileron-control forces without either reducing the low-speed control forces or impairing the landing characteristics.

The test results indicate the following:

1. The desired high-speed elevator-control forces can be obtained by replacing the original, fabric-covered, straight-sided elevators with metal-covered bulged-contour elevators incorporating a balance tab. The low-speed elevator control forces will remain essentially unchanged; however, in order to retain the desirable stalling characteristics of the original elevator, a tab gearing that will

return the tab to approximately neutral at high elevator deflections is required.

2. The desired high-speed aileron-control forces can be obtained by replacing the original, fabric-covered, true-contour ailerons incorporating a 0.375:1 balance tab with metal-covered, straight-sided, extended-span ailerons incorporating a 1:1 balance tab. From 5- to 10-percent improvement in the low-speed flaps-down control will be effected by increasing the maximum aileron throw from 20° up and 15° down to 22° up and 17° down.

3. Approximately 9 miles per hour could be added to the top speed by sealing the airplane; about 3 miles per hour could be added to the top speed by fairing the nose guns and removing the lower-periscope deflector; when the 500-pound bomb racks are in place, about 7 miles per hour could be added to the top speed by fairing the bomb racks.

INTRODUCTION

The subject airplane is a high-performance airplane which has seen extended service in both the European and Pacific theatres of war. The basic design has proved to be highly successful when used as a light-bombardment airplane. However, it was desired to extend the over-all usefulness of the airplane and to utilize it as a ground-support attack airplane. Pilots found the airplane exceedingly tiring to fly in this latter function where constant and violent

maneuvers were required. In the opinion of the combat pilots, a reduction of from 25 to 50 percent in the high-speed maneuvering elevator- and aileron-control forces would be required to make the airplane suitable for ground-support attack operations.

Therefore the airplane was tested in the Ames 40- by 80-foot wind tunnel to determine the modifications necessary to obtain the desired high-speed elevator- and aileron-control-force reductions. Also since any increase in top speed would further enhance the usefulness of the airplane, tests were made to indicate possible drag reductions.

DESCRIPTION OF AIRPLANE

The subject airplane is a twin-engine, midwing land monoplane with a tricycle landing gear and is powered by two radial air-cooled engines.

A drawing of the airplane is shown in figure 1, and the test airplane mounted in the wind tunnel is shown in figure 2. Detailed data of the airplane are given in Appendix A.

Gunnery equipment of the airplane is made up of a variety of arrangements of .50-caliber machine guns,

37-millimeter cannon, and 75-millimeter cannon. The airplane tested, however, was equipped with three .50-caliber machine guns in each wing and eight .50-caliber machine guns mounted in the nose. In addition, various combinations of bombs, torpedoes, or fuel tanks may be mounted under both wings.

The propellers were removed previous to mounting the airplane in the wind tunnel and remained off throughout the tests. Modified oil-cooler inlets, which were wooden duplicates of the inlets with which future airplanes were to be equipped, were installed in place of the production inlets. Wing-surface irregularities caused by screws and by the leading-edge joint of the wing armor plate between the fuselage and the nacelles were filled with clay and smoothed over. For the wind-tunnel tests, the main landing gear was removed and specially made fittings were substituted in its place, by means of which the airplane was mounted to the tunnel support struts.

All control surfaces tested were equipped with cantilever-beam, electrical strain gages for measurement of hinge moments. Electrically driven actuators were used to vary the control-surface deflection, and selsyn transmitter-receiver units were used to indicate the control-surface setting. These various pieces of equipment were all mounted entirely within the airplane.

TESTS, RESULTS, AND DISCUSSION

The test results are presented in the form of standard NACA coefficients. A complete list of all coefficients and symbols used in the presentation of data within this report is given in Appendix B. All results have been corrected for tunnel-wall effects, support tares and interference, and stream inclination. The tunnel-wall corrections which were applied are described in Appendix C.

Longitudinal Characteristics

As previously mentioned, pilots had found it exceedingly tiring to fly the airplane functioning as a ground-support attack airplane, and had expressed the opinion that the maneuvering control forces should be reduced 25 to 50 percent. This indicated that for the attack center-of-gravity position (23 percent M.A.C.) the elevator-control-force gradient should be reduced from the previous value of 80 pounds per g to at least 60 pounds per g and if possible to 35 pounds per g. (Reference 1 requires that the maximum control-force gradient be less than 39 pounds per g for the forward center-of-gravity position, which is at 20 percent M.A.C. for this airplane. This would require that the control-force gradient be approximately 34 pounds per g for the 23 percent M.A.C. center-of-gravity position.)

It was imperative that any modifications made in the

endeavor to attain the foregoing control-force-gradient reductions not reduce the control-force gradient at the rearward center of gravity below the existing value of 16 pounds per g (reference 1 requires the minimum control-force gradient to be above 14 lb/g for this airplane); and also not reduce the elevator effectiveness below that of the original elevator, which was indicated to be marginal in flight tests.

In order to obtain the desired control-force characteristics, it was necessary to increase positively both the basic hinge-moment parameters C_{h_δ} and $C_{h_{\alpha_t}}$. The original elevators were fabric-covered and straight-sided and were equipped with a trimming tab. In order to accomplish the necessary increments in C_{h_δ} and $C_{h_{\alpha_t}}$, it was decided to make three modifications to the elevator: (1) to replace the fabric covering with metal, thus reducing surface deformation in high-speed flight and the consequent negative increments of both C_{h_δ} and $C_{h_{\alpha_t}}$; (2) to incorporate a bulge in the elevator contour, as shown in figure 3, which would result in positive increments of both C_{h_δ} and $C_{h_{\alpha_t}}$; and if necessary (3) to make use of a balance tab which would produce, in effect, a positive increment of C_{h_δ}.

The method of testing was to first determine the characteristics of the original elevators and then the characteristics of the modified elevators so that a comparison between the two could be made. The longitudinal tests were run at a tunnel dynamic pressure of 25 pounds per square foot

(V = 100 mph, R = 7,300,000). The data obtained from the tests are shown in figures 4 and 5 in the form of pitching-moment-coefficient and hinge-moment-coefficient characteristics for the airplane equipped with the original and with the modified elevators, respectively. Pitching-moment coefficients are presented for a center of gravity located 25 percent M.A.C. aft of the leading edge of the M.A.C. and 5.13 percent M.A.C. above the fuselage reference line.

The results[1] obtained disclose that bulging the surface such that the trailing-edge angle was increased 6° resulted in an increase in C_{h_δ} of 0.0022 (from -0.0047 to -0.0025) and an increase in $C_{h_{\alpha_t}}$ of 0.0020 (from -0.0020 to 0). It is of interest to note that, in an effort to predict the effect of the bulge, calculations made in accordance with reference 2 predicted an increase of 0.0026 in C_{h_δ} and 0.0020 in $C_{h_{\alpha_t}}$ for a 6° increase in trailing-edge angle.

Using the elevator gearing shown in figure 6, the control-force gradients for the airplane in steady turning flight have been computed from the wind-tunnel data and are shown in figure 7 as a function of center-of-gravity location.

---

[1]Since the tests were run at a dynamic pressure of 25 pounds per square foot, the effects of surface deformation were negligible. The test results therefore indicate the effect of the bulged contour only and do not include the effect of surface deformation. The advantages of metal-covered surfaces will be realized only in high-speed flight.

These gradients have been computed for rated power[1] at sea level for a gross weight of 32,000 pounds and airspeeds of 350 and 240 miles per hour. An airspeed of 350 miles per hour is considered to represent high-speed attack conditions, while 240 miles per hour was chosen to represent the lower range of maneuvering speed (240 mph also enabled a check to be obtained from the previous flight-test data).

To provide a correlation between the control-force gradients computed from the basic wind-tunnel data and the control-force gradients obtained in previous flight tests, data have been taken from flight tests and plotted in figure 7 along with the control-force gradients computed from the wind-tunnel data for the same flight conditions. It will be seen that a very good correlation exists.

A comparison between the curves for the original elevator and the bulged elevator reveals that bulging the elevator contour reduced the control-force gradient from 80 pounds per g to 60 pounds per g, a reduction of 25 percent (350 mph, 23 percent M.A.C. center-of-gravity position). It should also be noted that the proportionate reduction in control-force gradient obtainable by bulging the elevators decreases as the center-of-gravity position moves aft. Thus

[1]The results of power-on tests of a 0.2375-scale model have been used to correct the airplane pitching moments for power effects. The hinge-moment data were not so corrected since they were found to be in good agreement with those calculated from power-on flight tests.

a favorable rearward shift in the maneuvering neutral point results.

However, the control-force gradient of 60 pounds per g obtained with the tested amount of bulge is still too high. (As previously mentioned, a control-force gradient of 35 lb/g is considered desirable when operating at high-speed low-level attack conditions with the forward center-of-gravity location.) Hence, an analysis has been made in Appendix D to determine the possible changes which would further reduce the control-force gradients.

The analysis of Appendix D indicates that the control-force gradient can be reduced to the desired value of 35 pounds per g by the use of a balance tab in conjunction with the tested amount of bulge. The balance-tab requirement is relatively small, a tab effectiveness ($\partial C_{h_e}/\partial \delta_t$) of 0.001 for an elevator-tab ratio of 1:1 being sufficient. The control-force gradients for the airplane equipped with the bulged elevator and the balance tab are shown in figure 7 for the previously described flight conditions. These results indicate that the bulge and balance-tab combination will satisfy the desired elevator-control-force characteristics: a control-force gradient of 35 pounds per g will be obtained for attack conditions (23 percent M.A.C. c.g. position, 350 mph speed), and at the same time the variation of control-force gradient with center-of-gravity location will be reduced with the result that a control-force gradient of 18 pounds per g

will be obtained for low-speed turns with rearward center of gravity (240 mph speed, 34 percent M.A.C. c.g. position).

Further tests were necessary to enable the size of the balance tabs to be determined. Since the balance tabs were to be located just outboard of the existing trim tabs, the assumption was made (which was later substantiated by flight tests) that the characteristics of the trim tabs would closely approximate the characteristics of the balance tabs. Therefore trim-tab effectiveness was determined in order to provide data for the design of the balance tabs.

The effects of trim-tab deflection on the characteristics of the bulged elevators are shown in figure 8. A trim-tab effectiveness ($\partial C_{h_e}/\partial \delta_t$) of 0.0033 is indicated by figure 8. From these results the size of the balance tabs can be determined, dependent upon actual manufacturing practicalities, structural details, and the method used of driving the balance tabs.

Use of an ordinary type of balance tab in which the tab deflection is proportional to elevator deflection will manifestly reduce the control forces at high deflections just as at low deflections. However, since the stalling characteristics of the airplane equipped with the original elevators were considered to be very good, due in part to heavying-up of control forces as the stall was approached, it was desirable to minimize the tab effects at the higher elevator deflections. To do this required a tab-drive linkage providing a variable

balance ratio such that a positive balance was obtained for elevator deflections attained during accelerated-flight maneuvers but that the tab be essentially neutral at the elevator deflections required to stall the airplane. The tab-drive linkage designed to attain these results is indicated diagrammatically in figure 9. The resulting variation between elevator deflection and balance-tab deflection is also shown in figure 9.

To satisfy the third requirement to be met by any modifications made to the elevators (that no loss in elevator effectiveness during landings could be sustained), additional data were obtained to indicate the relative effectiveness of the two elevators - original and bulged - at high deflections. These data, presented in figure 10, disclose that although for the lower deflections the effectiveness of the bulged elevators is lower than that of the original elevators, the peak effectiveness of the bulged elevators is about 4 percent higher than that of the original elevators. Therefore the bulged elevators should give somewhat better landing characteristics than the original elevators.

Particular attention should be given to the deflection at which the elevators stall, which is from 25° to 27°, dependent upon the airplane angle of attack. Obviously then, the elevator stops should be set to limit the elevator deflection to approximately 25° and not 30°, as originally

specified. This, in fact, may have contributed to accidents during landings caused by collapse of the nose gear, the nose-gear failure probably resulting from excessive impact loads due to inability to hold the tail down after the elevators stalled.

Lateral Characteristics

To make the airplane suitable for ground-support attack operations, it was further necessary to reduce the high-speed aileron-control forces from 25 to 50 percent. It was required that these reductions be achieved without loss in low-speed lateral control since, as reported from flight tests, the lateral control was marginal during approaches and landings. In fact, it was considered very desirable to improve the low-speed flaps-down effectiveness by about 10 percent.

In the endeavor to attain the high-speed control-force reductions, the original, fabric-covered, true-contour ailerons were modified as follows: (1) the ailerons were covered with metal to minimize surface deformation at high speeds and the consequent increase in control forces; (2) a straight-sided contour was incorporated in place of the true contour to directly reduce the control forces; and (3) the balance-tab ratio was to be changed as necessary to utilize the balance tabs to the fullest extent possible in reducing the control forces. The aileron span was extended to the wing tip, to offset the anticipated loss in effectiveness incurred by use

of straight-sided ailerons in place of true-contour ailerons. Additional low-speed effectiveness was then to be obtained by increasing the aileron travel from the maximum of 20° up and 15° down, as originally specified, to a maximum of 22° up and 17° down[1]. The modifications made to the ailerons are shown in figure 11. The aileron gearing is shown in figure 12.

For the wind-tunnel tests, the original aileron was mounted in place on the right wing and the modified aileron on the left wing. The characteristics of the original and modified ailerons were then determined at a dynamic pressure of 25 pounds per square foot (V = 100 mph, R = 7,300,000) and are shown in figures 13 to 16, inclusive.

The rolling characteristics of the airplane have been computed[2] from the basic wind-tunnel data and are shown in figures 17 and 18. Figure 17 shows the variation of control force with pb/2V in high-speed flight and figure 18 shows the over-all rolling characteristics. Results of the previous flight tests have been plotted on the two figures to give a correlation between flight results and

[1]The maximum travel that the wing and aileron structure will permit is 22° up and 17° down.

[2]Rolling characteristics have been computed by use of the relation $pb/2V = \Delta C_l/C_{l_p}$. The value of C_{l_p} was obtained for the purposes of this report from reference 3. A correction for the slope of the lift curve was applied, giving a value of $C_{l_p} = 0.58$ for this airplane. The value of pb/2V obtained was reduced 20 percent to correct for the losses in rolling velocity resulting from the dynamic effects of wing twist and sideslip.

wind-tunnel results. Considerable discrepancy will be seen to exist between the curves obtained from the flight tests and the curves obtained from the wind-tunnel tests. This discrepancy can not be entirely explained at the present time, but may be due in part to heavying-up of control forces resulting from fabric deformation. (This could not be taken into account in reducing the wind-tunnel data, as previously explained regarding the elevators.) However, the improvements in aileron control henceforth indicated were adjusted so as to be proportional to the flight-test data.

On the basis of the foregoing remarks, a comparison between the curves shown in figure 17 indicates that the modified ailerons with no balance tab will reduce the high-speed aileron-control forces about 15 percent below those experienced with the original aileron having a 0.375:1 balance-tab ratio. A comparison of the curves for the flaps-down condition in figure 18 indicates essentially no change in the low-speed flaps-down characteristics (the extended aileron span and lack of balance tabs increased the effectiveness approximately the same amount that the straight-sided contour reduced the aileron effectiveness). These results signified that additional high-speed aileron-control-force reductions would have to be obtained by proper use of the balance tabs; further, to overcome the loss in effectiveness

due to use of the balance tabs, the low-speed flaps-down effectiveness would have to be increased by increasing the aileron travel.

Additional data were required to enable determination of the proper balance ratio for the tabs. These data are shown in figures 19 and 20. It is evident from these figures that the balance ratio must be limited to 1:1, otherwise overbalance will result.

It therefore appeared that an aileron incorporating a 1:1 balance tab to further reduce control forces, with the maximum travel increased to 22° up and 17° down to provide additional effectiveness at low speeds would give the desired results. The rolling characteristics have been computed for this aileron configuration and are shown in figures 17 and 18. The curves in figure 17 indicate that the high-speed aileron-control forces will be reduced approximately 80 percent by use of the modified ailerons with a 1:1 balance-tab ratio. In addition, as shown in figure 18, the increased aileron travel will result in a gain of from 5 to 10 percent in the low-speed flaps-down lateral control.

Minimum Drag Characteristics

To determine the improvements that could be obtained in the top speed of the airplane, tests were made to indicate the drag of each of the various drag-producing items. The

loss in the top speed of the airplane due to each of the items could then be determined. The drag-producing items have been classified into three groups: (1) leakage items, (2) component protuberances, and (3) adjunct protuberances. The leakage items are the joints through which air could leak out of the wings, fuselage, or nacelles. The airplane with all leakage items sealed is shown in figure 21. The component protuberances are the protuberances that are component parts of the airplane such as the guns, radio loop, etc. Figures 2 and 22 show the airplane in the service configuration with the component protuberances in place. The adjunct protuberances are the removable auxiliary items such as the bombs, fuel tanks, etc. The airplane with the various adjunct protuberances in place is shown in figure 23.

Preparatory for mounting in the wind tunnel, the airplane was completely sealed and all protuberances were removed. The method of testing was to unseal the airplane by sections and evaluate the increment of leakage drag caused by each section; next, to add the component protuberances one at a time and evaluate the increment of drag due to each protuberance; and finally, to add the adjunct protuberances and evaluate the increment of drag due to each.

The drag results are presented in the form of minimum drag polars which were run at a dynamic pressure of 70 pounds per square foot (V = 165 mph, R = 12,200,000). The minimum

drag polars for each successive change in configuration are shown in figures 24, 25 and 26. It is to be noted that the tests were run in the order in which they are presented in the figures; therefore, the configuration for each curve is the configuration of the preceding curve plus the item noted on the curve[1].

A summary of the results obtained from the leakage drag tests (fig. 24) is presented in the following table. Shown in the table are the increments of drag attributable to each item, and the increase[2] in top speed which could be realized if the item were sealed.

[1]The exceptions to this are the curves for the wing rib unsealed and the landing-flap door in place. The tests for these curves were not run in the sequence shown in the figures; however, the values have been corrected to account for the intervening runs so that the proper drag increment is indicated.

[2]The calculated velocity increments are based upon the reported sea-level high speed of 360 miles per hour. A high-speed power-on drag coefficient of 0.0263 was calculated, based upon the reported high-speed and war-emergency power of 2370 horsepower per engine. The assumption was made that the total propulsive efficiency was 95 percent: 85-percent-propeller propulsive efficiency plus an additional 10-percent efficiency due to jet thrust and Meredith effect.

	Item	ΔC_D at C_L=0.19	ΔV at top speed (mph)
1.	Nose seals removed, including the seals around the nose at fuselage station 0	0.0002	1
2.	Nose-wheel doors unsealed	.0001	$\frac{1}{2}$
3.	Cockpit canopy unsealed	.0002	1
4.	Bomb-bay spoiler well unsealed	-.0004	-
5.	Bomb-bay doors unsealed	.0000	0
6.	Steps and drift meter unsealed	.0000	0
7.	Fuselage armor plate unsealed	.0001	$\frac{1}{2}$
8.	Fuselage butt joints unsealed	.0001	$\frac{1}{2}$
9.	Rear-gunner escape hatch and oblique-camera doors unsealed	.0000	0
10.	Wing-fuselage fillet unsealed	.0002	1
11.	Cowl and cowl flaps unsealed	.0002	1
12.	Nacelle access doors unsealed	.0001	$\frac{1}{2}$
13.	Nacelle butt joints unsealed	.0000	0
14.	Main landing-gear doors unsealed	.0002	1
15.	Wing butt joints unsealed	-.0001	-
16.	Wing-deflection slots unsealed	-.0002	-
17.	Wing-access plates and gun-compartment plates unsealed	.0001	$\frac{1}{2}$
18.	Wing-gun ejection chutes unsealed	.0003	$1\frac{1}{2}$
	Summation of favorable increments. (Items 1, 2, 3, 5 to 14, 17 and 18.)	.0019	9

From the table it can be seen that the airplane is quite well sealed. Although an additional 9 miles per hour can be added to the top speed by completely sealing the airplane, difficulties associated with sealing will limit the actual improvement in top speed that can be gained.

The drag increments and corresponding losses in top speed due to addition of each of the component protuberances (fig. 25)

are shown in the following table:

Item	ΔC_D at C_L=0.19	ΔV at top speed (mph)
1. Nose guns (faired)	0.0002	1
2. Removal of nose-gun fairings	.0002	1
3. Nose louvers	-.0002	-
4. Radio antenna and mast	.0000	0
5. Enclosed loop antenna	.0001	$\frac{1}{2}$
6. Upper turret and periscope	.0010	5
7. Lower turret and periscope	.0008	4
8. Lower-periscope deflector	.0004	2
9. Aft air-conditioning scoop and exit	.0001	$\frac{1}{2}$
10. Forward air-conditioning scoop and exit	.0001	$\frac{1}{2}$
11. Modification to landing-flap doors	.0001	$\frac{1}{2}$

These results show that the airplane is fairly clean. By fairing the nose guns and removing the lower-periscope deflector, 3 miles per hour can be added to the top speed of the airplane. The functions of the remainder of the items however, require their existence, and hence little can be accomplished in the way of improvement.

The landing-flap doors are the doors which close the gap between the lower-surface wing skin and the landing flaps. These doors require an elaborate linkage to move them down and out of the way when the landing flaps are being either lowered or raised. The linkage caused considerable trouble on existing airplanes and it was desired to replace the doors and linkage with a fixed extension of the lower-surface wing

skin. Tests were therefore made to determine if replacing the doors and linkage with a fixed extension of the lower-surface wing skin would have an appreciable effect on either the high-speed drag or the maximum lift.

For the purpose of these tests, a fixed extension of the lower-surface wing skin was simulated by trimming the trailing edges of the original doors sufficiently to allow the landing flaps to be lowered or raised without moving the doors. As shown in the table, the modification to the landing-flap doors caused only a small increment in the high-speed drag coefficient and would result in only 1/2-mile-per-hour loss in top speed. Hence, replacing the landing-flap doors and linkage with a fixed extension of the lower-surface wing skin will be satisfactory as far as the drag is concerned. The effect of the modified doors on the maximum lift will be discussed in the next section.

The results of the tests made to determine the drag characteristics of the adjunct protuberances (figs. 26(a) and (b)) are summarized in the following table:

Item	ΔC_D at C_L=0.19	ΔV at top speed (mph)
1. 14 rocket racks	0.0015	7
2. 14 rockets and racks	.0051	21
3. Four 500-lb bomb racks	.0027	12
4. Four 500-lb bombs and racks	.0084	32
5. Two fuel-tank racks	.0006	$2\frac{1}{2}$
6. Two fuel tanks and racks	.0027	12
7. Eight rockets and two fuel tanks	.0056	$22\frac{1}{2}$
8. Eight rockets and two 500-lb bombs	.0070	$27\frac{1}{2}$
9. Two fuel tanks and two 500-lb bombs	.0078	30
10. Bomb-bay doors open	.0084	32

This table discloses that, with the exception of the bomb racks, the various items cause no undue increase in drag. The bomb racks appear to create excessive drag when compared to the fuel-tank racks. In spite of the much greater size of the fuel-tank racks, the decrease in speed attributable to each fuel-tank rack is about 1-1/4 miles per hour; whereas the decrease in speed attributable to each bomb rack is about 3 miles per hour. Thus it appears that fairing the bomb racks will increase the top speed at least 1-3/4 miles per hour per rack or 7 miles per hour for all four racks.

Maximum Lift Characteristics

In conjunction with the foregoing tests, additional tests were made to determine the effect of various configurations on the maximum lift characteristics of the airplane.

Included were an evaluation of the effects on maximum lift of wing leakage, addition of the wing guns, opening the cowl flaps, opening the oil-cooler doors, the modified doors of the landing flaps, the various adjunct protuberances, and various flap deflections.

The results of the maximum lift tests are shown in figure 27 in the form of lift, drag, and pitching-moment curves. The data were obtained at a dynamic pressure of 25 pounds per square foot (V = 100 mph, R = 7,300,000). It can be seen from figure 27 that none of the items affect the maximum lift appreciably. For example, the difference between the maximum lift coefficient of the airplane in the clean and sealed configuration and the maximum lift coefficient of the airplane in the service configuration (an increment in the maximum lift coefficient of 0.05) will result in only about 1/2-mile-per-hour decrease in the landing speed.

Figure 27 also shows that when the modified landing-flap doors were in place, no decrease in the maximum lift coefficient was experienced; in fact, there was an increase. (The modified landing-flap doors were previously discussed in regard to their effect on minimum drag.) Hence it can be concluded that replacing the landing-flap doors with a fixed extension of the lower-surface wing skin will have no significant aerodynamic effects; it will result in only small increases in drag and in maximum lift.

In figure 28 are presented the lift, drag, and

pitching-moment curves for the airplane with various flap deflections. The maximum-trim-lift coefficients were computed from the data of figure 28 and are shown in figure 29 as a function of flap deflection. It can be seen from figure 29 that the maximum flap deflection of 52° produces the highest trim-lift coefficient obtainable with the existing flap system.

CONCLUSIONS

The results of the tests of the airplane reported herein may be summarized as follows:

1. The elevator-control-force gradients for high-speed maneuvering flight will be reduced about 50 percent by replacing the original, fabric-covered, straight-sided elevators with metal-covered bulged-contour elevators incorporating a balance tab. In addition to reducing the high-speed maneuvering control forces the desired amount, the modified elevators will satisfy the other critical flight conditions as follows: (a) the elevator-control-force gradients for low-speed maneuvering flight with the rearward center of gravity will not be reduced from the original values; in fact, they will undergo slight favorable increases; and (b) the elevator control during landings will be slightly increased (about 4 percent) above the original values. The desirable stalling characteristics of the original elevators (heavying-up of the elevator control forces as the stall is

approached) may be retained by utilizing a tab gearing that will return the balance tab to approximately neutral at high elevator deflections.

2. The aileron-control forces for high-speed maneuvering flight will be reduced about 80 percent by replacing the original, fabric-covered, true-contour ailerons incorporating a 0.375:1 balance tab with metal-covered, straight-sided, extended-span ailerons incorporating a 1:1 balance tab. The lateral control during approaches and landings may be increased from 5 to 10 percent by increasing the maximum aileron travel from 20° up and 15° down to 22° up and 17° down.

3. Approximately 9 miles per hour could be added to the top speed by completely sealing the airplane; however, difficulties associated with sealing will limit the actual improvement that can be gained. Three miles per hour can be added to the top speed by fairing the nose guns and removing the lower-periscope deflector. When the 500-pound bomb racks are in place, about 7 miles per hour can be added to the top speed by fairing the bomb racks.

Ames Aeronautical Laboratory,
National Advisory Committee for Aeronautics,
Moffett Field, Calif.

APPENDIX A

GENERAL DATA ON THE TEST AIRPLANE[1]

Power plant

The airplane is powered by two radial 18-cylinder, double-row, air-cooled engines with water injection, designated as R-2800-79. Power ratings are as follows:

Condition	bhp	rpm
War emergency	2370	2700
Military	2000	2700
Rated	1600	2400

Propellers . . . . . Constant speed, quick feathering

Three blades 6359A-18

Diameter (actual). . . . . .12 ft 7 in.

No spinners installed

Wing

Area, sq ft. 540.5

Span, ft 70.0

Aspect ratio 9.07

Taper ratio. 453

Mean aerodynamic chord, ft 8.13

Sweepback . . . . . 20-percent-chord line straight

[1]All data are taken from manufacturer's specifications and apply to the service airplane before any modifications were made.

Equivalent geometric dihedral (top of front spar), deg 4.5

Geometric twist, deg. . . . . -1.0

Incidence at root chord, deg. 2

Wing section

Root . . . . . NACA 65,2-215(a = 0.8)(b = 1.0)

Tip . . . . . NACA 65,2-215(a = 0.5)(b = 1.0)

Root chord, ft. 10.67

Tip chord, ft 4.83

Flaps

Type. . . . . .Partial-span double-slotted

Area (aft of hinge line), sq ft. 55.9

Effective span (to center line) (one side), ft. . . 22.82

Actual span (one side), ft. 15.8

Maximum travel, deg 52

Wing area affected (both sides), sq ft. 264.8

Total flap chord/wing chord 0.25

Ailerons

Type. . . . . .Sealed internal balance

Area (aft of hinge line)(two sides including tabs), sq ft. 27.2

Span, ft. 10.9

Wing area affected, sq ft 129.96

Maximum aileron travel, deg . . . . . 20 up ±1

15 down ±1

M.A.C., ft. 1.26

Wing area affected, sq ft	129.96
Balance area excluding cut-outs, sq ft	16.61
Balance area including cut-outs, sq ft	17.67
Balance ratio (based on area aft hinge line excluding cut-outs)	0.61
Hinge-line location, percent wing chord	79
Aileron tabs	
Type	Trim and balance
Span, ft	2.77
M.A.C. of tab, ft	0.42
Hinge-line location, percent aileron chord . . .	30
Area (aft of hinge line) (both sides), sq ft . .	2.38
Maximum travel, deg	± 7
Balance tab ratio	0.375:1
Trim tab on left side only	
Fuselage	
Length, ft	48.875
Horizontal tail	
Span, ft	22.69
Area (including fuselage), sq ft	116.1
Aspect ratio	4.43
Taper ratio	0.5
Mean aerodynamic chord, ft	5.36
Dihedral, deg	10.58
Incidence	0

Tail length (0.25 M.A.C. to hinge line horizontal tail), ft 30.45

Elevators

Type . . . . . Sealed overhang balance

Area (aft of hinge line), sq ft 32.7

M.A.C., ft 1.79

Hinge-line location (percent chord of horizontal tail) 65.45

Horizontal surface area affected, sq ft 93.62

Balance ratio (based on area aft of hinge line) . . . 0.315

Maximum travel, deg . . . . . Up 30 ±1/2

Down 16 ±1/2

Elevator tab

Type . . . . . Trim (no balance tab)

Span, ft 2.46

M.A.C. of tab, ft 0.52

Hinge-line location (percent elevator chord) . . 25

Area (aft of hinge line) (both sides) sq ft . . . 2.58

Maximum travel, deg . . . . . -12, 17

Control-system data

Control-column travel (no load), deg 37.5

Wheel travel (no load), deg . . . . . ±130

Control-column length, in. 27

Wheel diameter, in. 14

Pedal radius, in. 12

APPENDIX B

COEFFICIENTS AND SYMBOLS

The coefficients and symbols used in the presentation of data with this report are defined as follows:

C_L lift coefficient (L/qS)

C_D drag coefficient (D/qS)

C_m pitching-moment coefficient (M/qSc)

C_n yawing-moment coefficient (N/qSc)

C_l rolling-moment coefficient (L'/qSc)

C_{h_e} elevator hinge-moment coefficient (H_e/qS_ec_e)

C_{h_a} aileron hinge-moment coefficient (H_a/qS_ac_a)

ΔC_l increment of rolling-moment coefficient produced by a given aileron deflection

C_{D_P} parasite-drag coefficient $[C_D - (C_L^2/\pi A)]$

$\left(C_{h_\delta}\right)_{C_L}$ rate of change of elevator hinge-moment coefficient with elevator deflection $[(\partial C_{h_e}/\partial \delta_e)_{C_L}]$

$\left(C_{h_{\alpha_t}}\right)_{C_L}$ rate of change of elevator hinge-moment coefficient with angle of attack of the horizontal tail $[(\partial C_{h_e}/\partial \alpha_t)_{C_L}]$

$\left(C_{h_{C_L}}\right)_\delta$ rate of change of elevator hinge-moment coefficient with airplane lift coefficient $[(\partial C_{h_e}/\partial C_L)_\delta]$

L lift, lb

L' rolling moment, ft-lb

D drag, lb

M pitching moment, ft-lb

N yawing moment, ft-lb

H_e elevator hinge-moment, ft-lb (Positive hinge moment tends to deflect elevator downwards.)

H_a aileron hinge-moment, ft-lb (Positive hinge moment tends to deflect aileron downwards.)

q free-stream dynamic pressure, lb/sq ft

V airspeed, ft/sec or mph

V_i indicated airspeed, mph

σ density ratio (ρ/ρ_o)

ρ mass density of air at altitude, slugs/cu ft

ρ_o mass density of air at sea level, slugs/cu ft

g standard acceleration of gravity, ft/sec^2

p rolling velocity, radians/sec

$pb/2V$ helix angle of roll generated by wing tips in a roll, radians

S wing area, sq ft

b wing span, ft

c mean aerodynamic chord of wing, ft

A aspect ratio of wing (b^2/S)

l_w wing loading, lb/sq ft

l_h distance from center-of gravity to hinge line of elevator, ft

n normal acceleration in g's

f elevator-control force, lb

S_e area of elevator aft of hinge line, sq ft

c_e mean aerodynamic chord of elevator aft of hinge line, ft

S_a area of original aileron aft of hinge line, sq ft

c_a mean aerodynamic chord of aileron aft of hinge line, ft

α angle of attack referred to thrust line, deg

α_t angle of attack of horizontal tail, deg

δ_e elevator deflection, deg (positive downwards)

δ_a aileron deflection, deg (positive downwards)

$$K_1 = \frac{f}{C_{h_e} q} \; l_w \; \frac{(\partial C_m/\partial C_L)_\delta - (\partial C_m/\partial C_L)_{\text{tail off}}}{(\partial C_m/\partial \alpha_t)_{C_L}}$$

$$K_2 = \frac{f}{C_{h_e} q} \; l_w \; \frac{(\partial C_m/\partial C_L)_\delta}{(\partial C_m/\partial \delta_e)_{C_L}}$$

$$K_3 = 2.192 \; \frac{f}{C_{h_e} q} \; l_h \sigma [(n + 1)/n]$$

$$K_4 = K_3 \; \frac{(\partial C_m/\partial \alpha_t)_{C_L}}{(\partial C_m/\partial \delta_e)_{C_L}}$$

Subscripts outside of parentheses indicate the factors held constant during measurement of the parameter.

APPENDIX C

CORRECTIONS APPLIED TO THE FORCE MEASUREMENTS

Tunnel-wall corrections have been applied to the gross force measurements in the following manner:

$\Delta\alpha_T = 1.052\ C_L$ (added to uncorrected values of α)

$\Delta C_{D_T} = .0184\ C_L^2$ (added to uncorrected values of C_D)

$\Delta C_{M_T} = .043\ C_L$ (added to uncorrected values of C_M)

$C_l = .973\ C_{l_{gross}}$

$\Delta C_{N_T} = .024\ (C_l C_L)_{gross} \pm 0.036\, C_{L^2 gross}$ (subtracted from uncorrected values of C_N; in the second term + is used for the left aileron, - is used for the right aileron)

These corrections take into account the shape of the tunnel cross-section, the large size of the airplane relative to the tunnel $\left(\frac{\text{wing span}}{\text{tunnel width}} = 0.88\right)$ and the off-center position of the airplane (the wing was approx. 6 feet above the horizontal center line of the tunnel). The corrections to the rolling and yawing moments were determined by the methods of references 4 and 5. In these calculations the loading distribution was assumed to be represented by a uniformly loaded aileron superimposed on an elliptically loaded main wing.

APPENDIX D

ANALYSIS OF THE LONGITUDINAL CHARACTERISTICS TO DETERMINE THE MODIFICATIONS REQUIRED TO GIVE THE DESIRED ELEVATOR-CONTROL-FORCE REDUCTION

As previously explained in the main text, it was desired to reduce the stick-force gradient from 80 pounds per g to 35 pounds per g for high-speed-attack conditions without appreciably reducing the minimum stick-force gradient for low-speed turns with aft center of gravity. To allow a rapid graphical solution to be obtained of the effects of changes in the hinge-moment parameters $C_{h_{\alpha_t}}$ and C_{h_δ} on the stick-force gradient in steady turning flight the following equation was developed:

$$\frac{\Delta f}{n-1} = (K_1+K_3)C_{h_{\alpha_{t_o}}} - (K_2+K_4)C_{h_{\delta_o}} + (K_1+K_3)\Delta C_{h_{\alpha_t}} - (K_2+K_4)\Delta C_{h_\delta}$$

In the equation, $C_{h_{\alpha_{t_o}}}$ and $C_{h_{\delta_o}}$ are the basic values of the hinge-moment parameters of the original elevators having the sealed-overhang balance, and $\Delta C_{h_{\alpha_t}}$ and ΔC_{h_δ} are the changes in the basic values which result from modifications made to the elevators. The values of the aerodynamic parameters used in the equation were obtained from the power-off tests of the airplane as presented in this report[1]. For a

[1]The exception to this is the value of the tail-effectiveness parameter $\frac{(\partial C_m/\partial C_L)_\delta - (\partial C_m/\partial C_L)_{\text{tail off}}}{(\partial C_m/\partial \alpha_t)_{C_L}}$ which was obtained from the power-off tests of a 0.2375-scale model in the Langley 19-foot pressure tunnel.

specified flight condition, the equation was solved to determine the various combinations of $\Delta C_{h_{\alpha_t}}$ and ΔC_{h_δ} which would satisfy a given stick-force gradient.

For the high-speed attack conditions (350 mph airspeed, 23 percent M.A.C. center-of-gravity position) the equation was solved for stick-force gradients of 80 pounds per g (the original stick-force gradient) and 35 pounds per g (the desired stick-force gradient). For low-speed turns with aft center of gravity (240 mph, 34 percent M.A.C. center-of-gravity location) the equation was solved for stick-force gradients of 14 pounds per g (the minimum allowable gradient) and 20 pounds per g (this latter value was chosen to allow making a convenient quantitative interpolation). The variations of $\Delta C_{h_{\alpha_t}}$ with ΔC_{h_δ} for the foregoing flight conditions and stick-force gradients are shown in figure 30. It can be seen that the shaded area on the figure defines the limits within which $\Delta C_{h_{\alpha_t}}$ and ΔC_{h_δ} must be kept in order to satisfy the desired stick-force gradients.

In order to determine the approximate amount of bulge required to give the desired high-speed stick-force gradient, the change in the parameters due to the effect of the tested amount of bulge was plotted in figure 30. A straight line was drawn through the origin and the test point and extended until it crossed the line for the gradient of 35 pounds per g. The intersection of these two lines determines the approximate amount of $\Delta C_{h_{\alpha_t}}$ and ΔC_{h_δ} to be supplied by bulging the

contour. It can be seen from figure 30 that approximately twice the amount of bulge would be required (an increase in trailing-edge angle of about 12°). It can also be seen from the figure that this large amount of bulge would be unsatisfactory as it would result in overbalance of the surface (ΔC_{h_δ} is greater than $C_{h_{\delta_o}}$, resulting in a positive or overbalanced C_{h_δ}). A large amount of bulge is also undesirable because of possible adverse Mach number effects.

A satisfactory solution that can be arrived at from figure 30 is to use the tested bulged surface and furnish an additional C_{h_δ} sufficient to bring the parameters within the shaded area. This increment of C_{h_δ} can be obtained by use of a boost tab. The required tab effectiveness for a 1:1 tab ratio can be read directly from the figure and is -0.0010. Thus a gradient of 35 pounds per g will be obtained for the high-speed attack conditions and a gradient of 18 pounds per g will be obtained for low-speed turns with aft center of gravity.

Other solutions to the problem could be made. For example, figure 30 shows that the limit of 35 pounds per g could be obtained by decreasing the bulge and increasing the boost tab the necessary amount. However, for low-speed turns with aft center of gravity the favorable margin would be reduced between the attained gradient and the minimum allowable gradient.

Therefore, the tested amount of bulge in combination

with a boost tab equivalent to a tab with an effectiveness of 0.0010 with a 1:1 ratio will be the optimum arrangement. This arrangement will reduce the stick-force gradient to the desired value of 35 pounds per g for high-speed attack conditions without appreciably reducing the minimum stick-force gradient for low-speed turns with aft center of gravity.

REFERENCES

1. Anon.: Stability and Control Characteristics for Airplanes. Spec. No. R-1815A, U.S. Army Air Forces, Apr. 7, 1945.

2. Crane, Robert M.: Computation of Hinge-Moment Characteristics of Horizontal Tails From Section Data. NACA CB No. 5B05, 1945.

3. Pearson, Henry A., and Jones, Robert T.: Theoretical Stability and Control Characteristics of Wings With Various Amounts of Taper and Twist. NACA Rep. No. 635, 1938.

4. Tani, Itiro, and Sanuki, Matao: The Wall Interference of a Wind Tunnel of Elliptic Cross Section. NACA TN No. 1075, 1944.

5. Graham, Donald J.: Tunnel-Wall Corrections to Rolling and Yawing Moments due to Aileron Deflection in Closed Rectangular Wind Tunnels. NACA ARR No. 4F21, 1944.

NATIONAL ADVISORY
COMMITTEE FOR AERONAUTICS

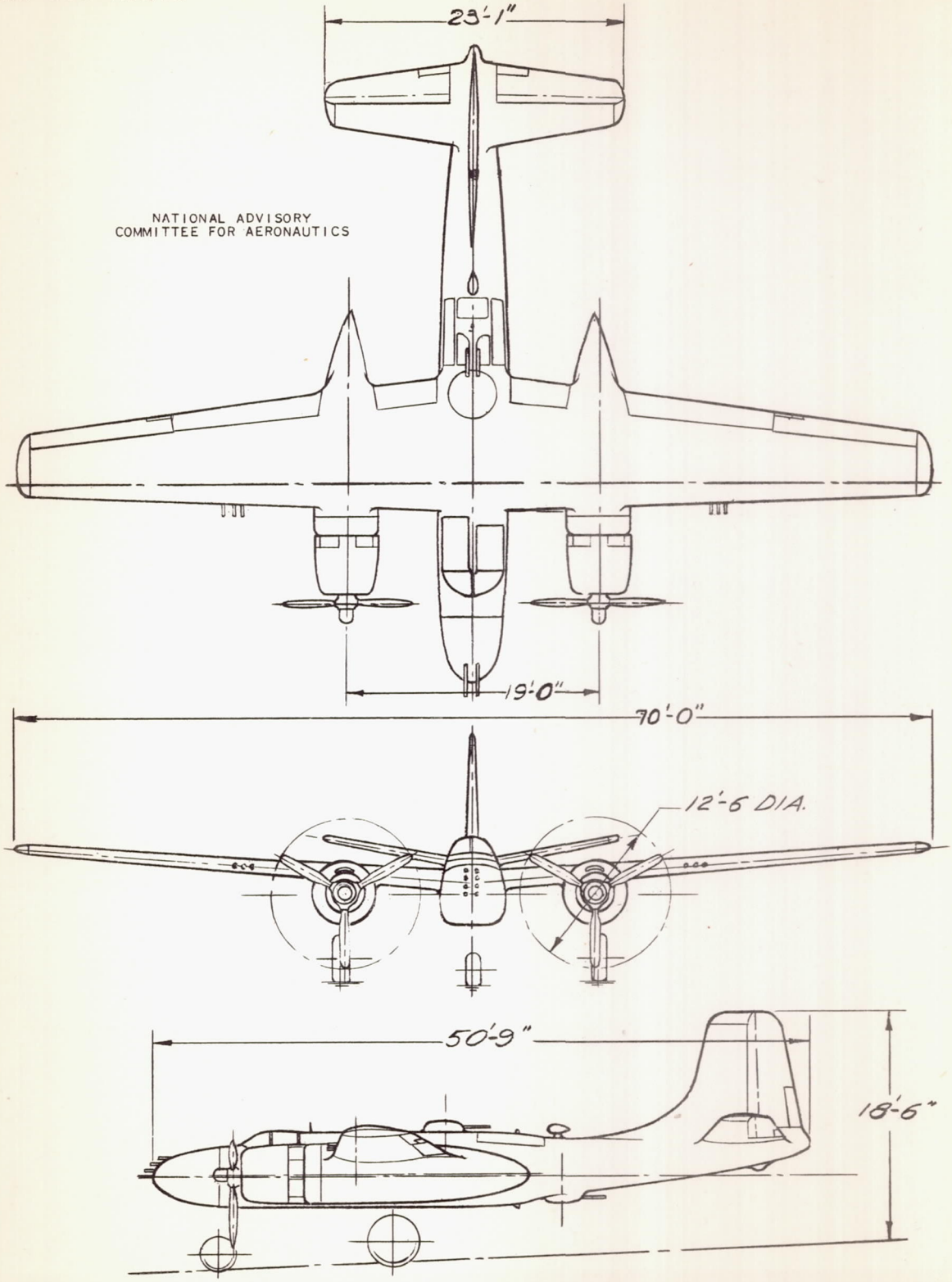

FIGURE 1.- THREE VIEWS OF TEST AIRPLANE

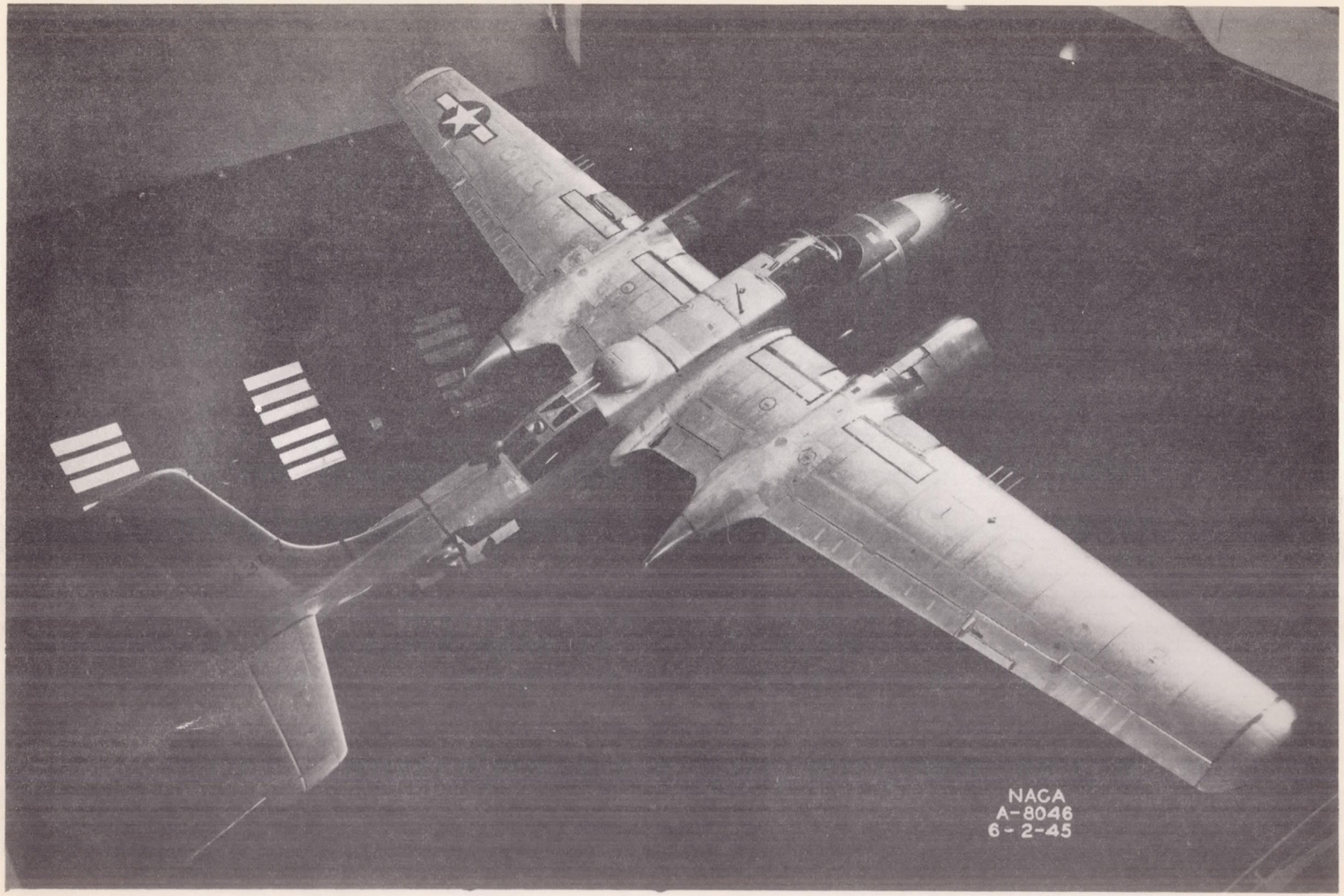

(a) Top view.

Figure 2.- The test airplane in the service configuration.

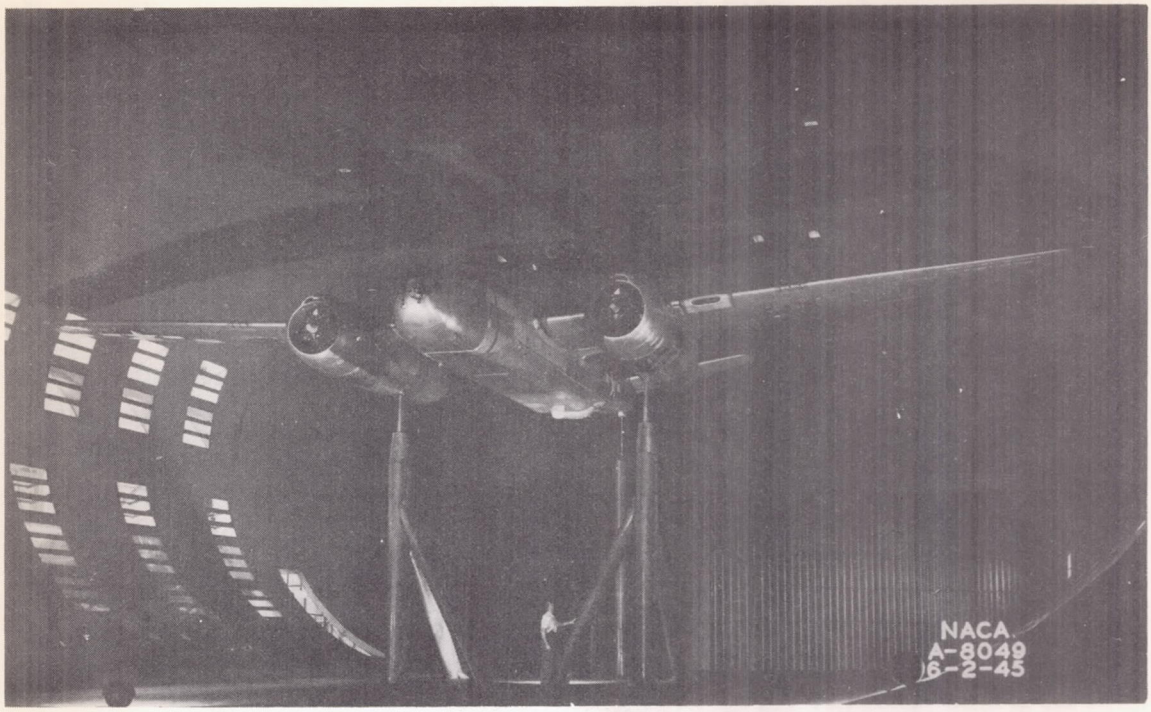

(b) Three-quarter front view.

Figure 2.- Continued.

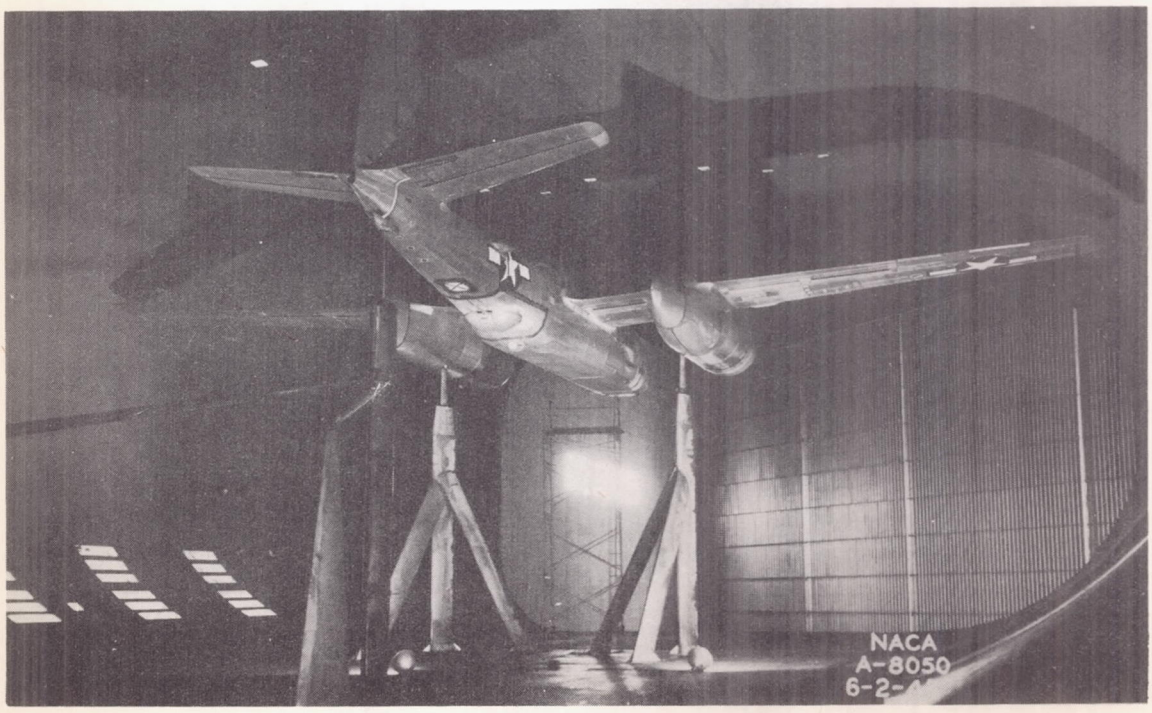

(c) Three-quarter rear view.

Figure 2.- Concluded.

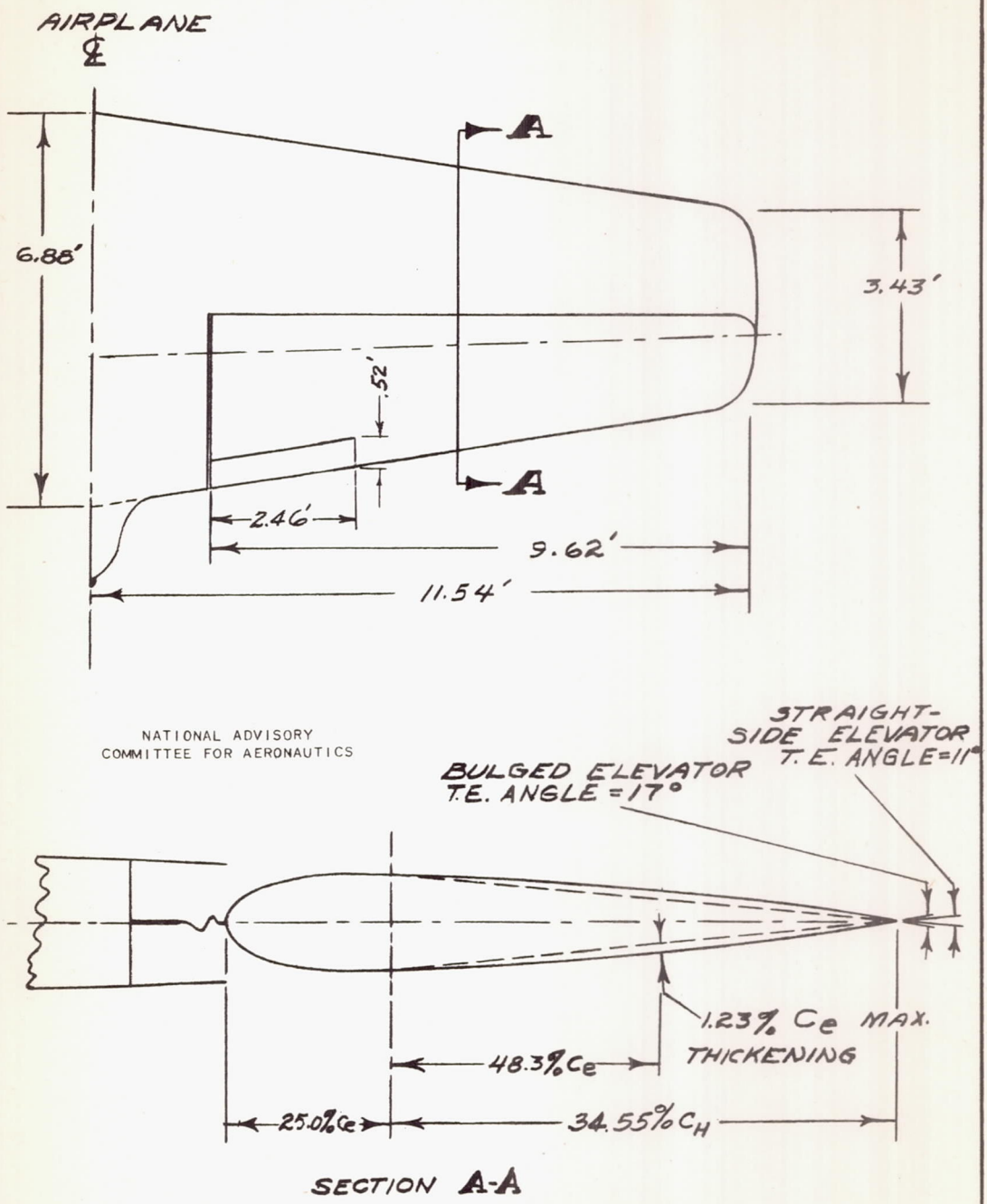

FIGURE 3.- HORIZONTAL TAIL

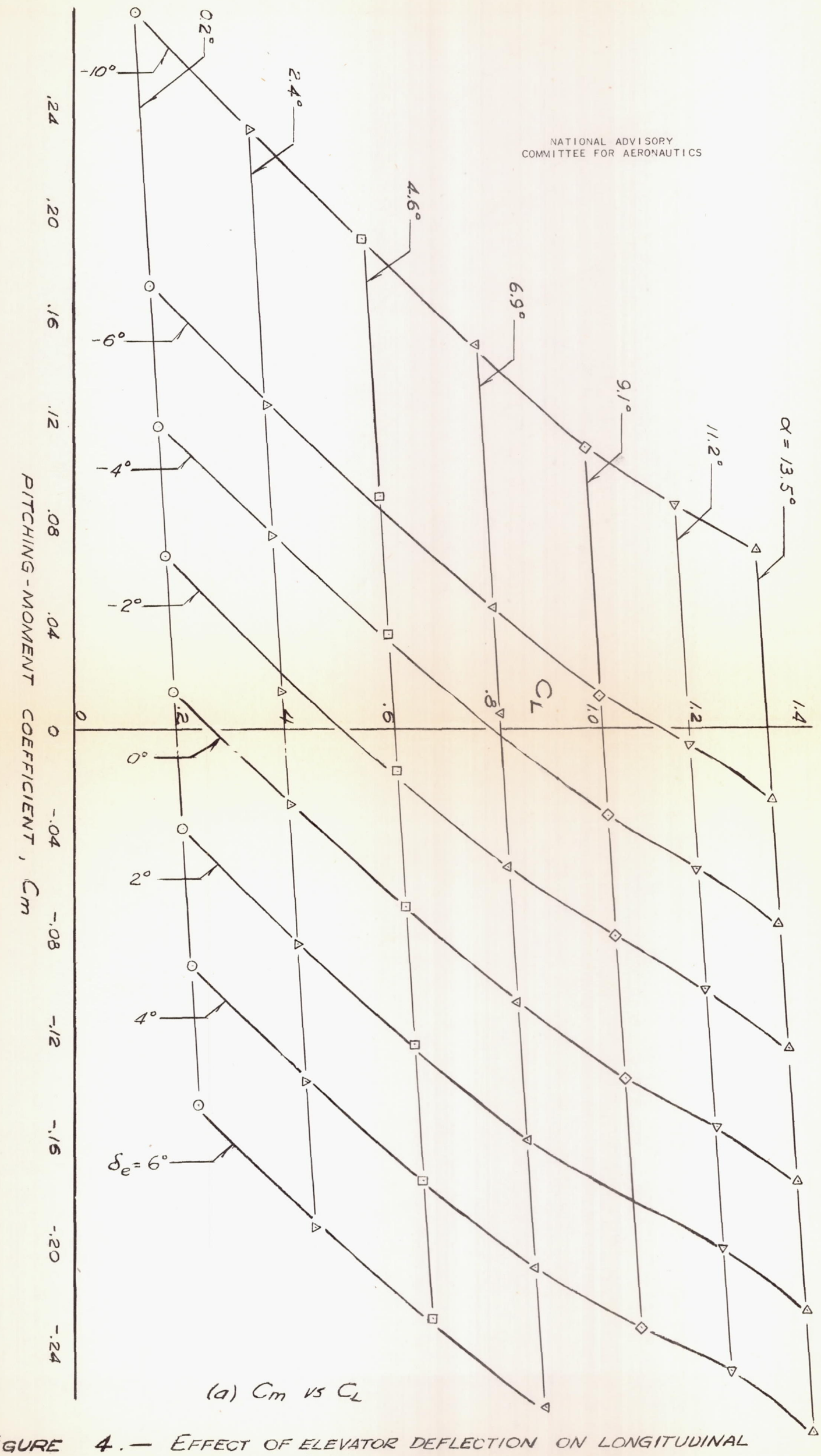

(a) C_m vs C_L

FIGURE 4.— EFFECT OF ELEVATOR DEFLECTION ON LONGITUDINAL CHARACTERISTICS. STRAIGHT-SIDED ELEVATORS.

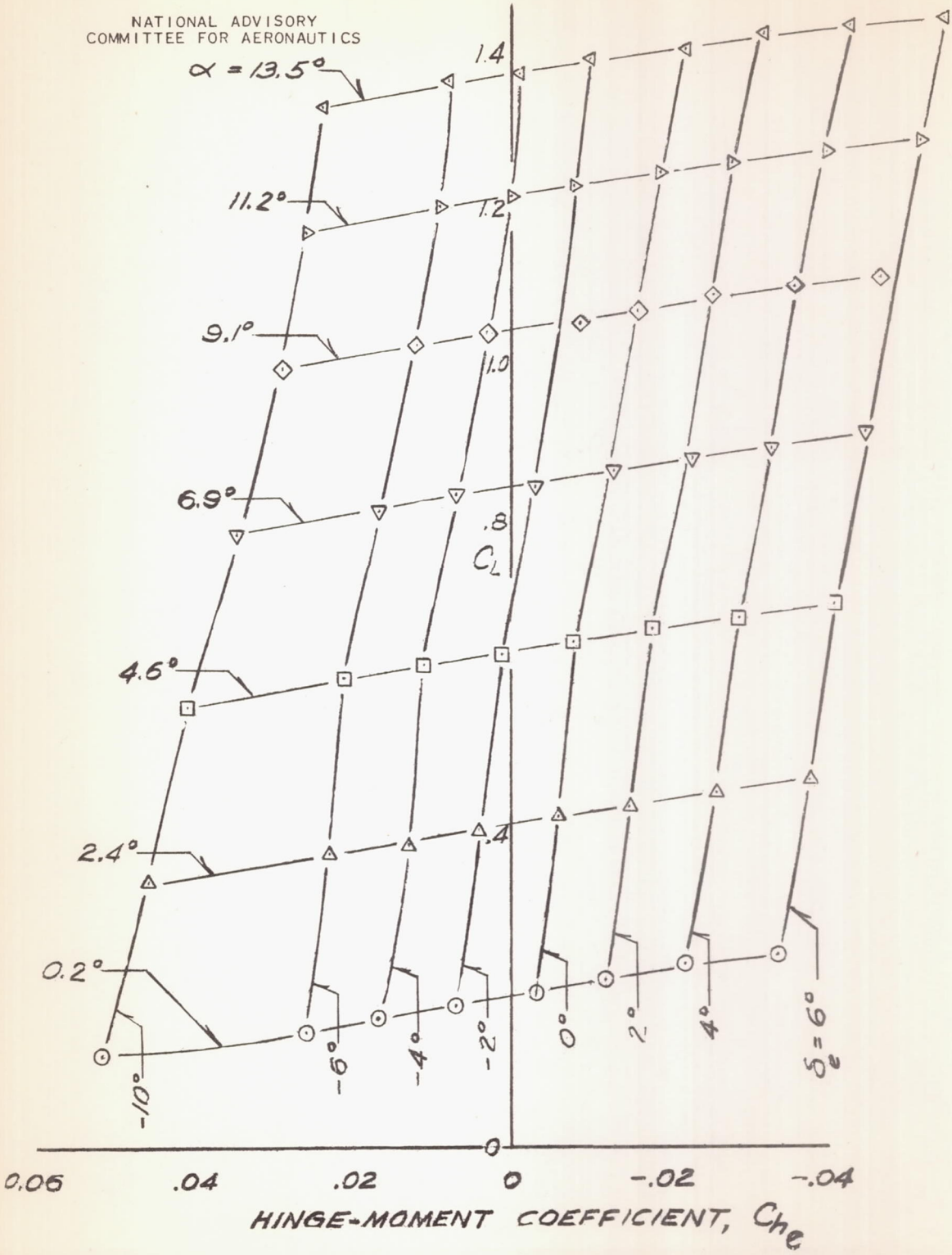

(b) C_{h_e} vs C_L

FIGURE 4.- CONCLUDED

NATIONAL ADVISORY
COMMITTEE FOR AERONAUTICS

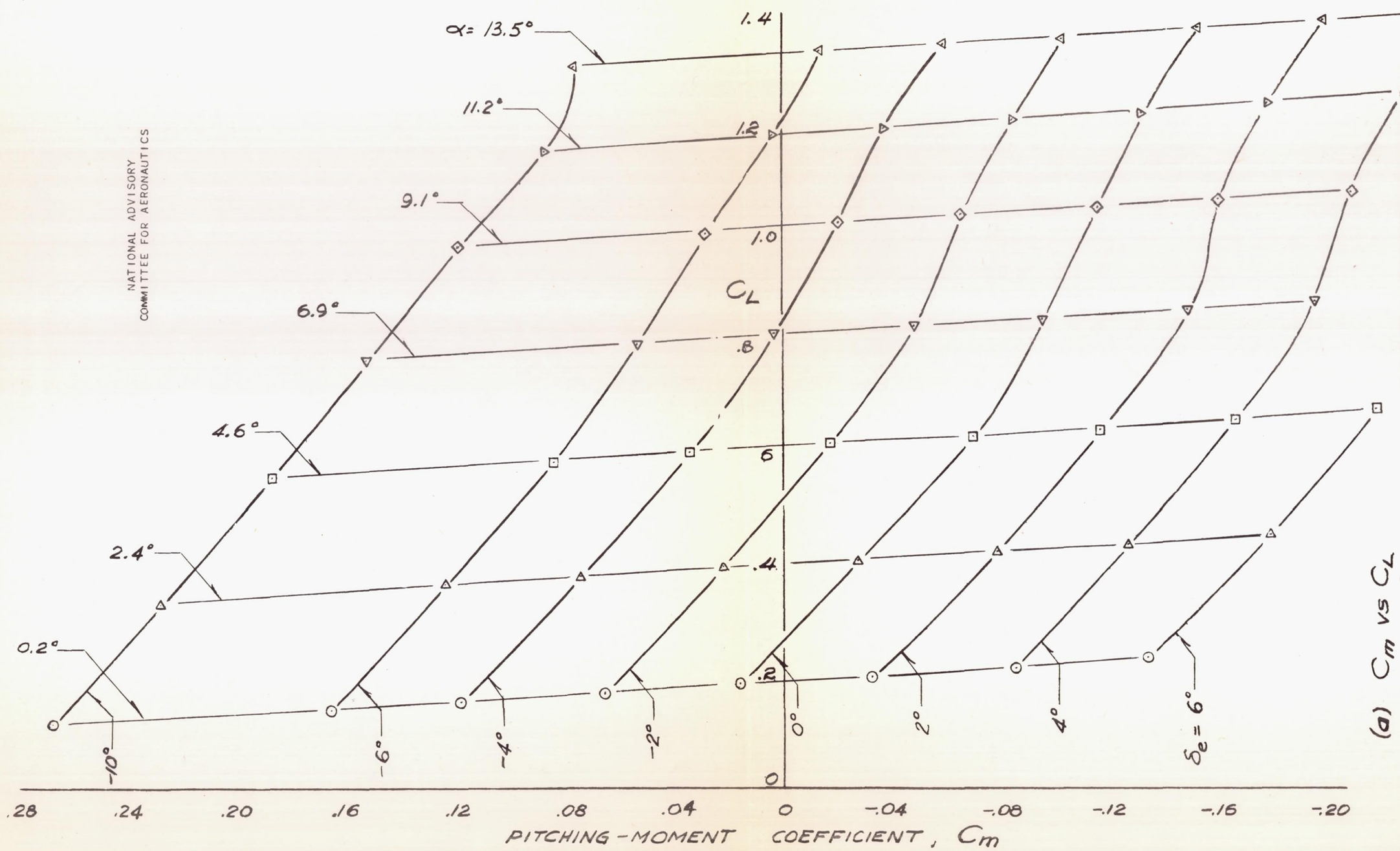

(a) C_m vs C_L

FIGURE 5.- EFFECT OF ELEVATOR DEFLECTION ON LONGITUDINAL CHARACTERISTICS. BULGED ELEVATOR.

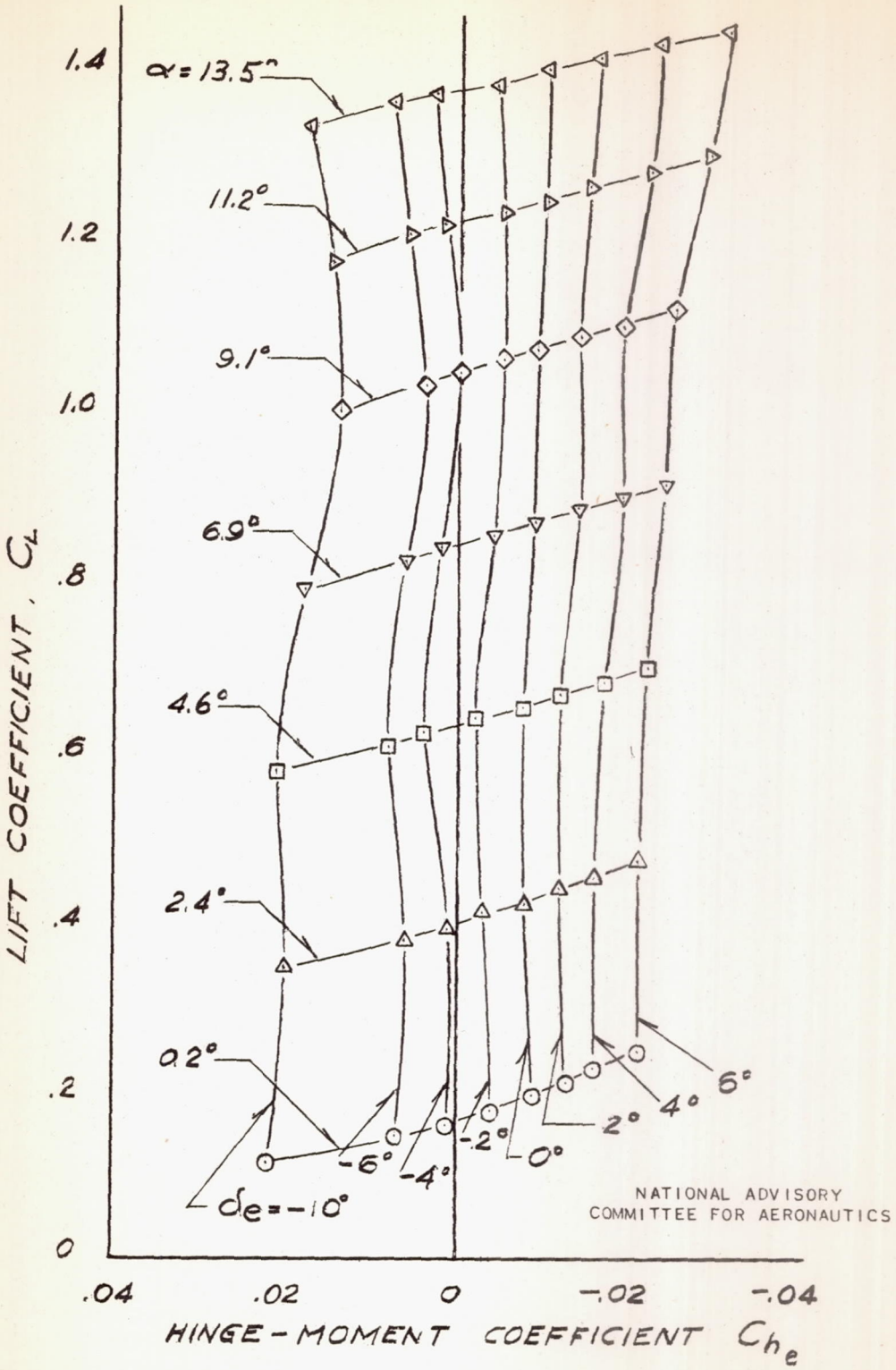

(b) C_{h_e} vs C_L

FIGURE 5. – CONCLUDED

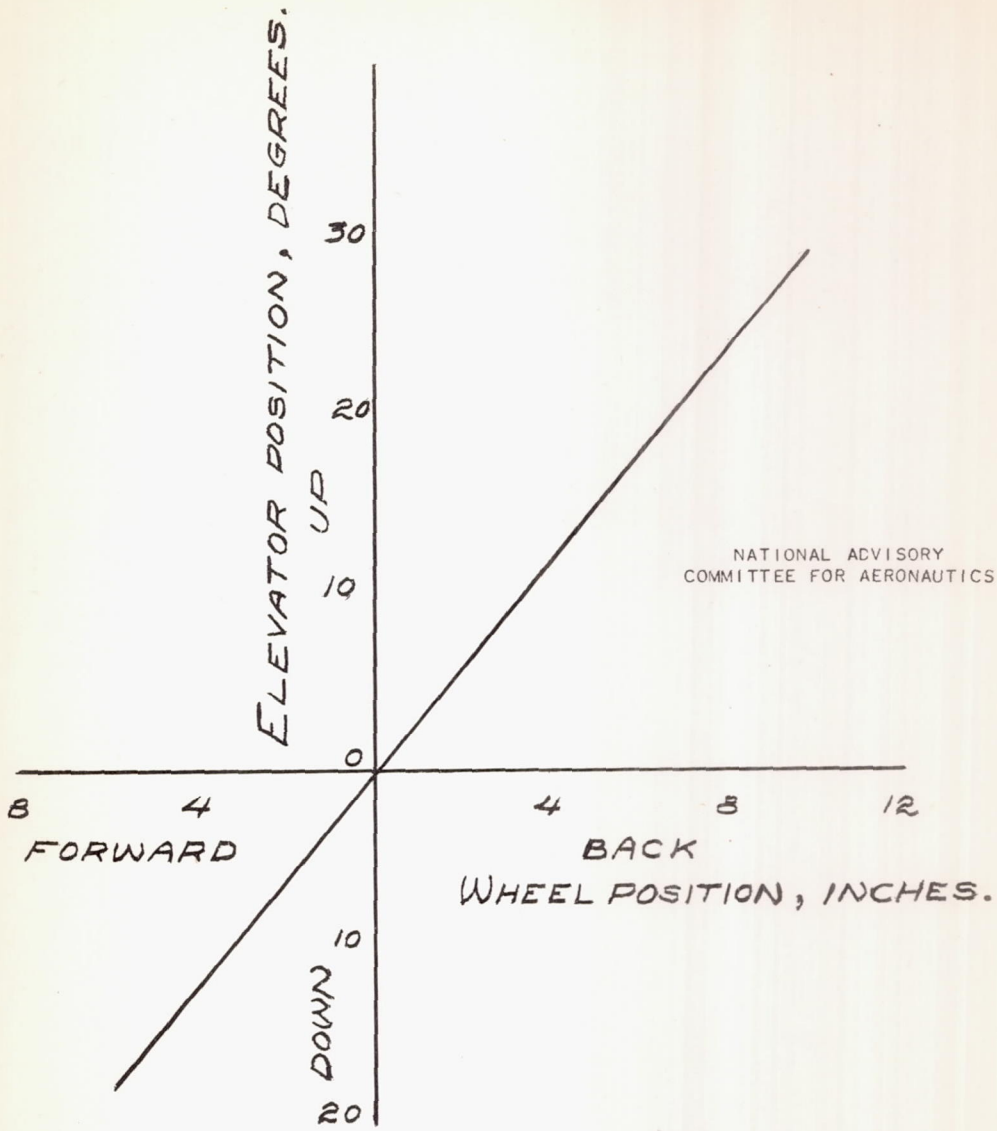

FIGURE 6.- VARIATION OF ELEVATOR POSITION WITH CONTROL WHEEL POSITION.

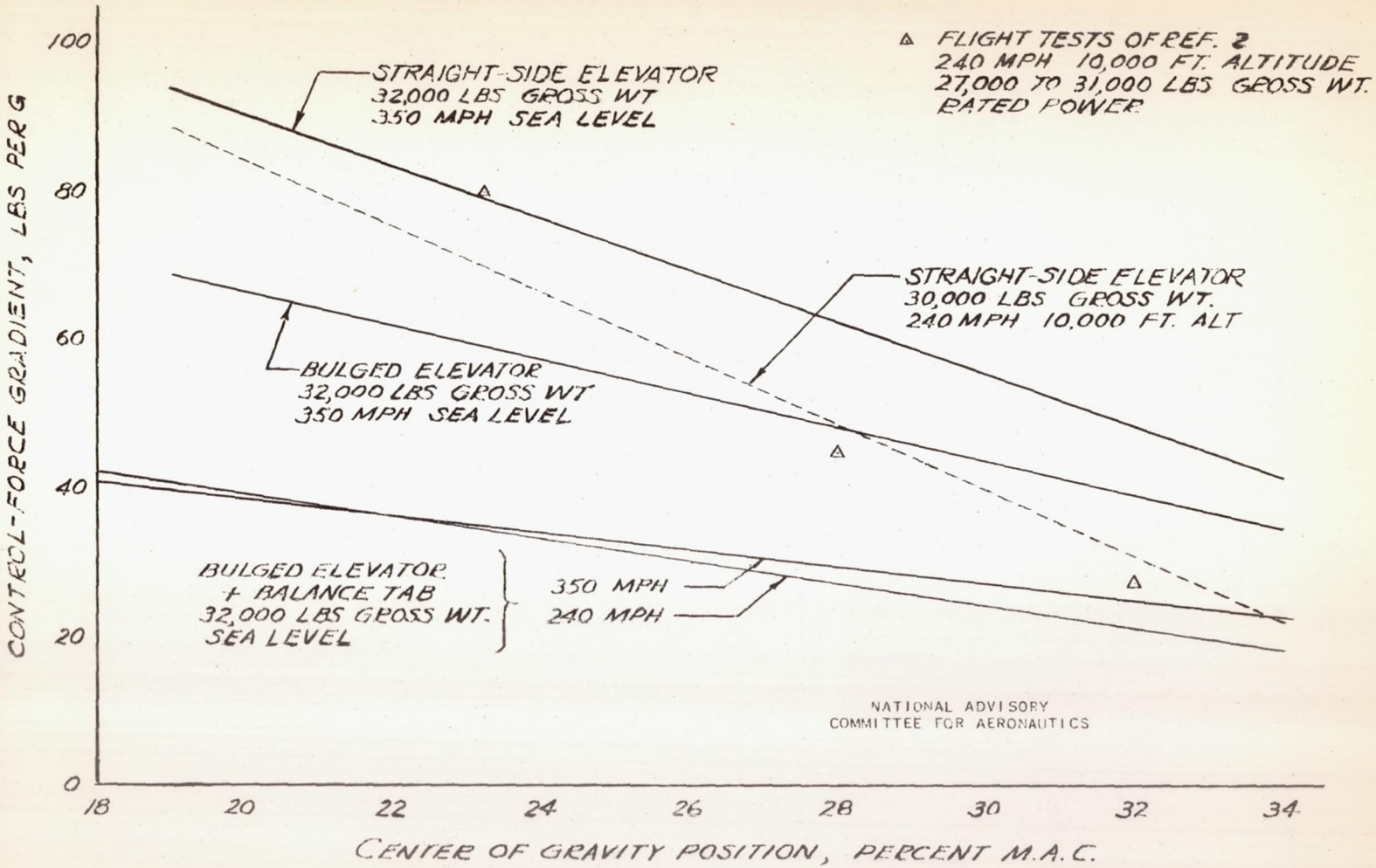

FIGURE 7.- EFFECT OF SEVERAL ELEVATOR CONFIGURATIONS ON THE VARIATION OF CONTROL-FORCE GRADIENT WITH CENTER-OF-GRAVITY POSITION FOR 3G IN STEADY TURNING FLIGHT

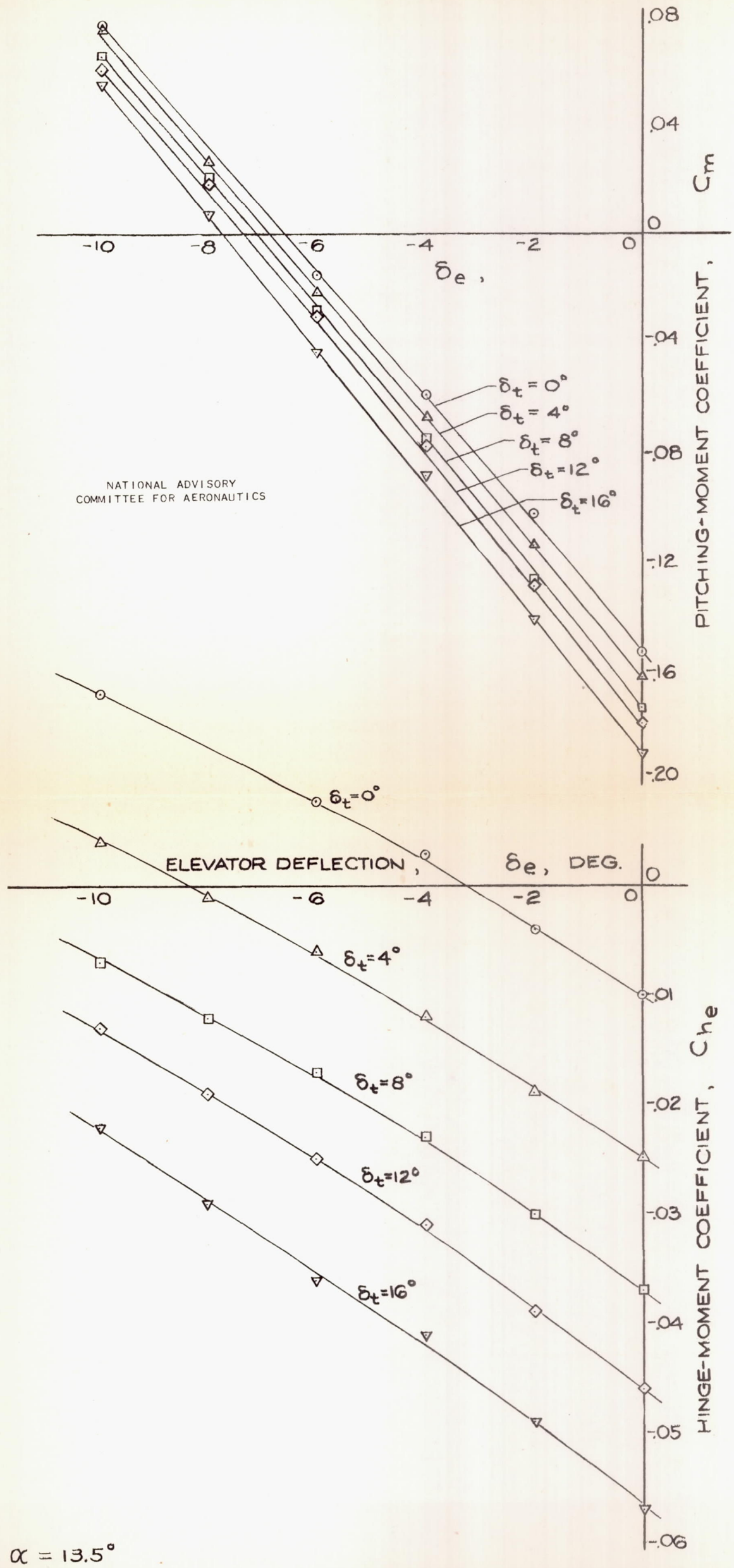

(a). $\alpha = 13.5°$

FIGURE 8:- EFFECT OF VARIOUS TAB ANGLES ON PITCHING MOMENT AND HINGE MOMENT. BULGED ELEVATOR WITH SEALED TAB.

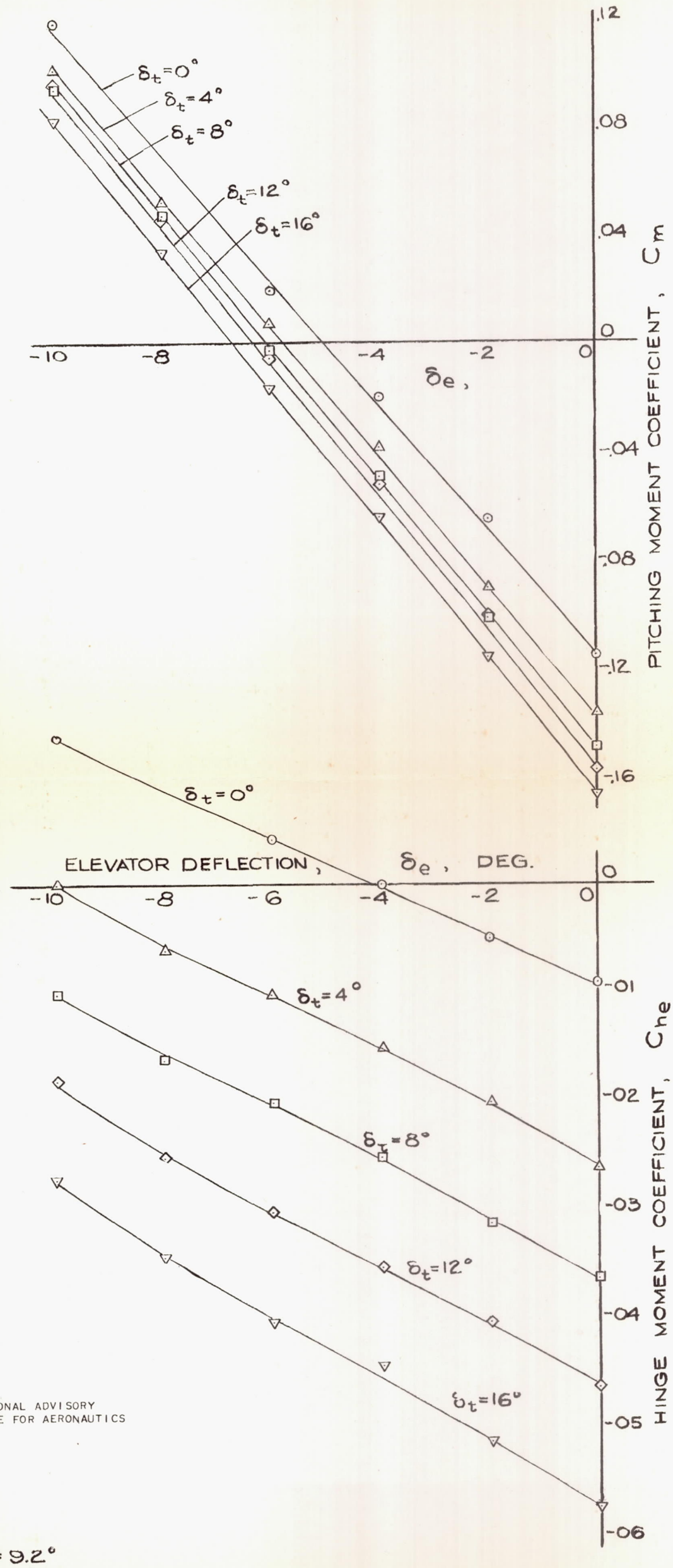

NATIONAL ADVISORY
COMMITTEE FOR AERONAUTICS

(b.) $\alpha = 9.2°$

FIGURE 8 :- CONTINUED.

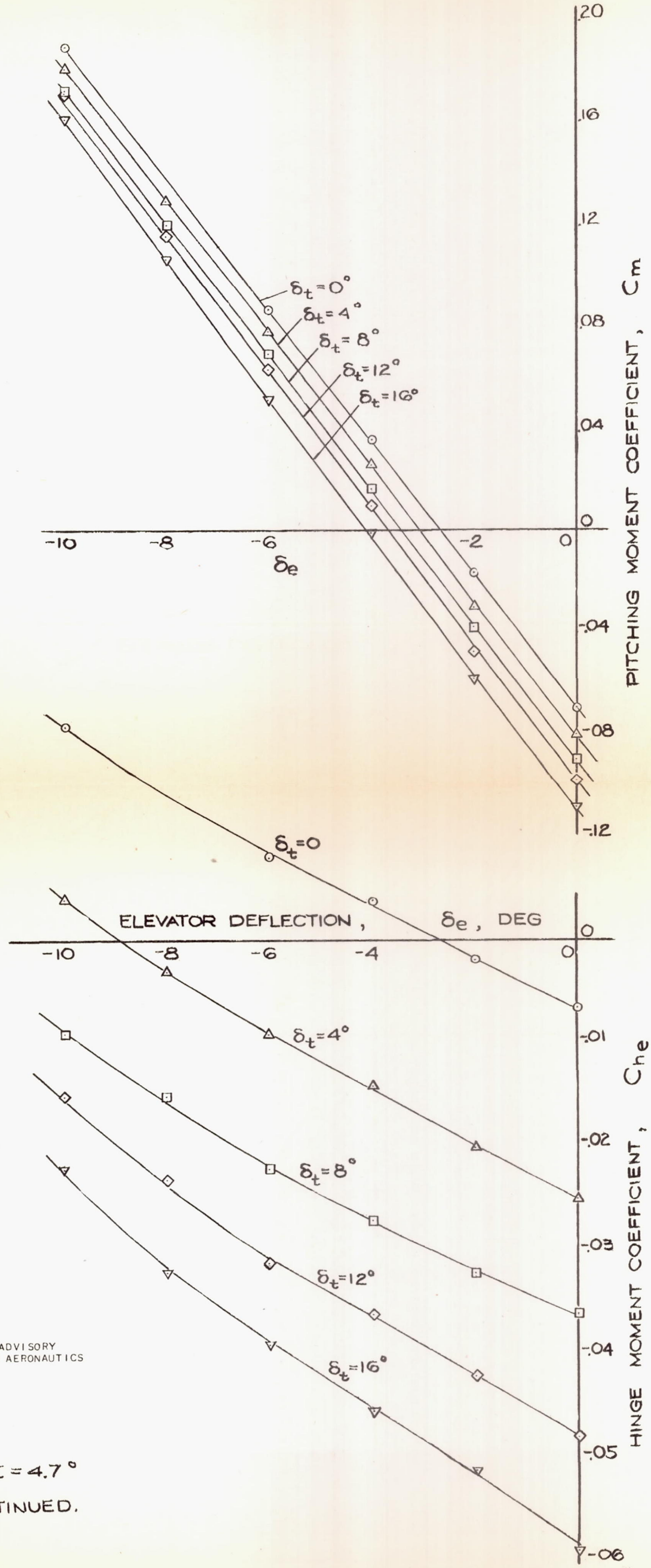

NATIONAL ADVISORY
COMMITTEE FOR AERONAUTICS

(c) $\alpha = 4.7°$

FIGURE 8 - CONTINUED.

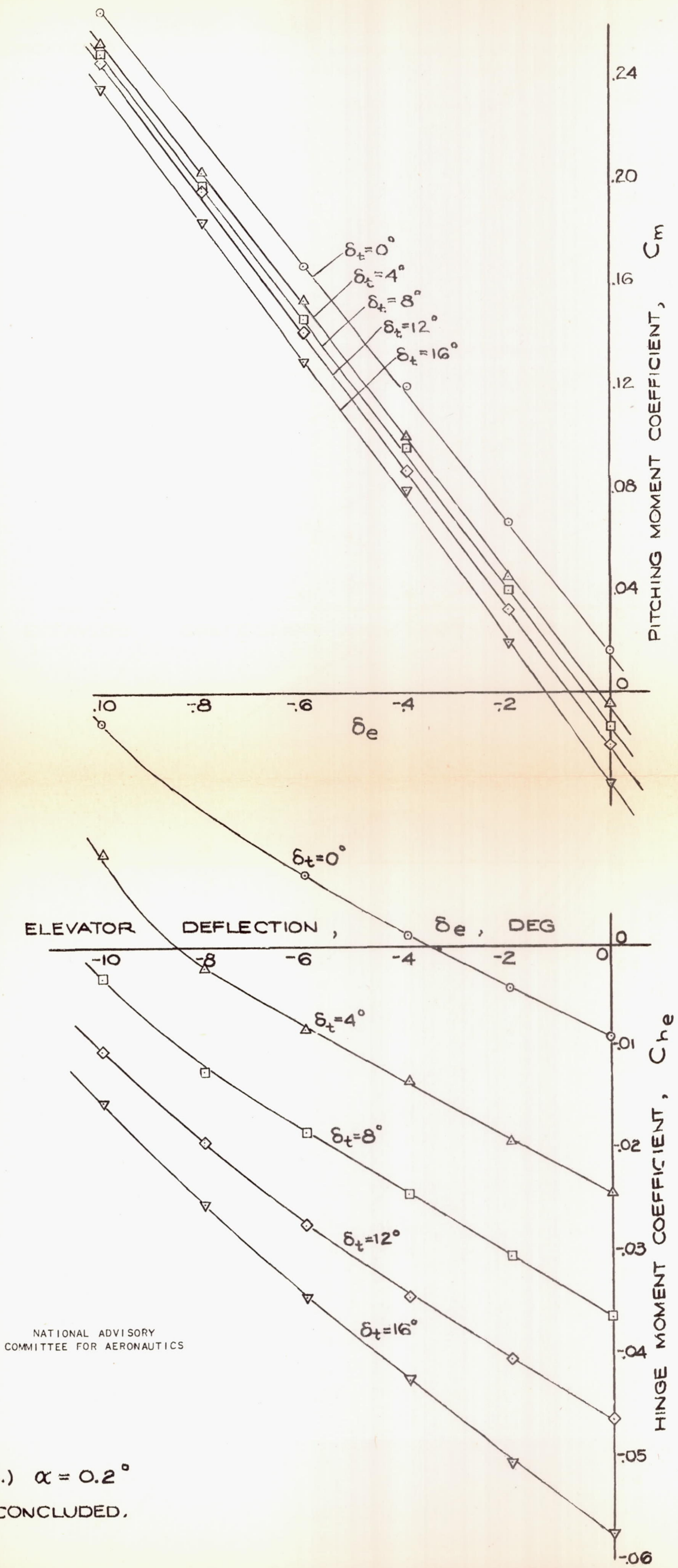

NATIONAL ADVISORY
COMMITTEE FOR AERONAUTICS

(d.) $\alpha = 0.2°$

FIGURE 8:- CONCLUDED.

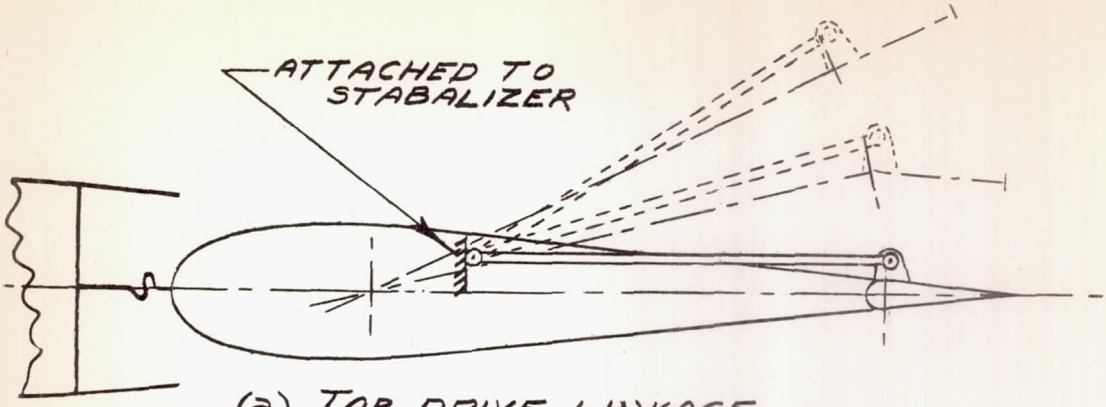

(a) TAB DRIVE LINKAGE.

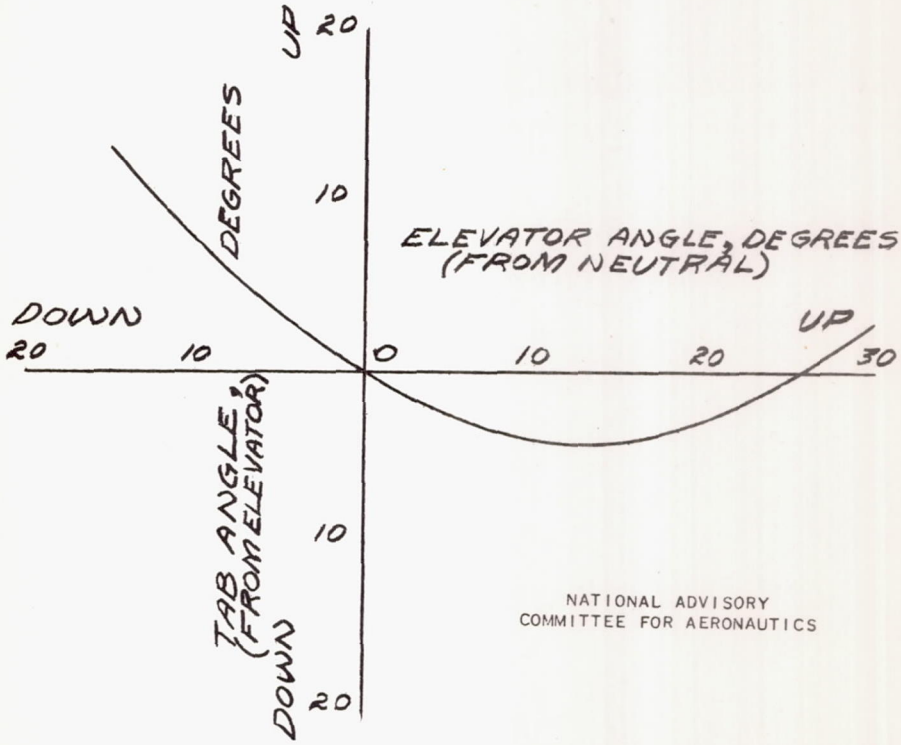

(b) VARIATION OF TAB POSITION WITH ELEVATOR POSITION.

FIGURE 9.- VARIABLE MOTION ELEVATOR BALANCE TAB.

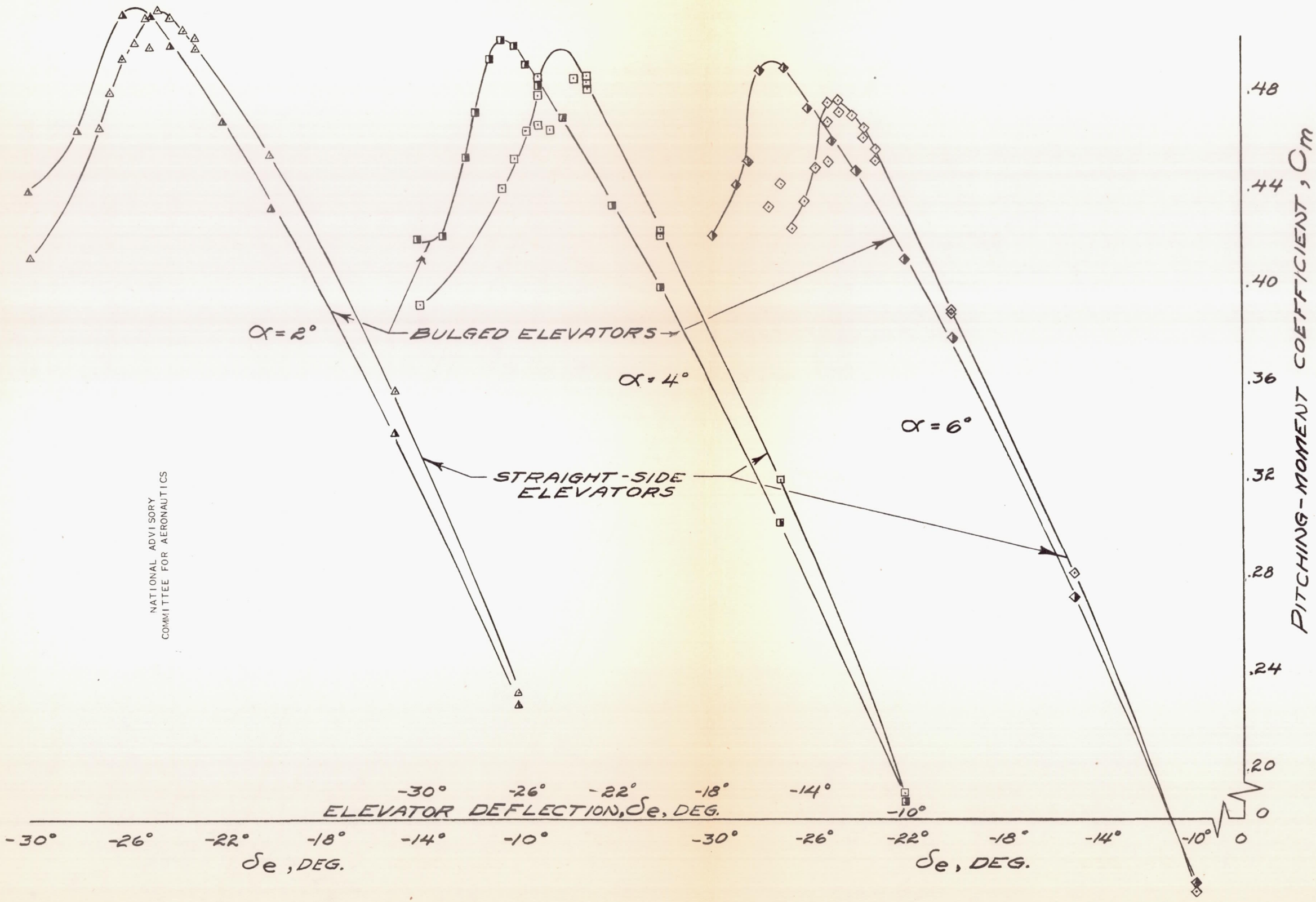

FIGURE 10.- COMPARISON OF ELEVATOR EFFECTIVENESS OF STRAIGHT-SIDED AND BULGED ELEVATORS AT HIGH DEFLECTIONS FOR SEVERAL ANGLES OF ATTACK.

NATIONAL ADVISORY
COMMITTEE FOR AERONAUTICS

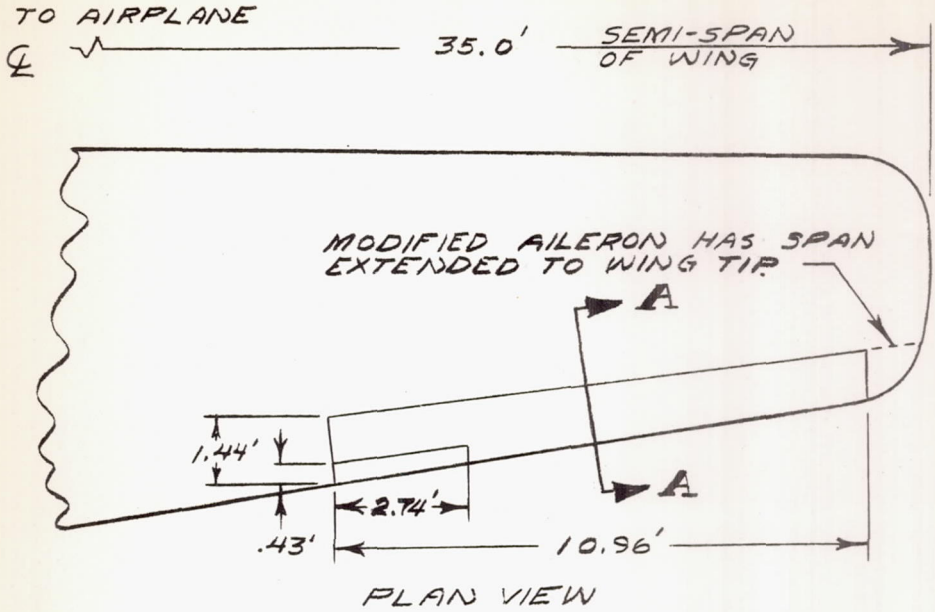

PLAN VIEW

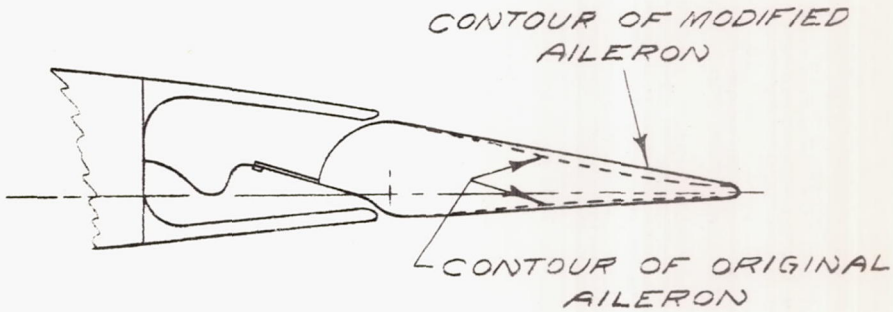

SECTION AT A-A ~ TYPICAL CROSS SECTION OF AILERON

NATIONAL ADVISORY
COMMITTEE FOR AERONAUTICS

FIGURE 11.- MODIFICATIONS TO AILERONS

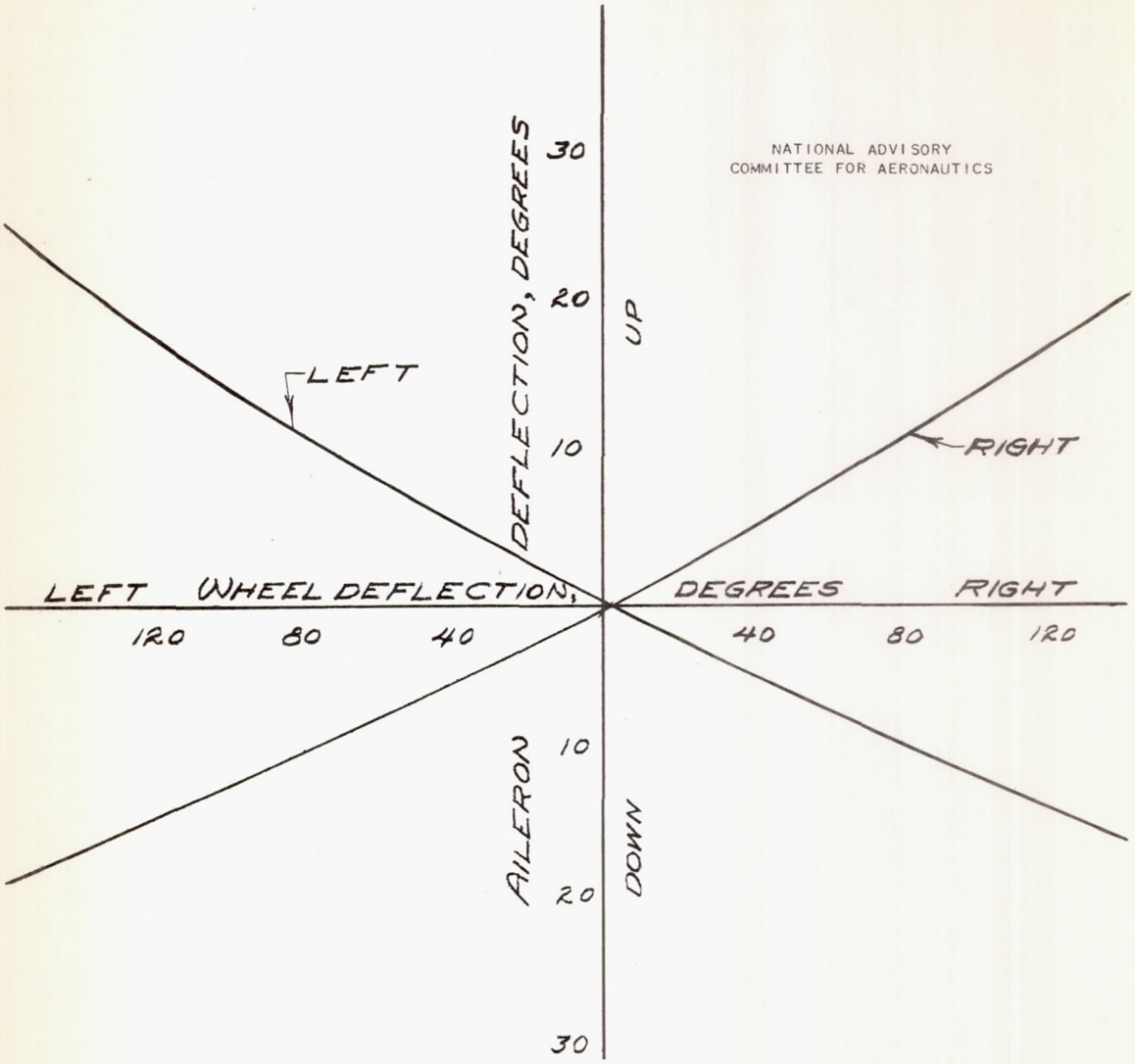

FIGURE 12.-VARIATION OF AILERON POSITION WITH CONTROL WHEEL POSITION

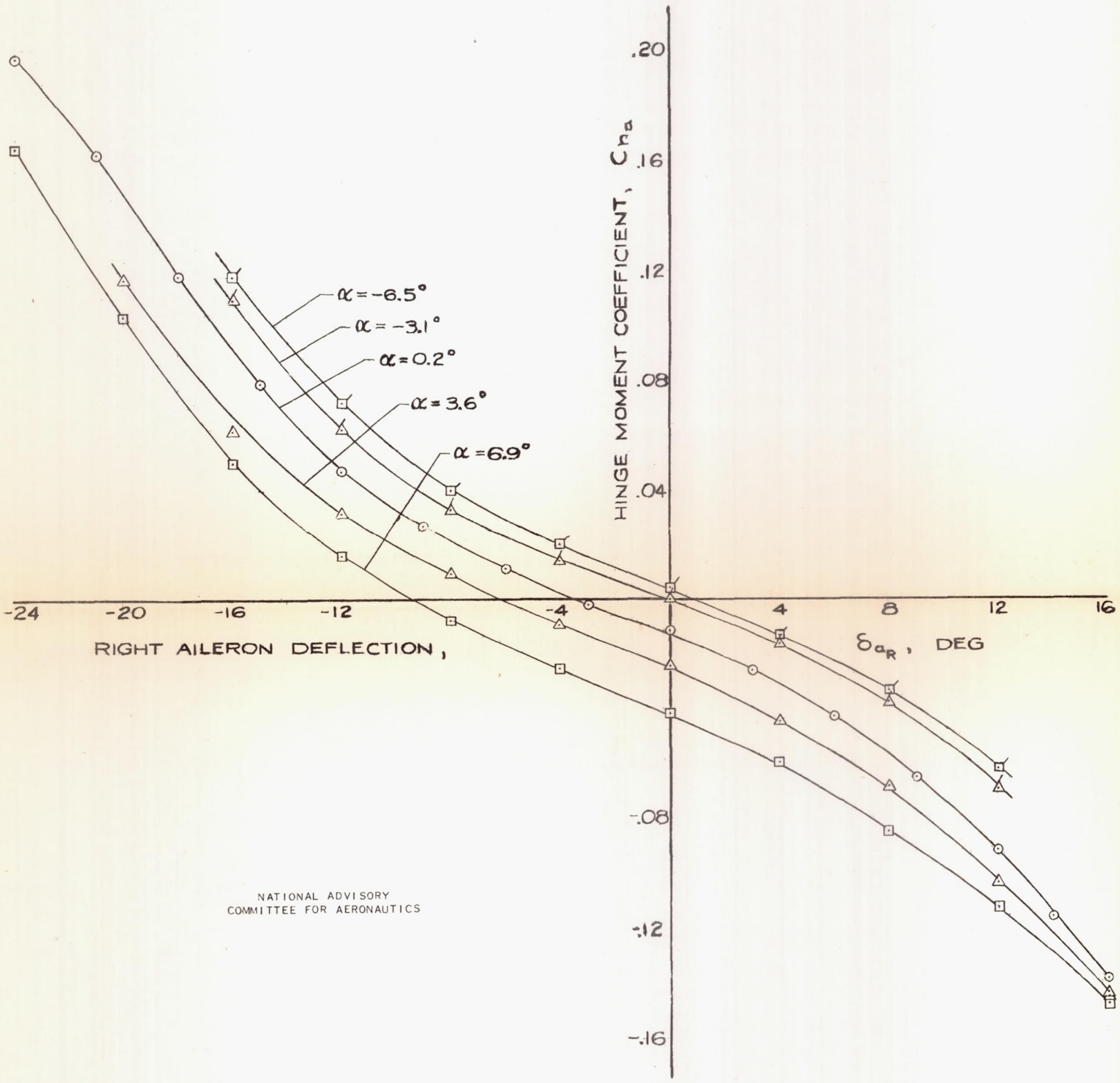

(a) C_{h_a} vs δ_{a_R}

FIGURE 13.- EFFECT OF AILERON DEFLECTION ON LATERAL CHARACTERISTICS WITH FLAPS UP. ORIGINAL AILERONS

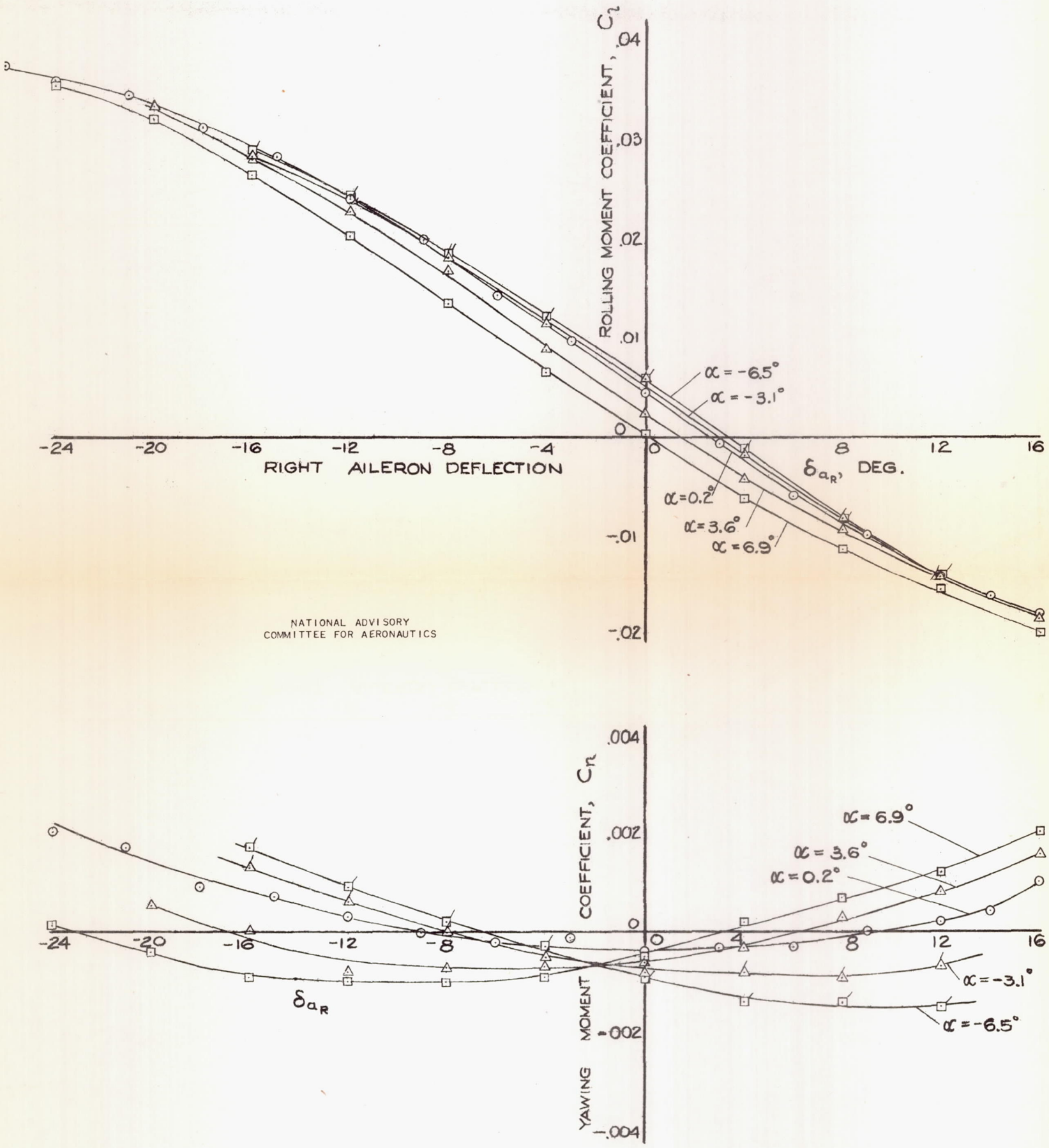

NATIONAL ADVISORY
COMMITTEE FOR AERONAUTICS

(b) C_l & C_n vs. δ_{a_R}

FIGURE 13:- CONCLUDED.

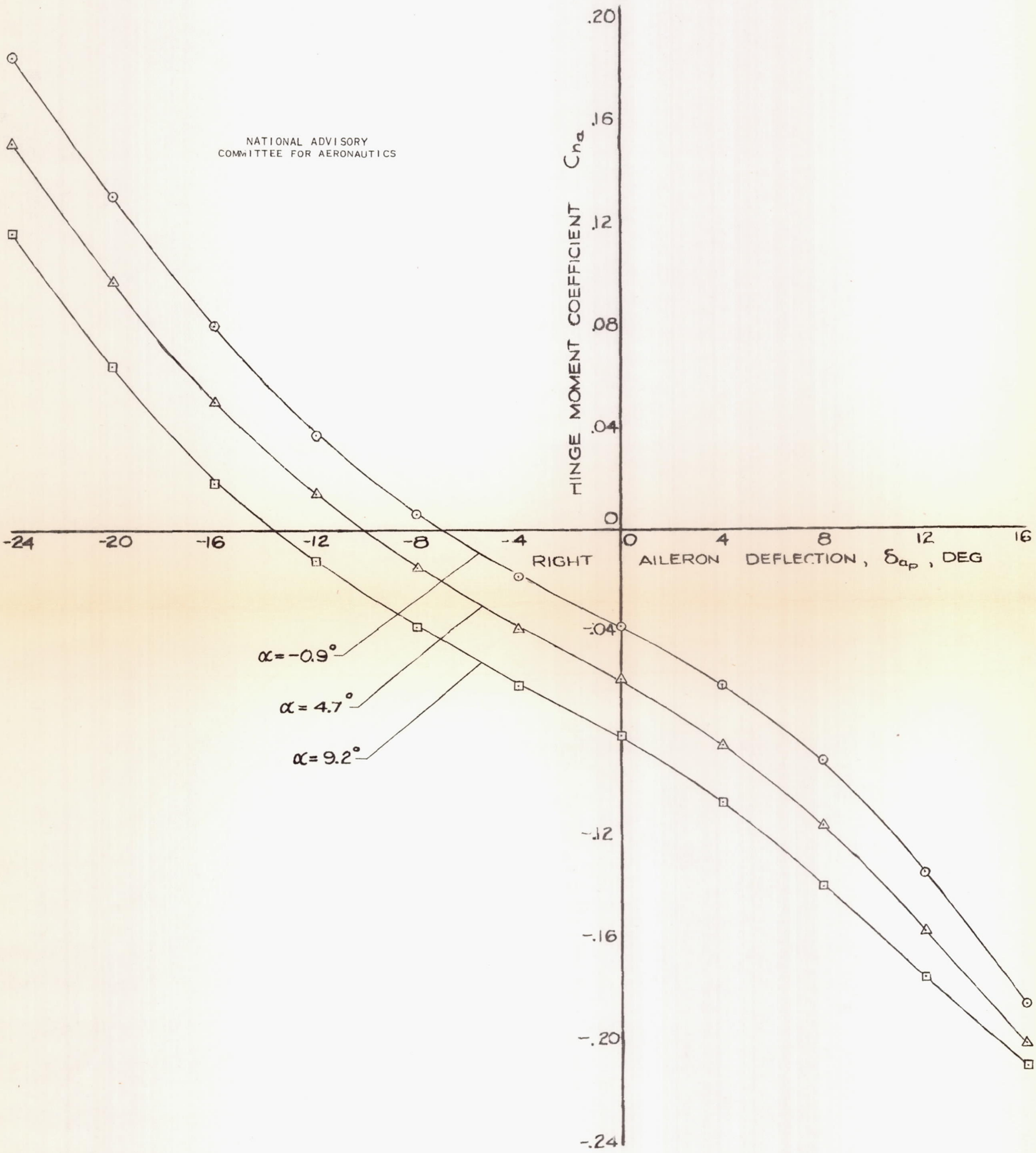

FIGURE 14.- EFFECT OF AILERON DEFLECTION ON LATERAL CHARACTERISTICS WITH FLAPS DEFLECTED 52°. ORIGINAL AILERONS.

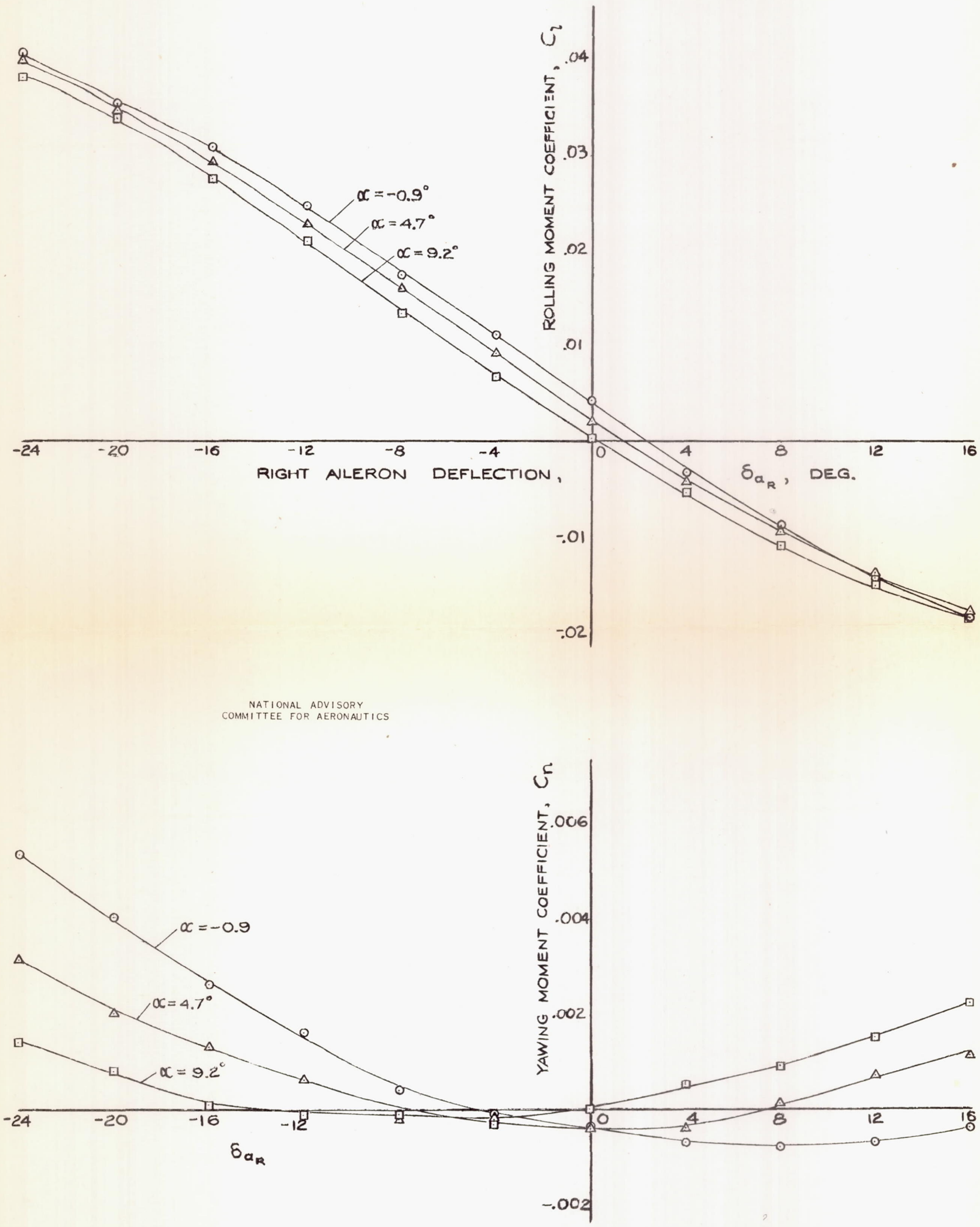

NATIONAL ADVISORY
COMMITTEE FOR AERONAUTICS

(b) C_l & C_n vs δ_{a_R}

FIGURE 14.- CONCLUDED.

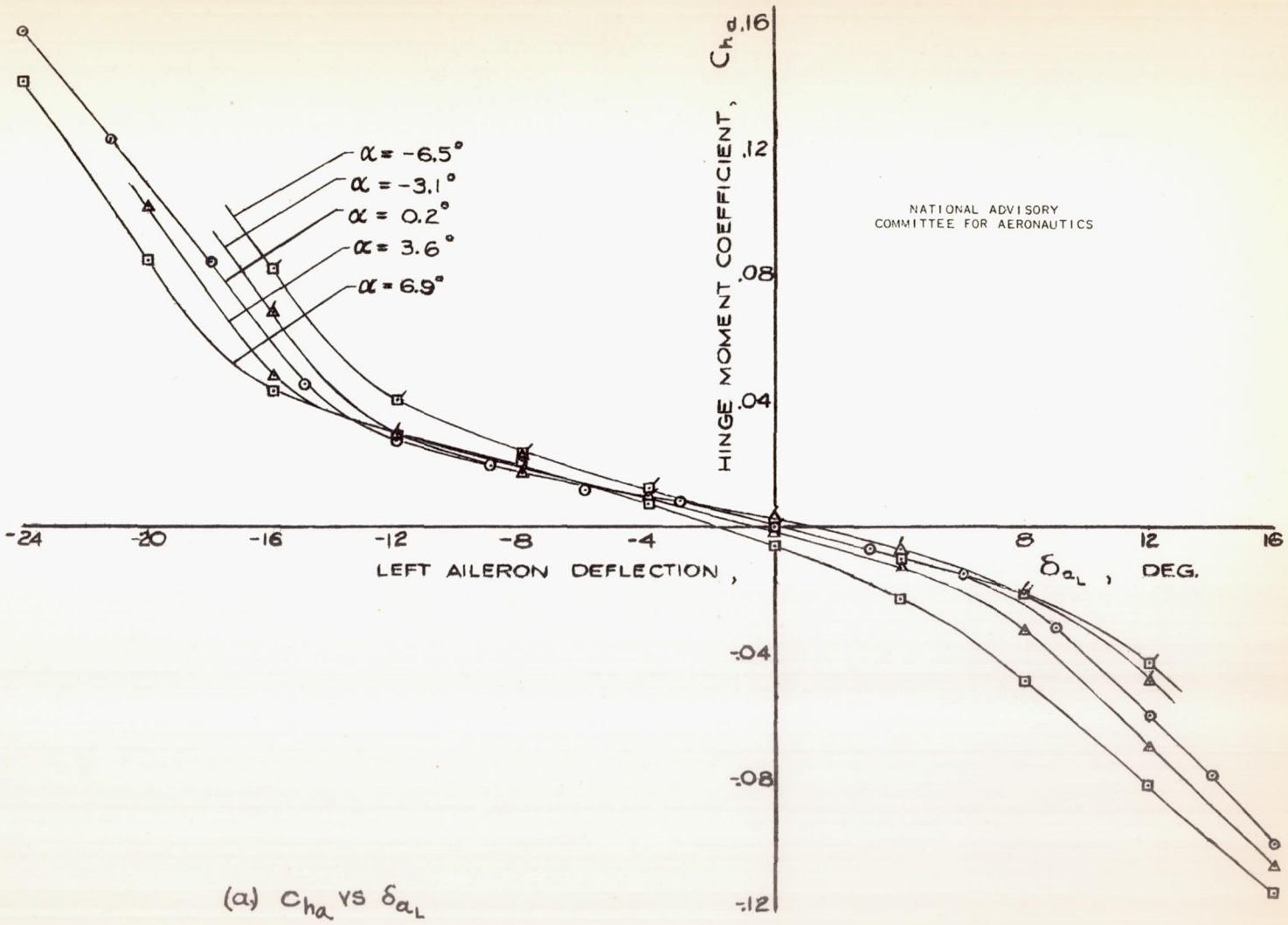

(a) C_{h_a} vs δ_{a_L}

FIGURE 15.- EFFECT OF AILERON DEFLECTION ON LATERAL CHARACTERISTICS WITH FLAPS UP. MODIFIED AILERONS.

NATIONAL ADVISORY
COMMITTEE FOR AERONAUTICS

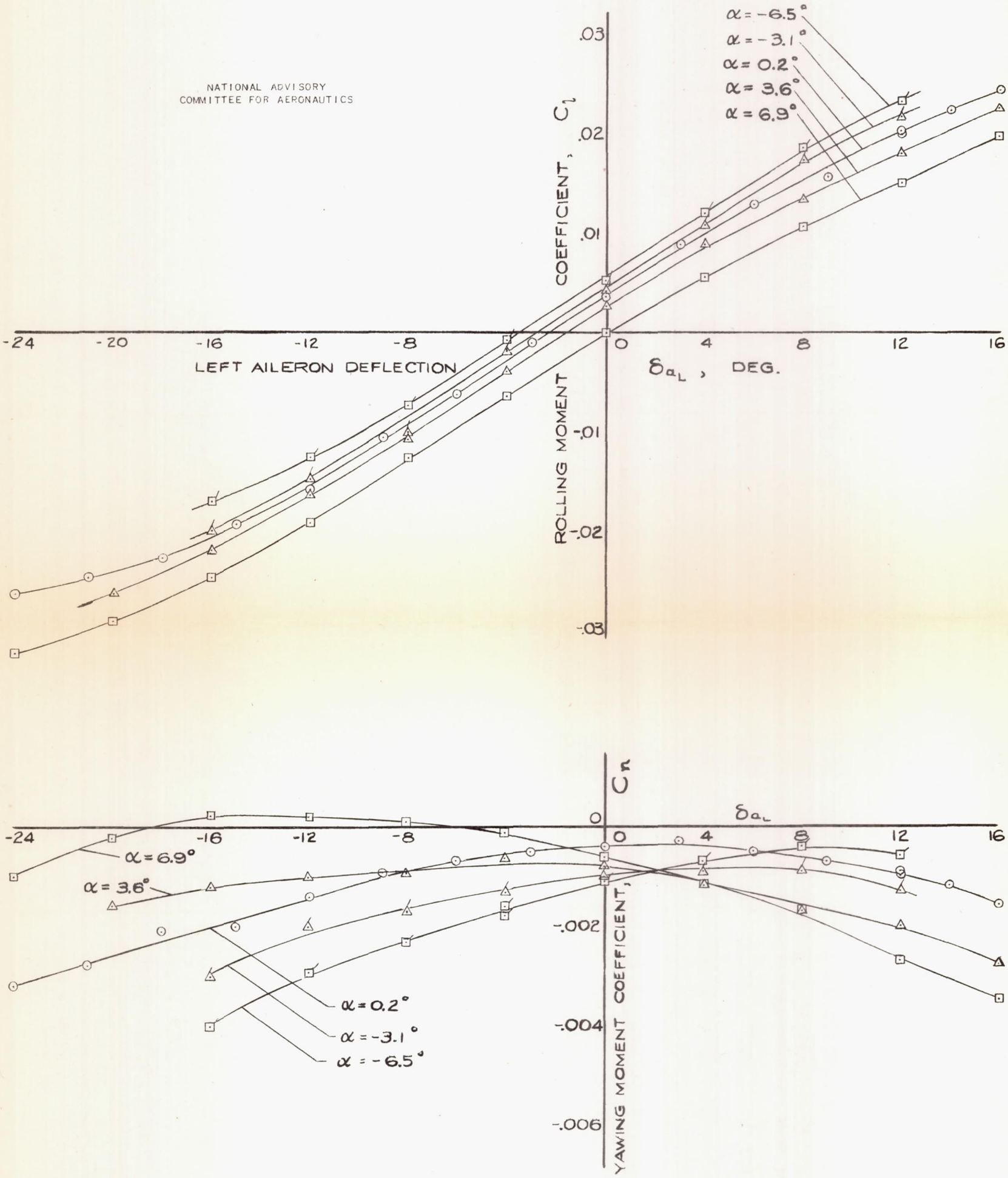

(b) C_l & C_n vs δ_{a_L}

FIGURE 15.- CONCLUDED.

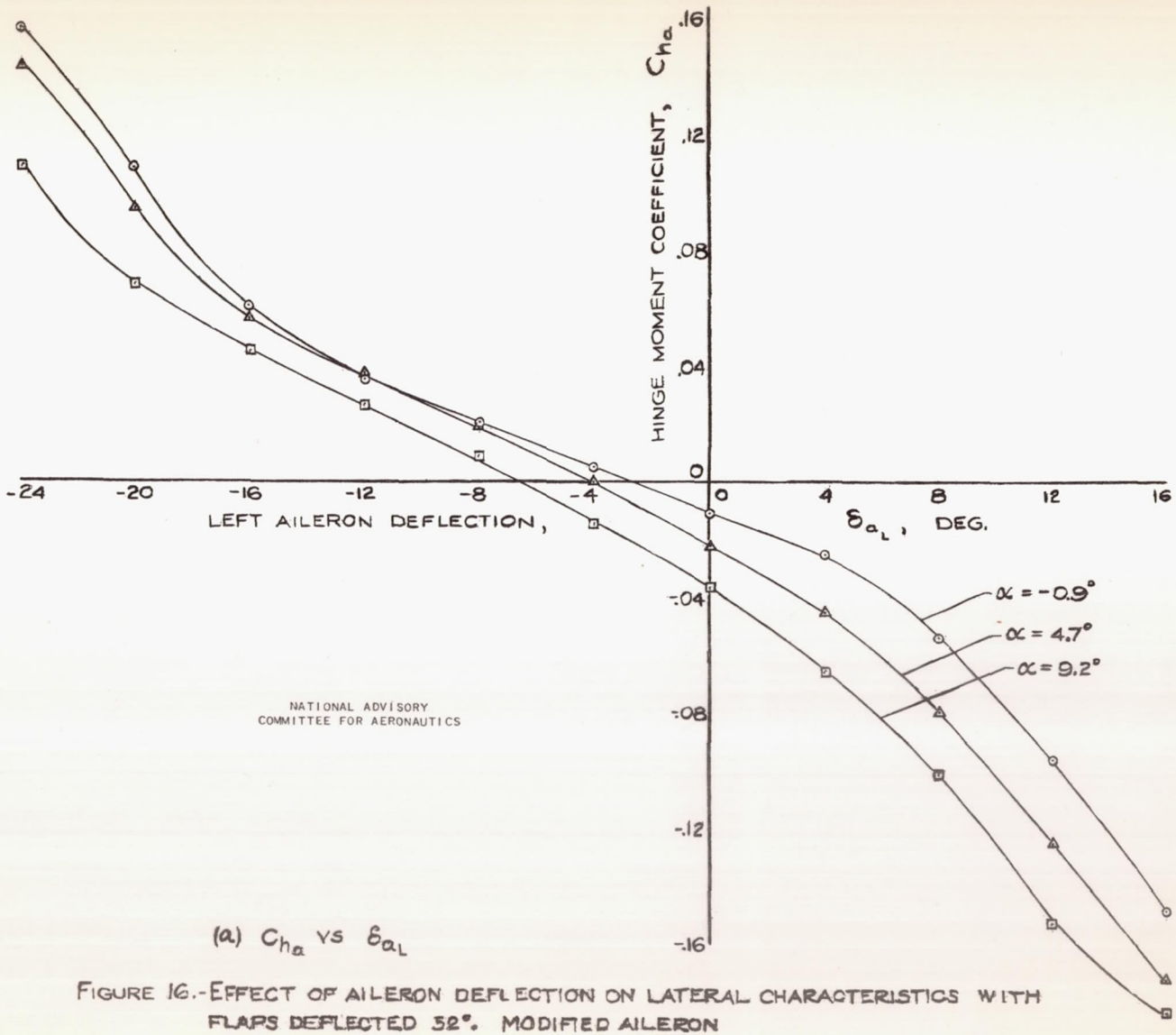

(a) C_{h_a} vs δ_{a_L}

FIGURE 16.-EFFECT OF AILERON DEFLECTION ON LATERAL CHARACTERISTICS WITH FLAPS DEFLECTED 52°. MODIFIED AILERON

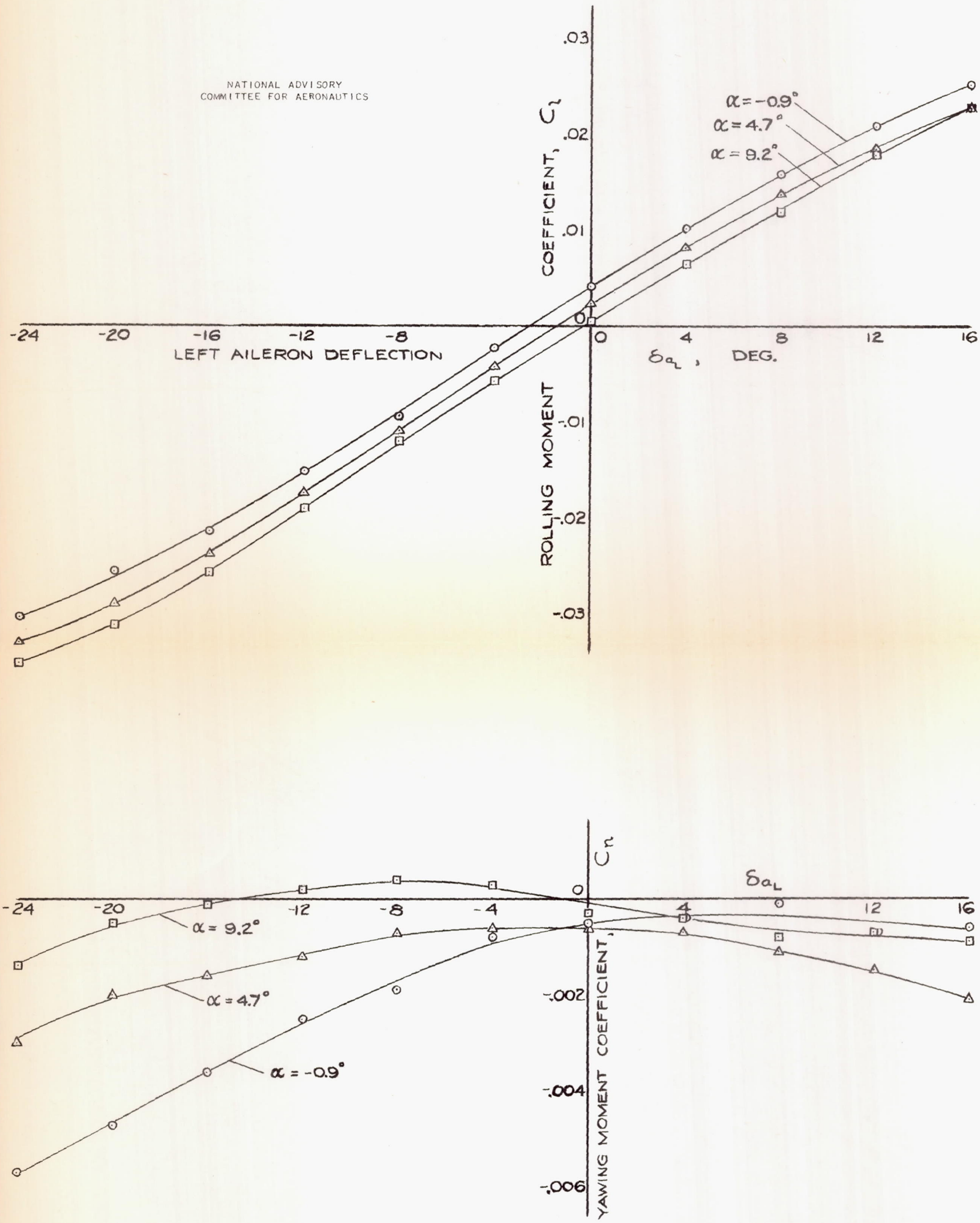

(b) C_l & C_n vs δ_{a_L}

FIGURE 16:- CONCLUDED.

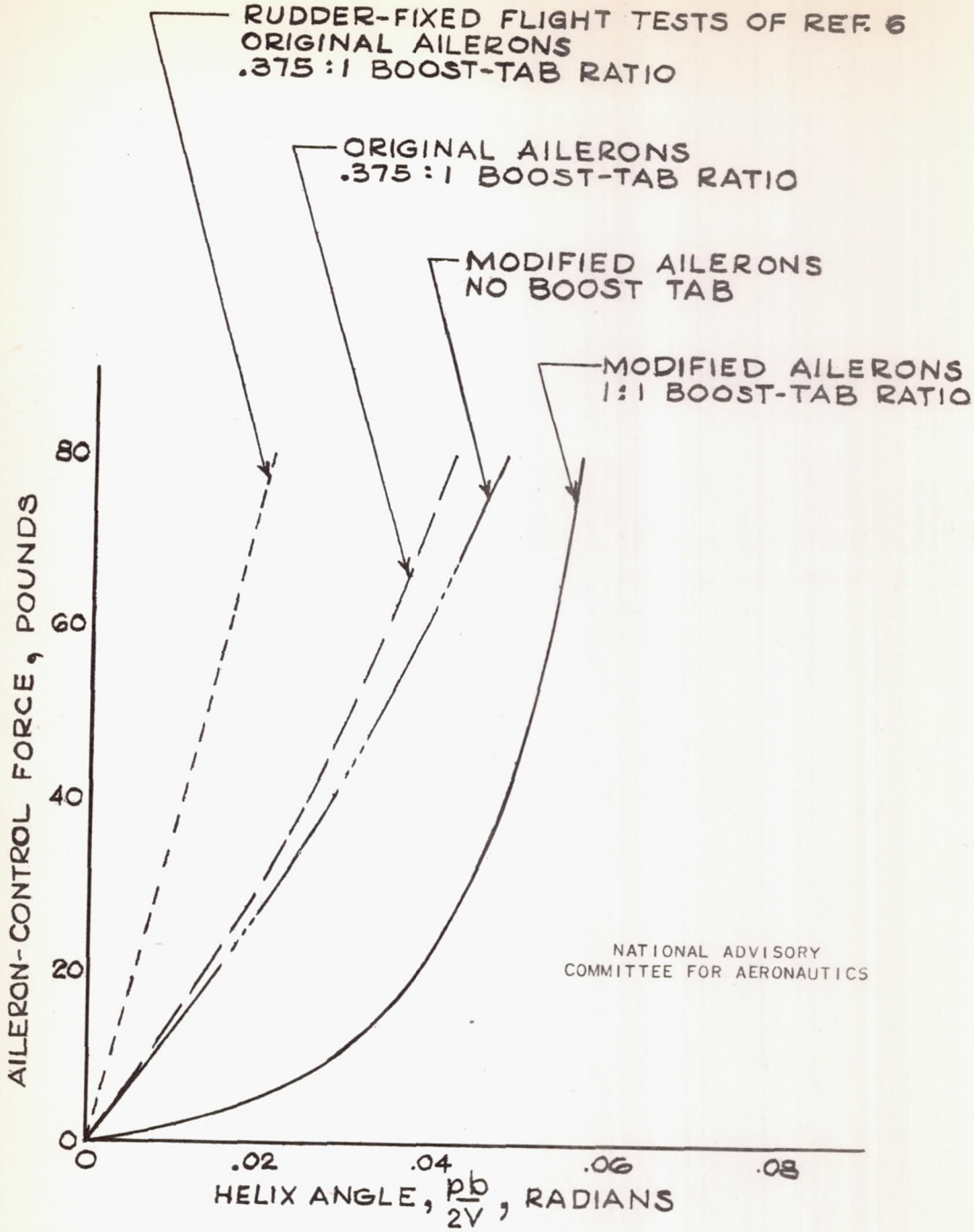

FIGURE 17.- EFFECT OF SEVERAL AILERON CONFIGURATIONS ON THE VARIATION OF WHEEL FORCE WITH $\frac{pb}{2V}$ AT 350 MILES PER HOUR INDICATED AIRSPEED.

NOTE: $\frac{pb}{2V}$ VALUES TO THE RIGHT OF THE BREAK IN THE FLAPS-UP CURVES ARE LIMITED BY AN 80 POUND CONTROL FORCE; OTHER VALUES ARE LIMITED BY THE MAXIMUM DEFLECTION NOTED ON THE CURVE.

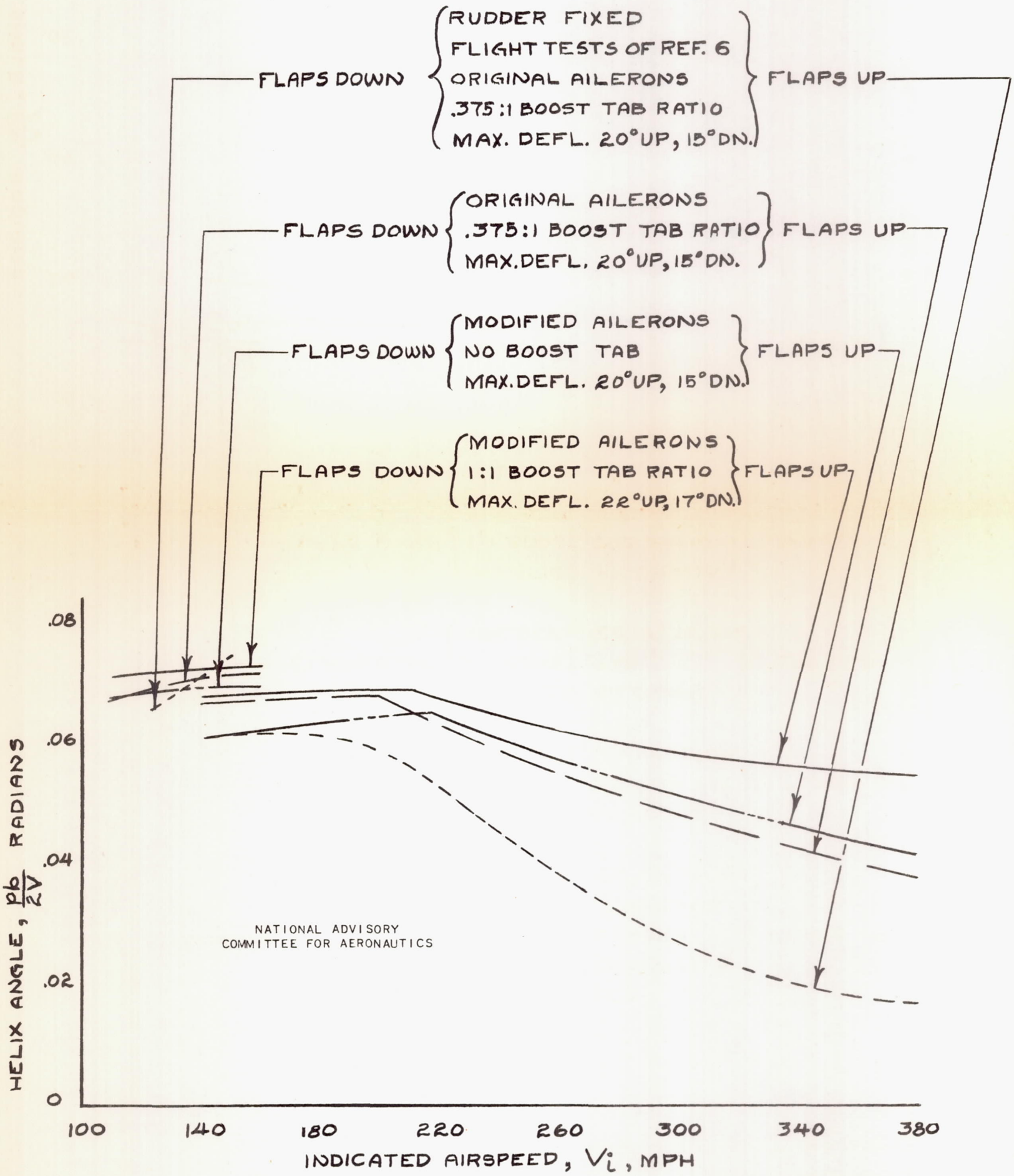

FIGURE 18.- EFFECT OF SEVERAL AILERON CONFIGURATIONS ON THE VARIATION OF $\frac{pb}{2V}$ WITH AIRSPEED.

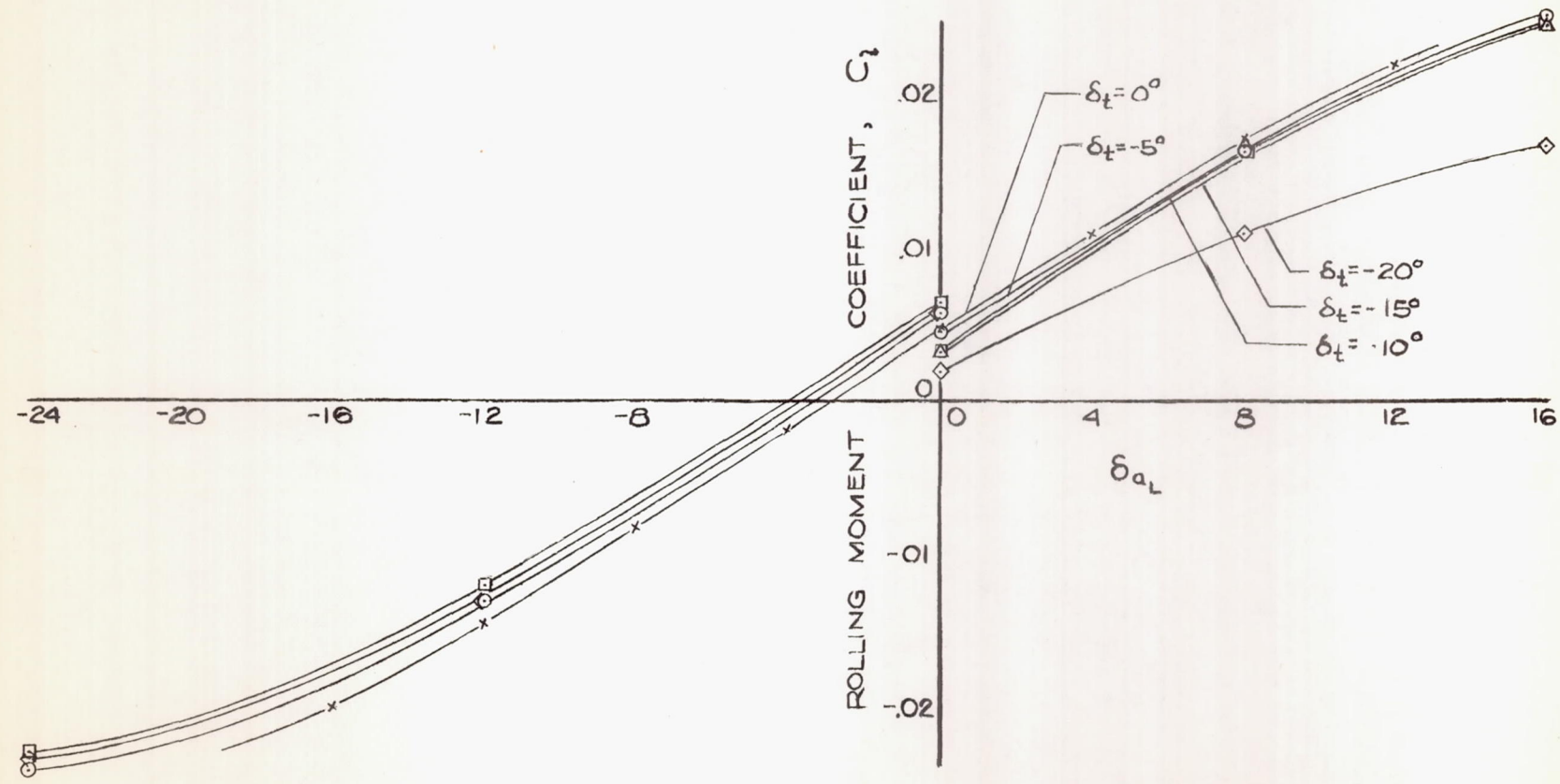

NATIONAL ADVISORY
COMMITTEE FOR AERONAUTICS

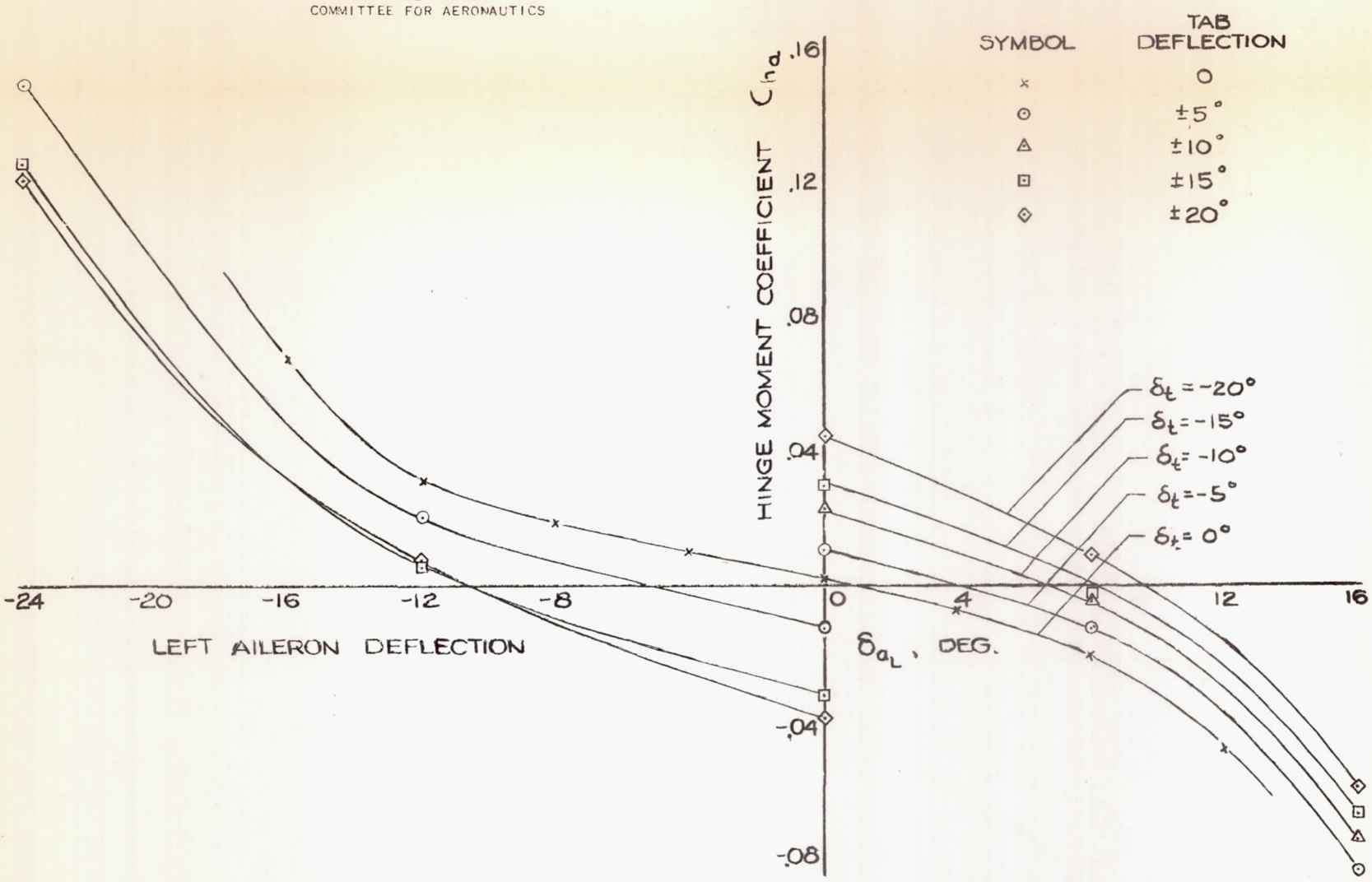

(a.) $\alpha = -3.1°$

FIGURE 19.- EFFECT OF VARIOUS TAB ANGLES ON THE ROLLING MOMENTS AND HINGE MOMENTS OF THE MODIFIED AILERON. FLAPS UP.

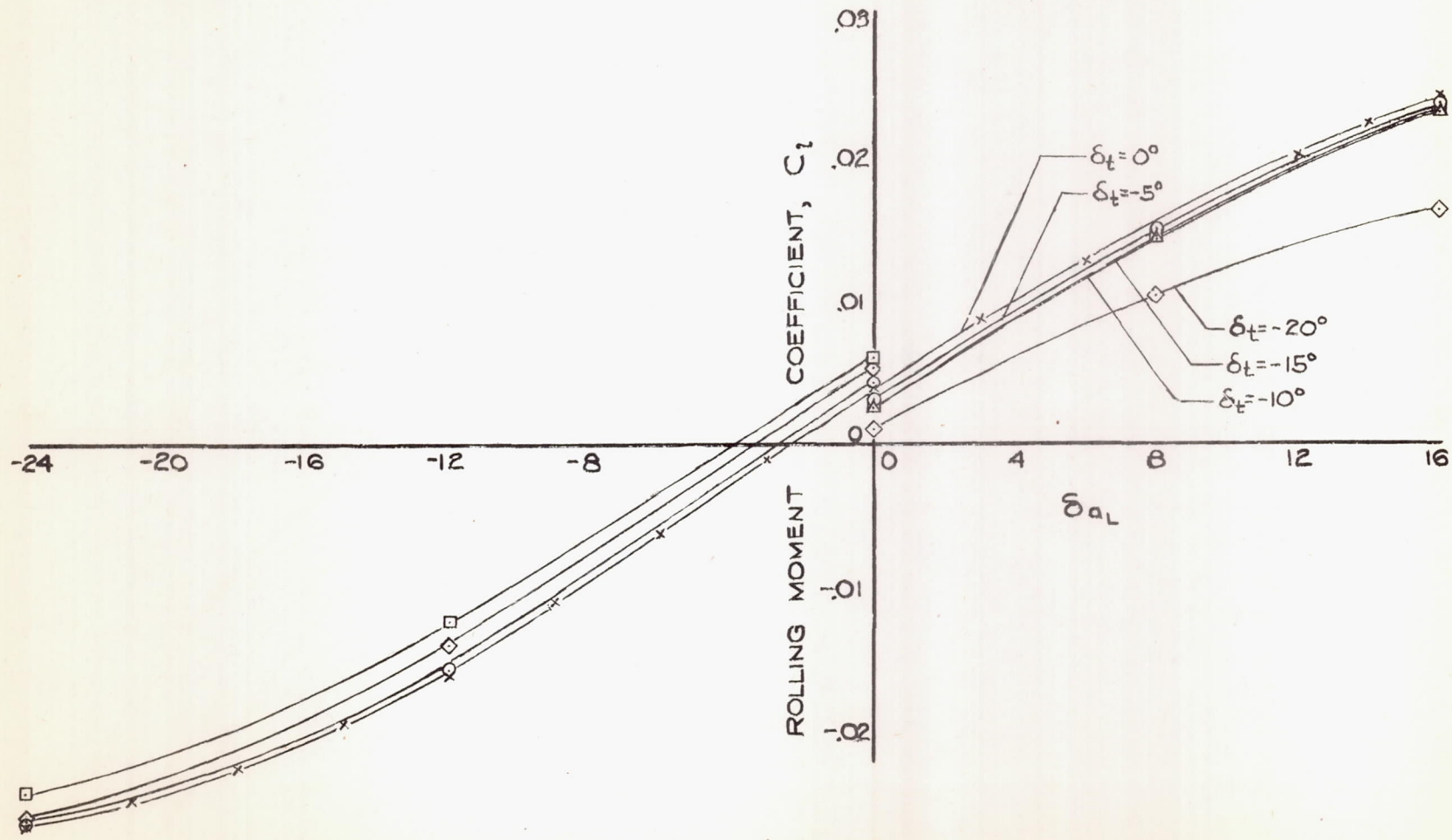

NATIONAL ADVISORY
COMMITTEE FOR AERONAUTICS

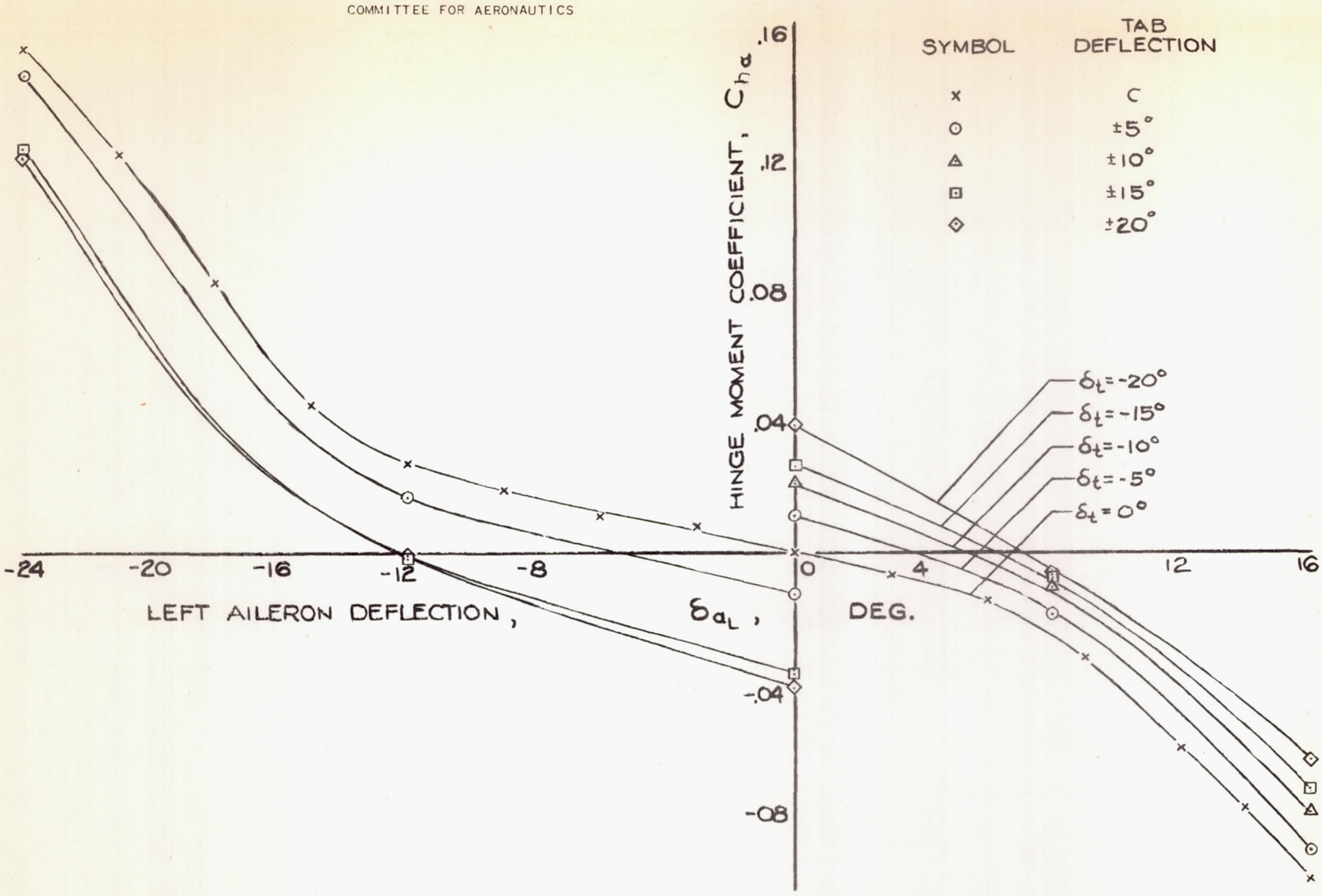

(b.) $\alpha = 0.2°$

FIGURE 19.- CONTINUED.

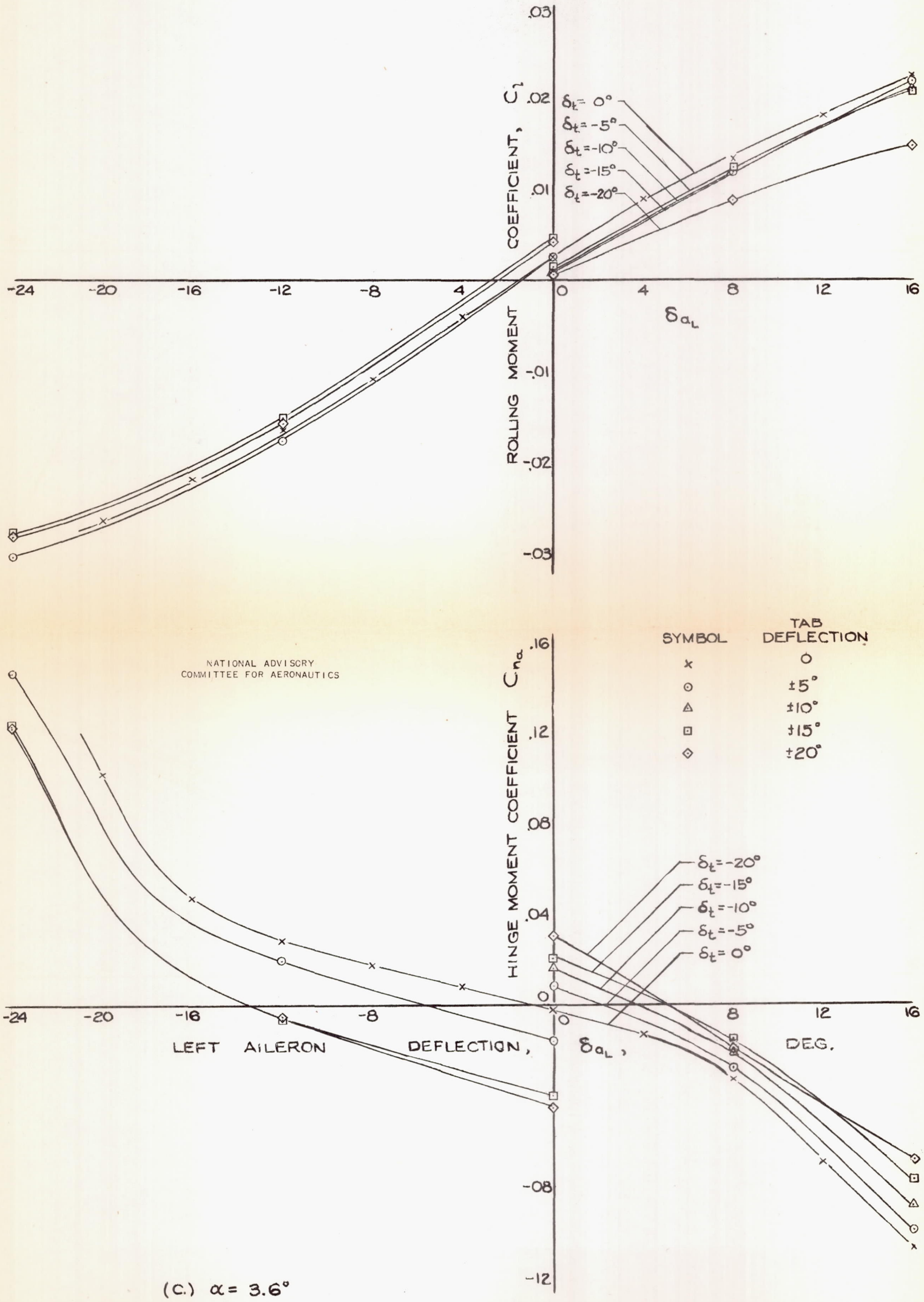

NATIONAL ADVISORY
COMMITTEE FOR AERONAUTICS

(C.) $\alpha = 3.6°$

FIGURE 19.- CONTINUED.

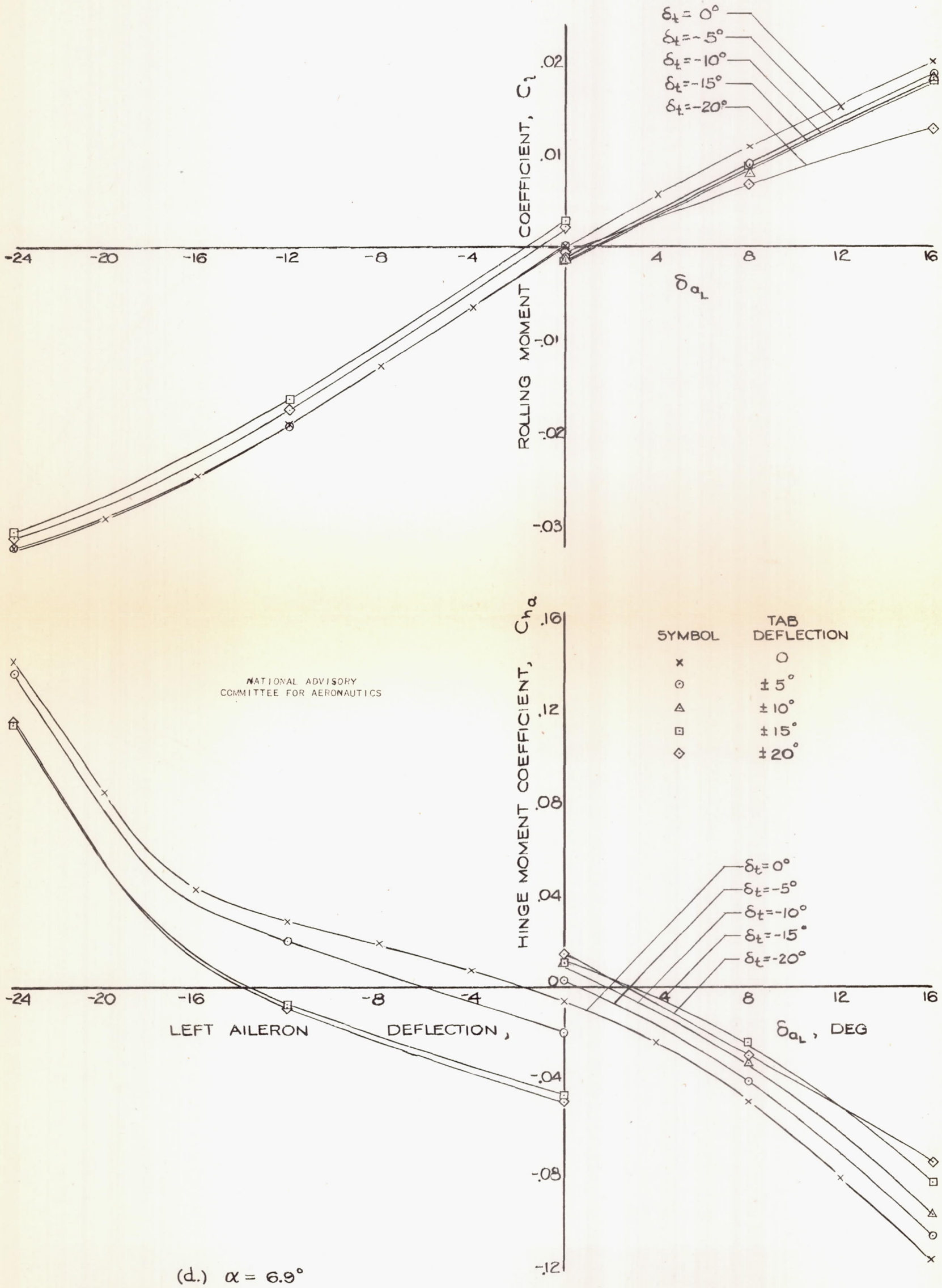

(d.) $\alpha = 6.9°$

FIGURE 19.- CONCLUDED.

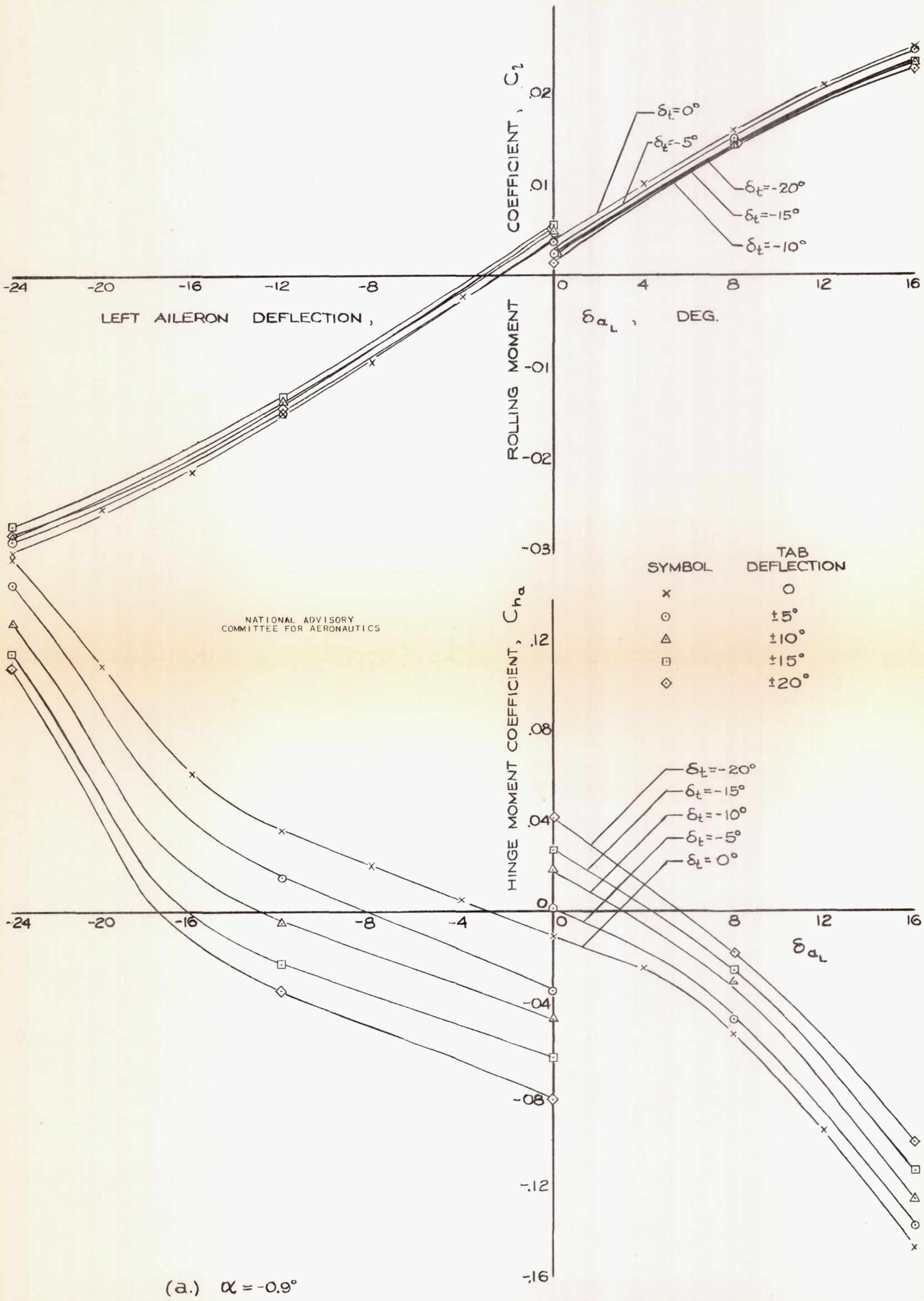

(a.) $\alpha = -0.9°$

FIGURE 20:- EFFECT OF VARIOUS TAB ANGLES ON THE ROLLING MOMENTS AND HINGE MOMENTS OF THE MODIFIED AILERON.
FLAPS DEFLECTED 52°

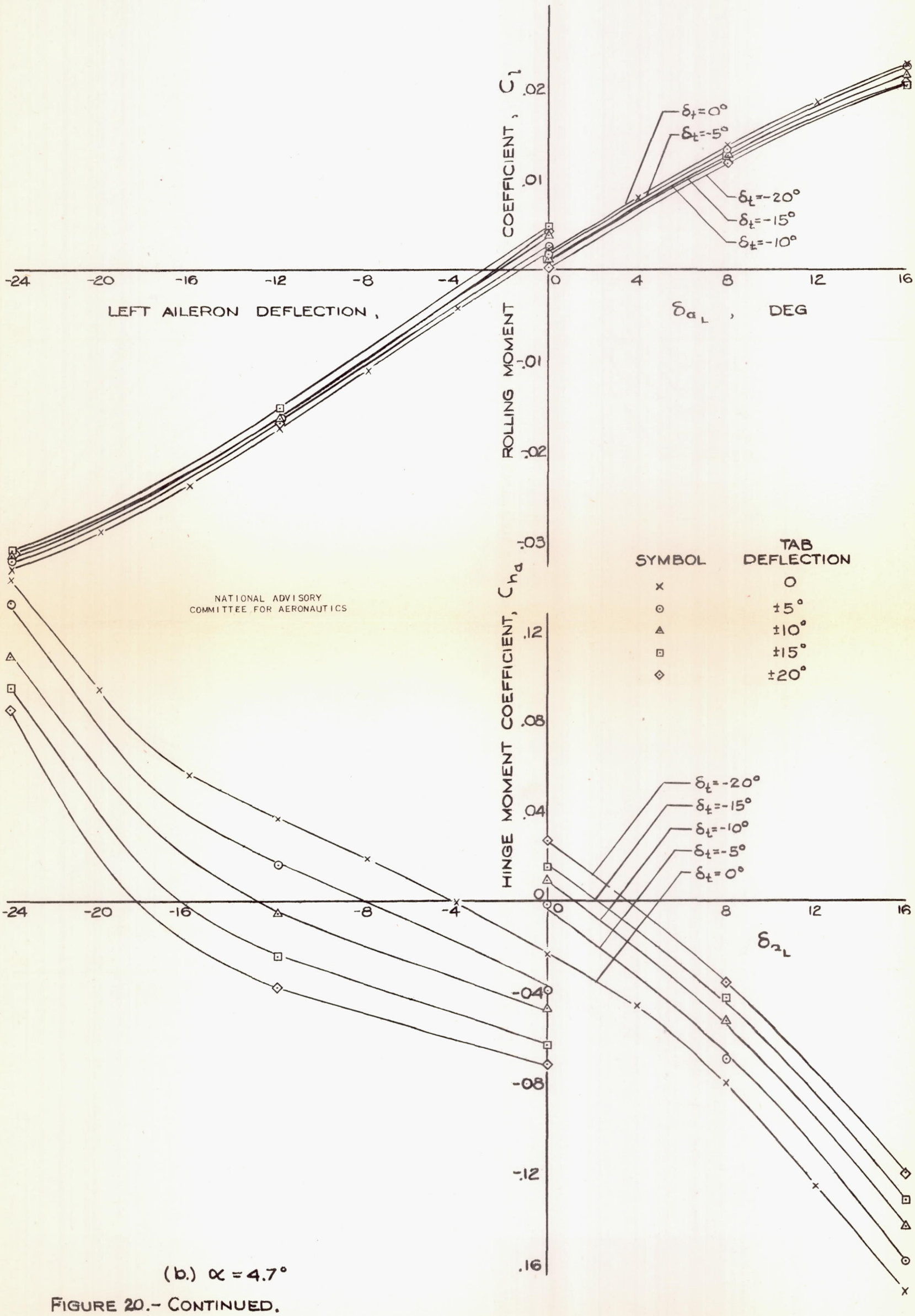

(b.) $\alpha = 4.7°$

FIGURE 20.- CONTINUED.

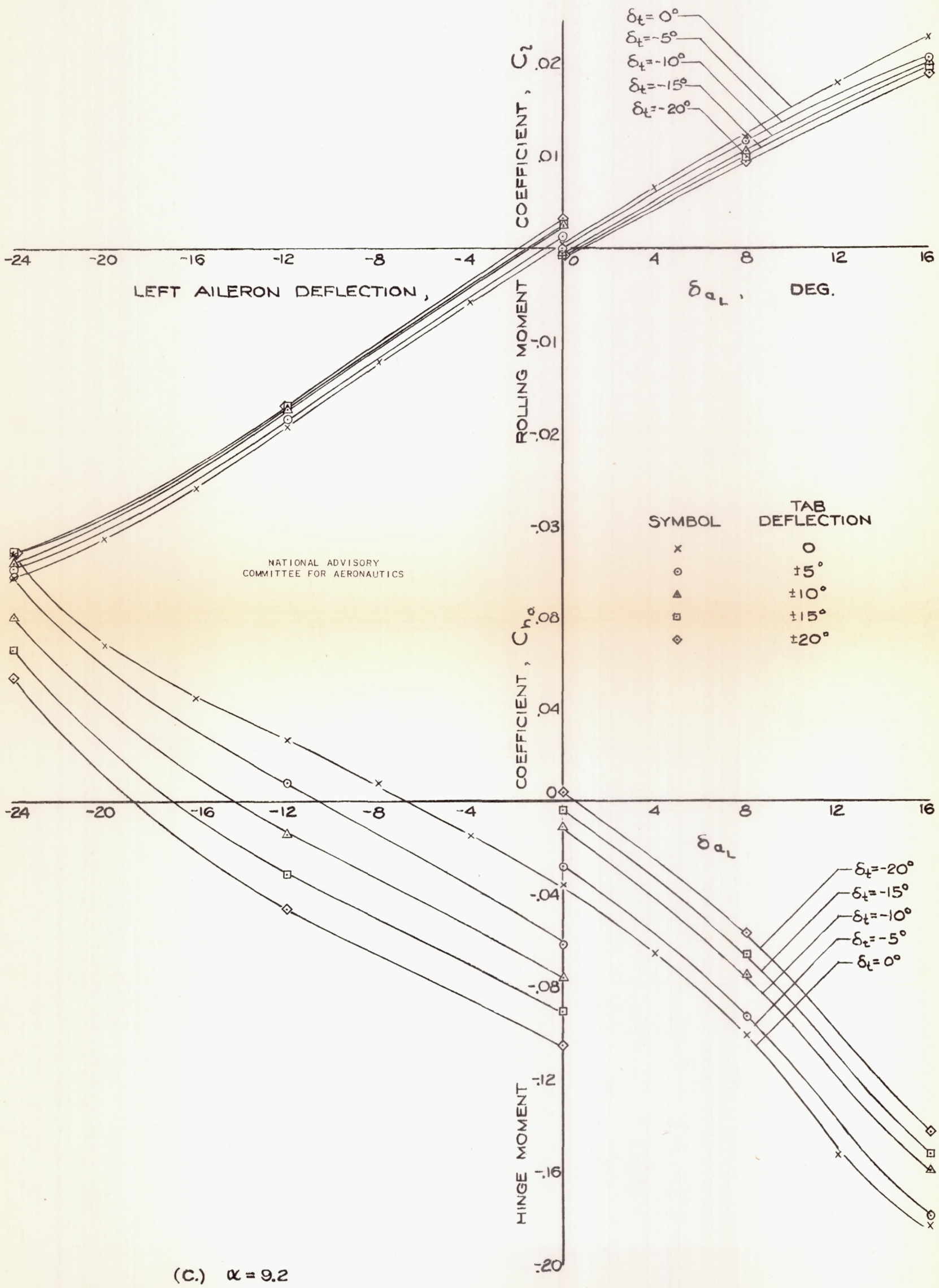

(C.) $\alpha = 9.2$

FIGURE 20:- CONCLUDED.

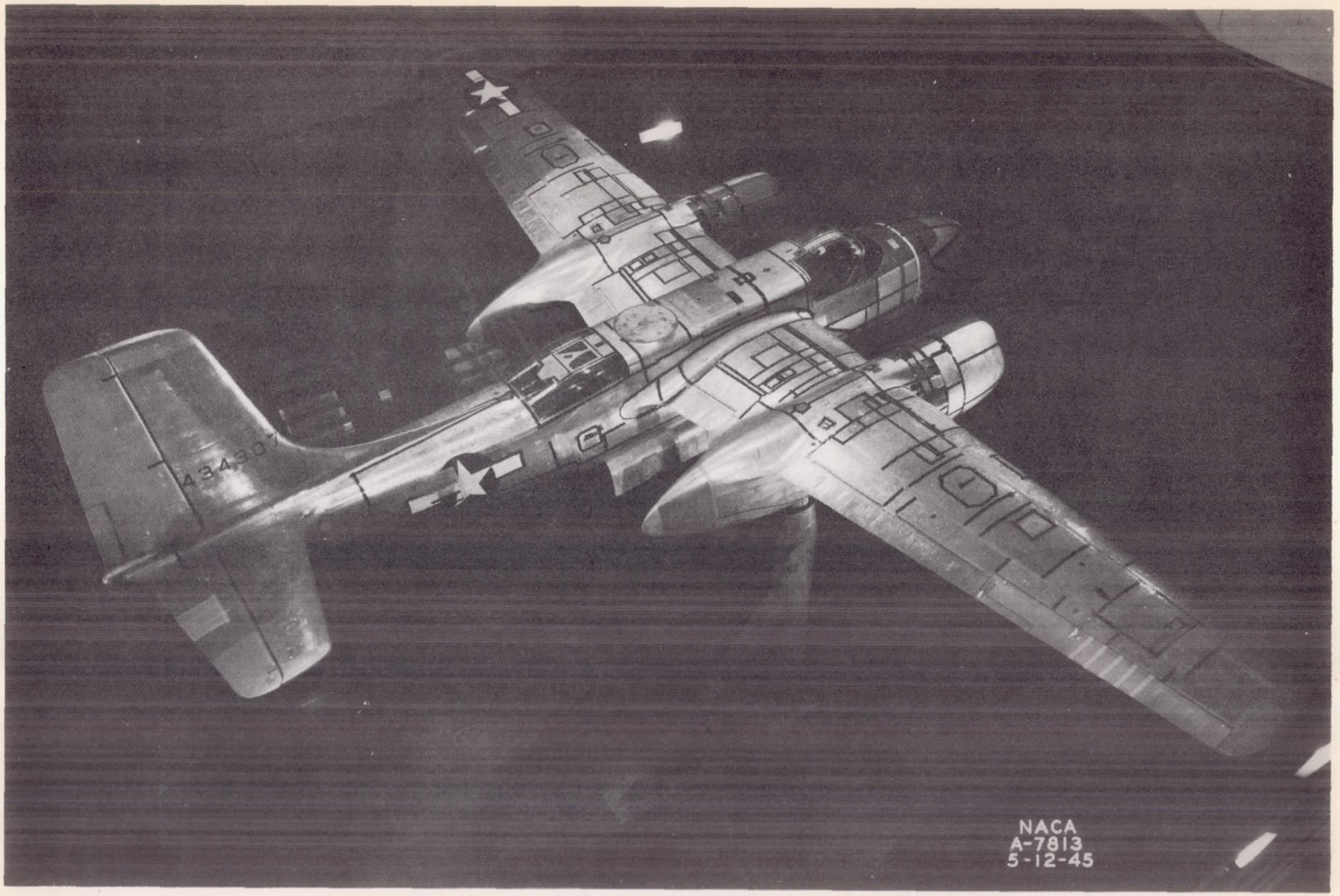

(a) Top view.

Figure 21.- The test airplane in the clean and sealed condition.

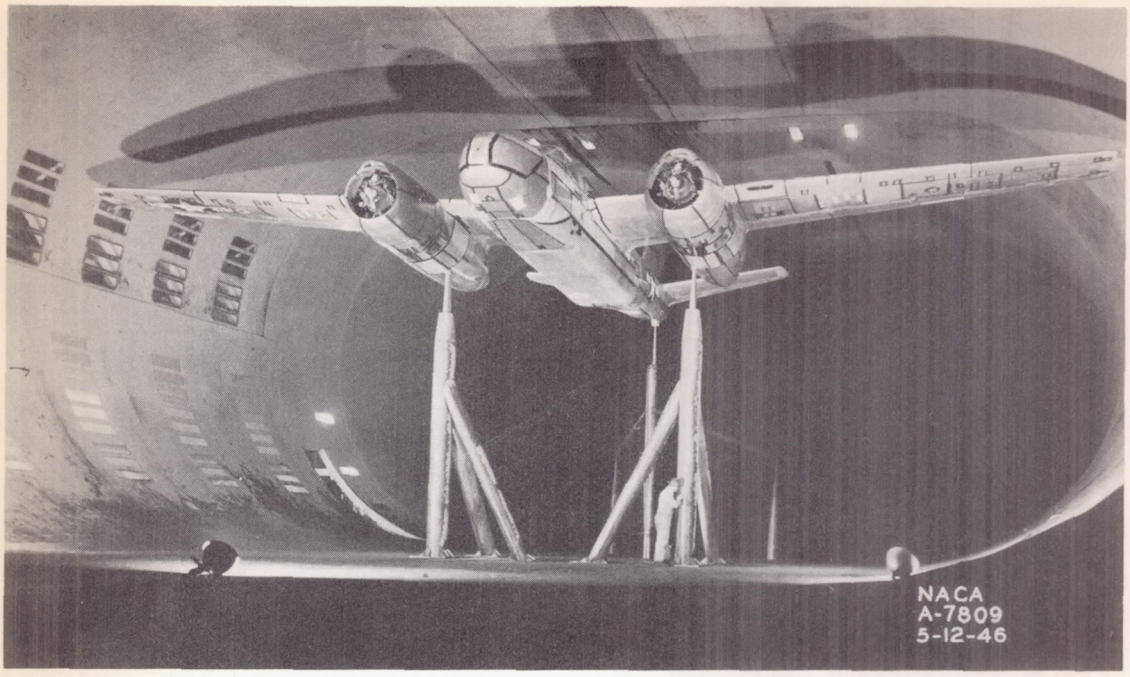

(b) Three-quarter front view.

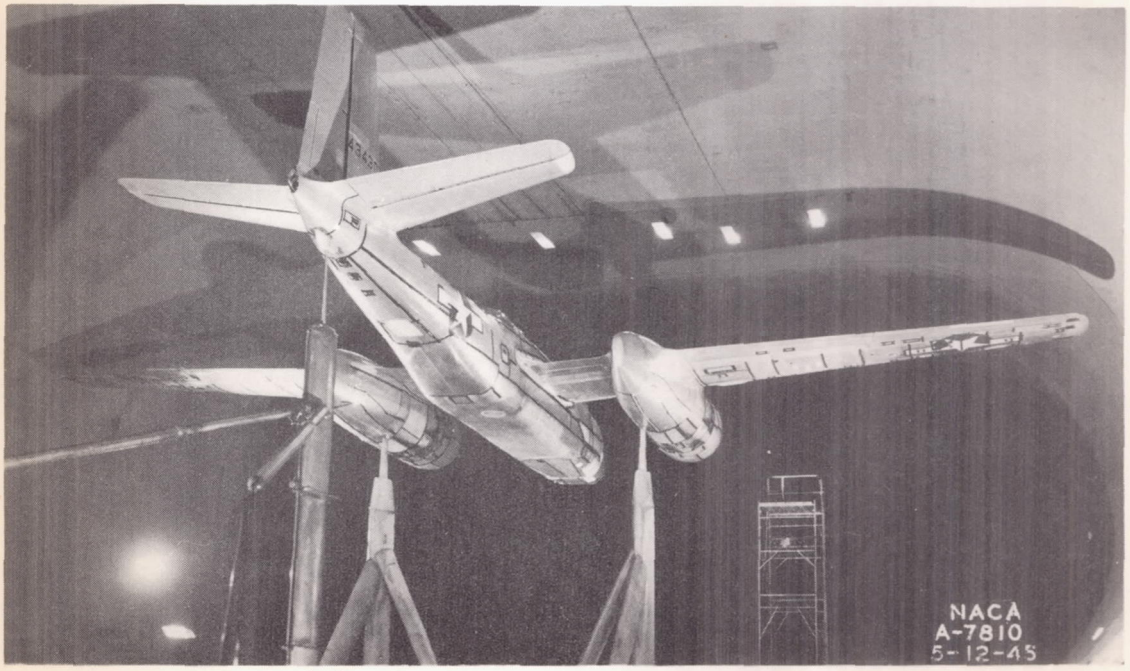

(c) Three-quarter rear view.

Figure 21.- Continued.

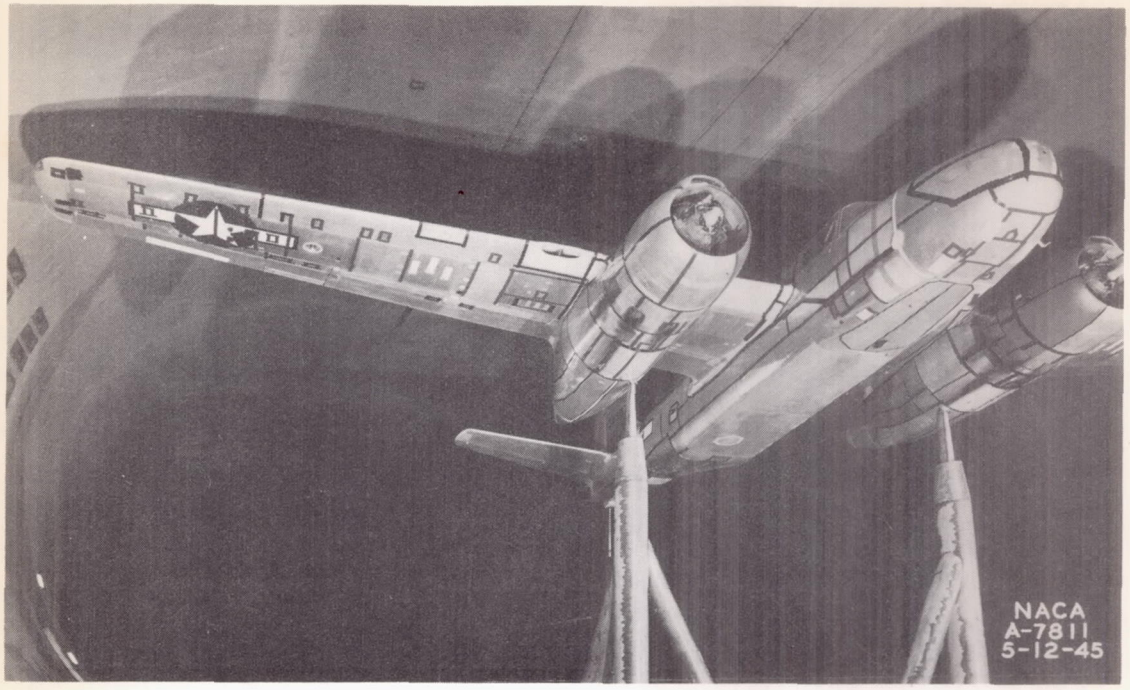

(d) Three-quarter lower front close-up.

Figure 21.- Continued.

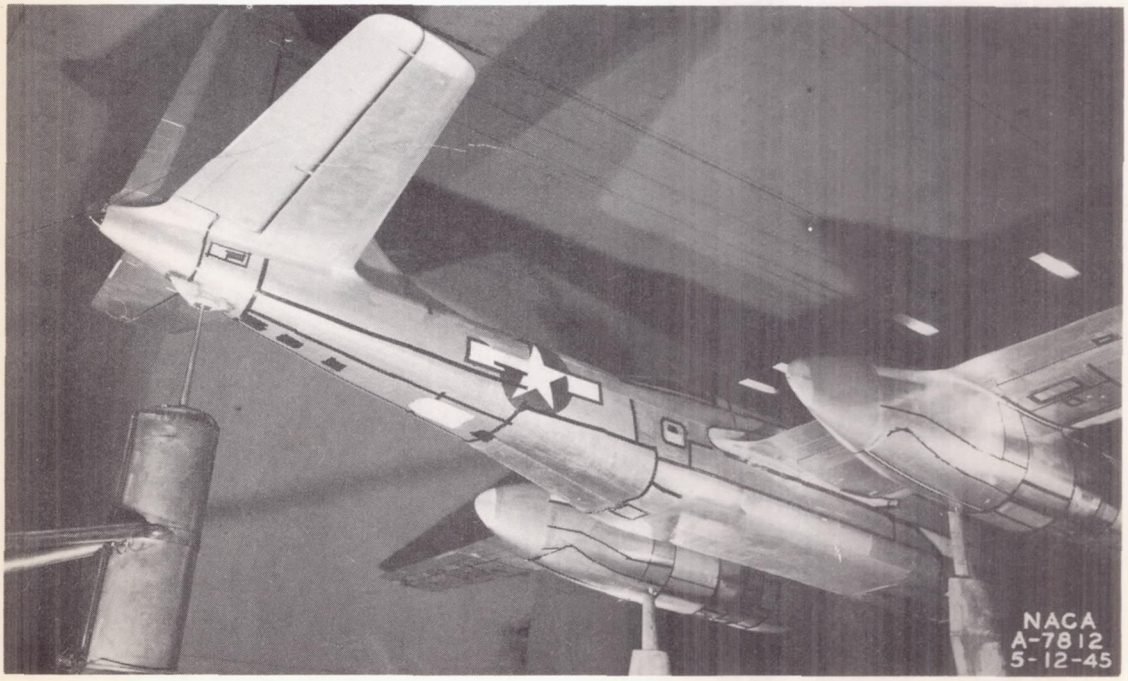

(e) Three-quarter lower rear close-up.

Figure 21.- Concluded.

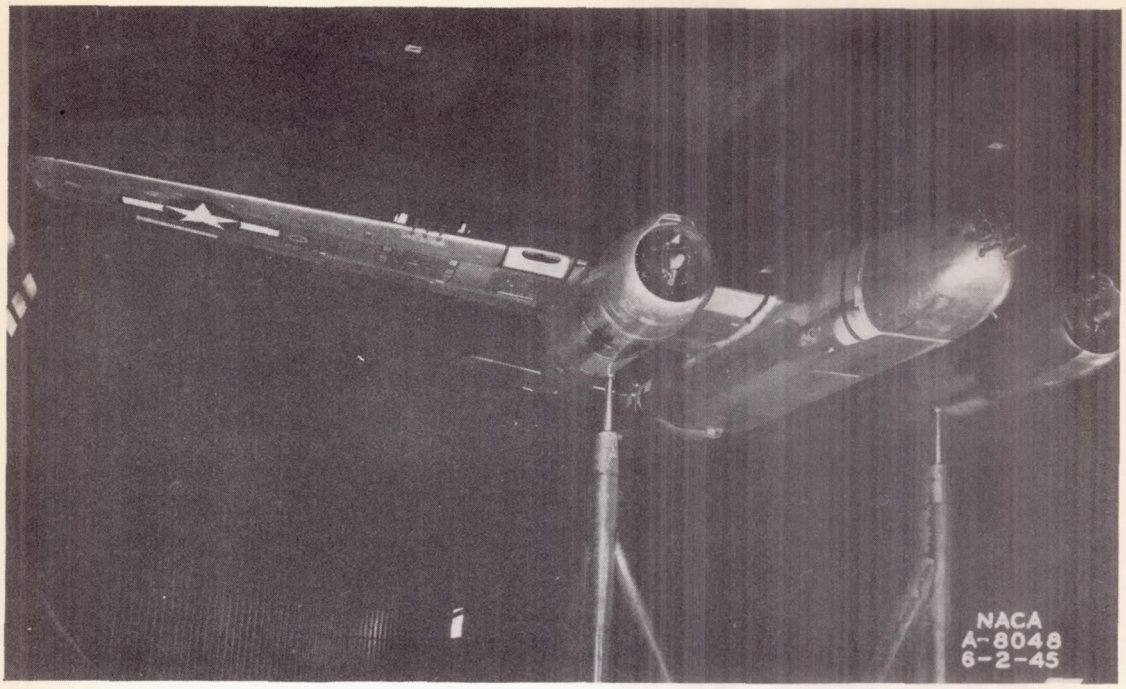

(a) Three-quarter lower front view.

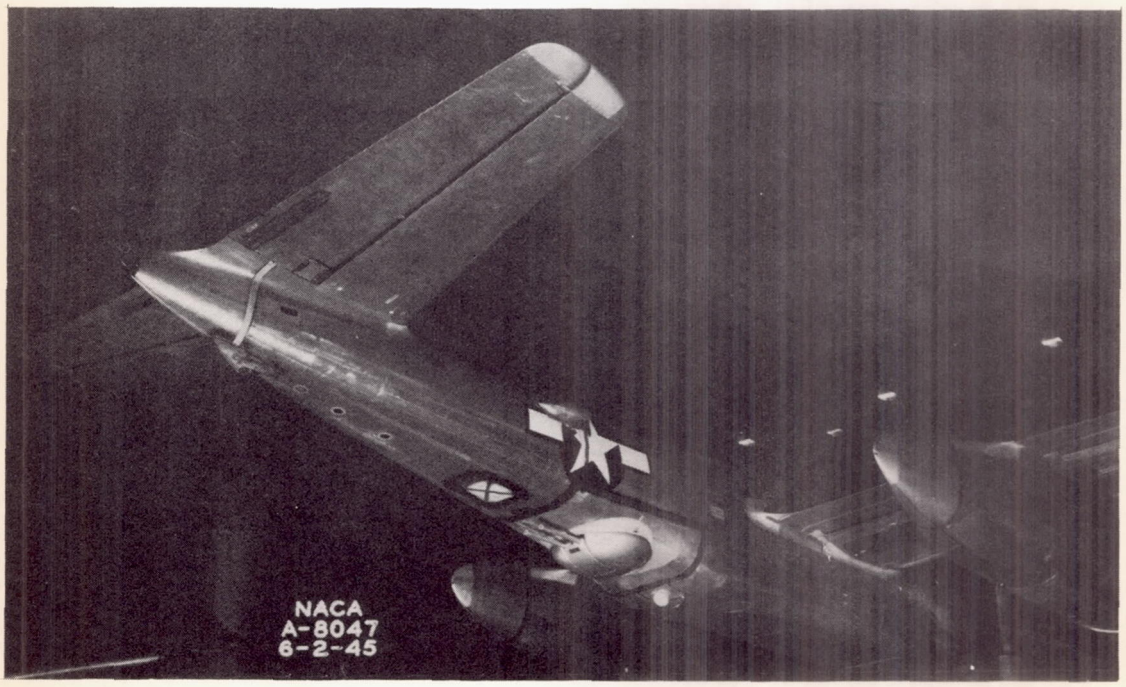

(b) Three-quarter lower rear view.

Figure 22.- Detail of component protuberances.

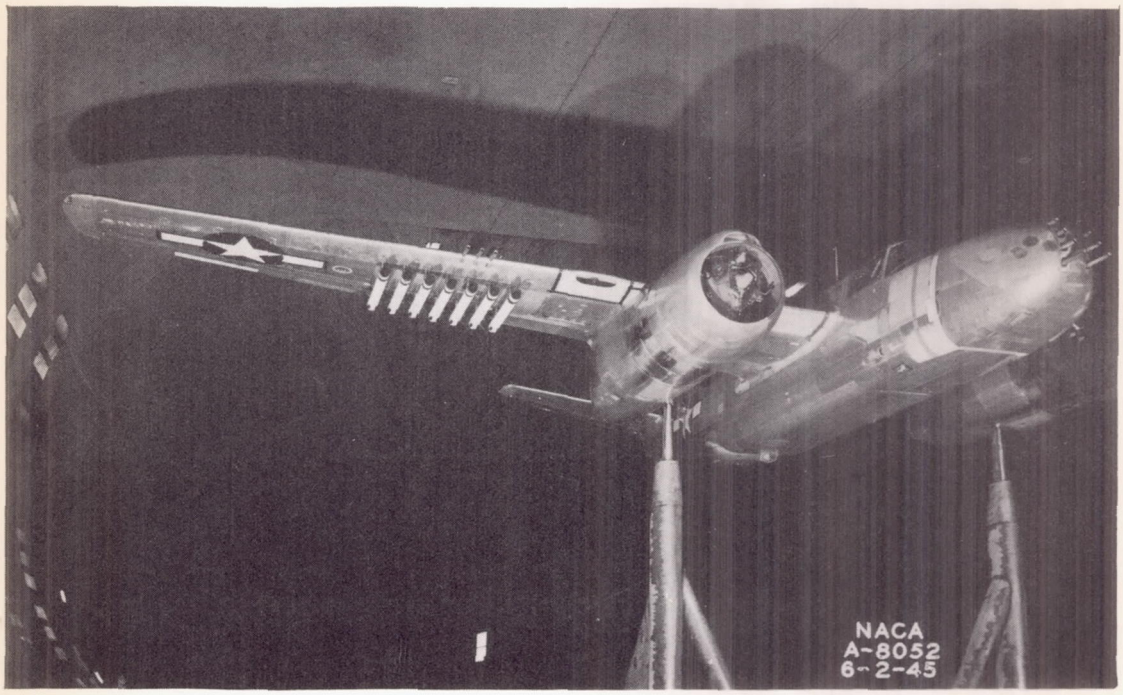

(a) Seven rockets.

Figure 23.- Detail of adjunct protuberances.

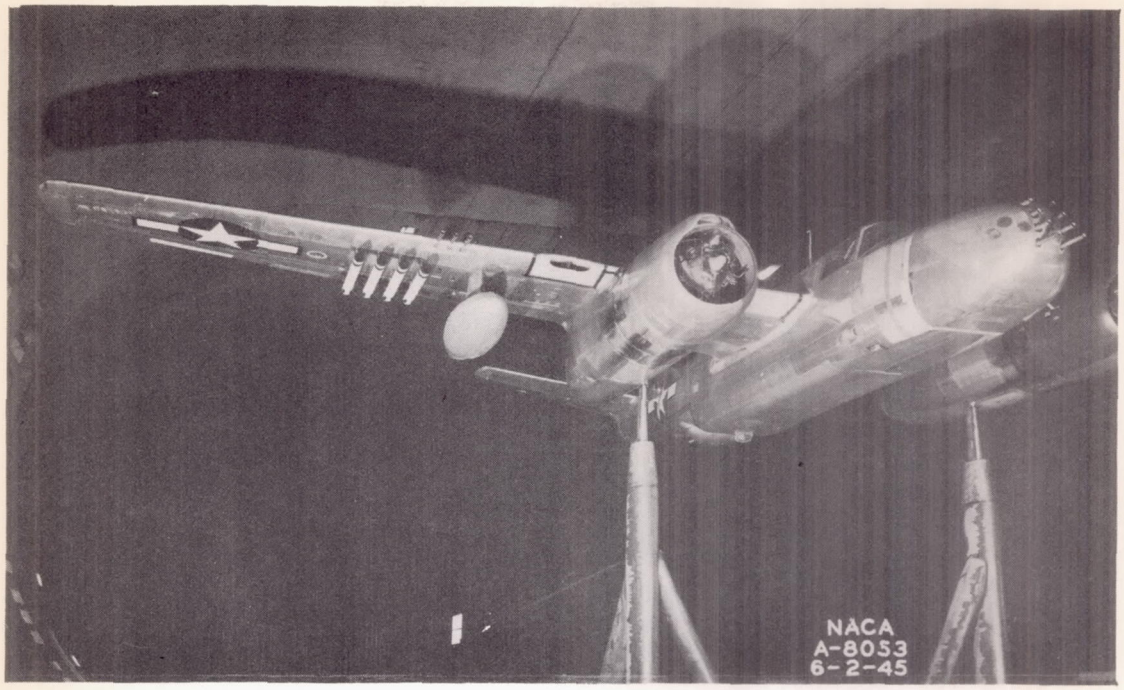

(b) Four rockets and one fuel tank.

Figure 23.- Continued.

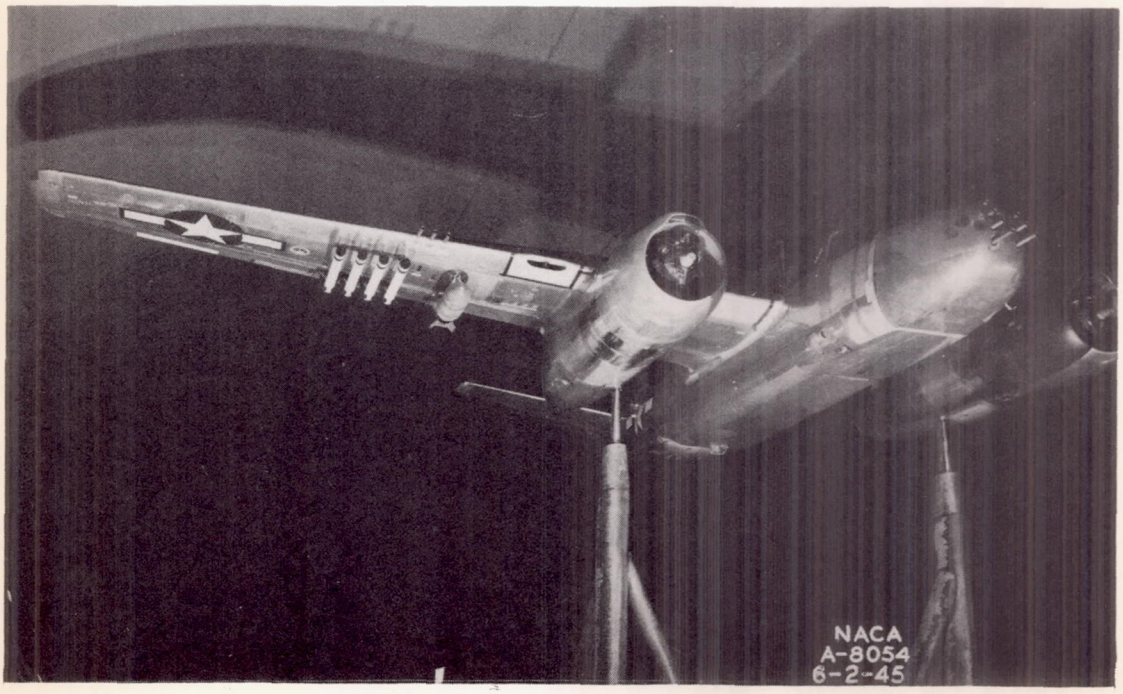

(c) Four rockets and one 500-pound bomb.

Figure 23.- Continued.

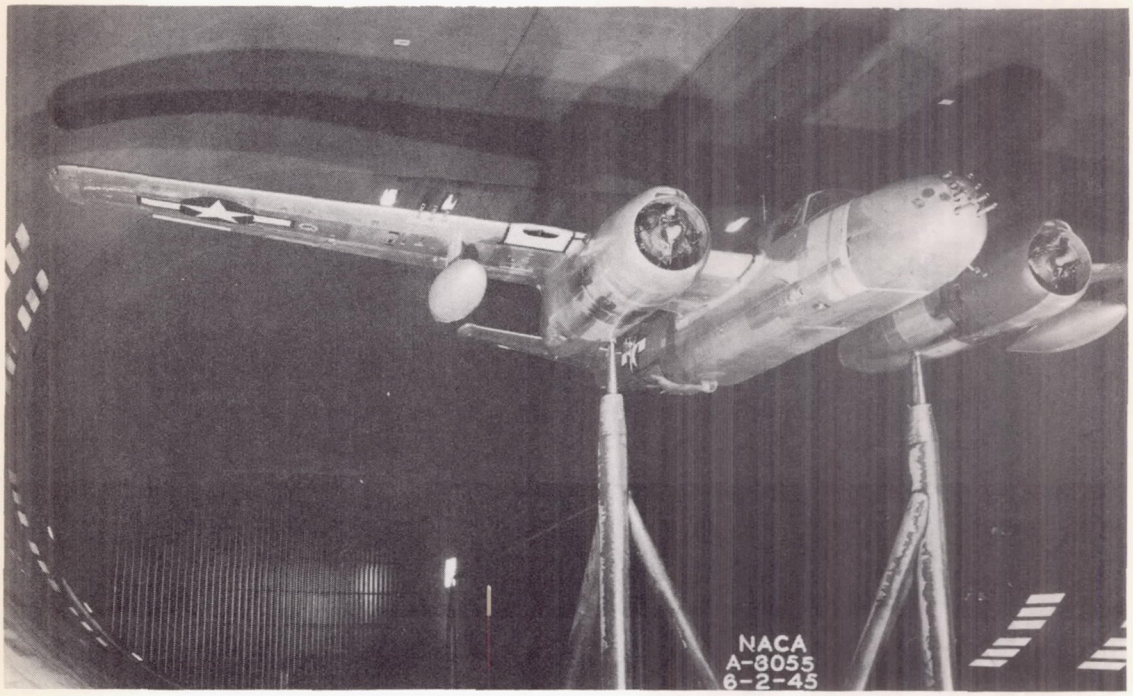

(d) One fuel tank.

Figure 23.- Concluded.

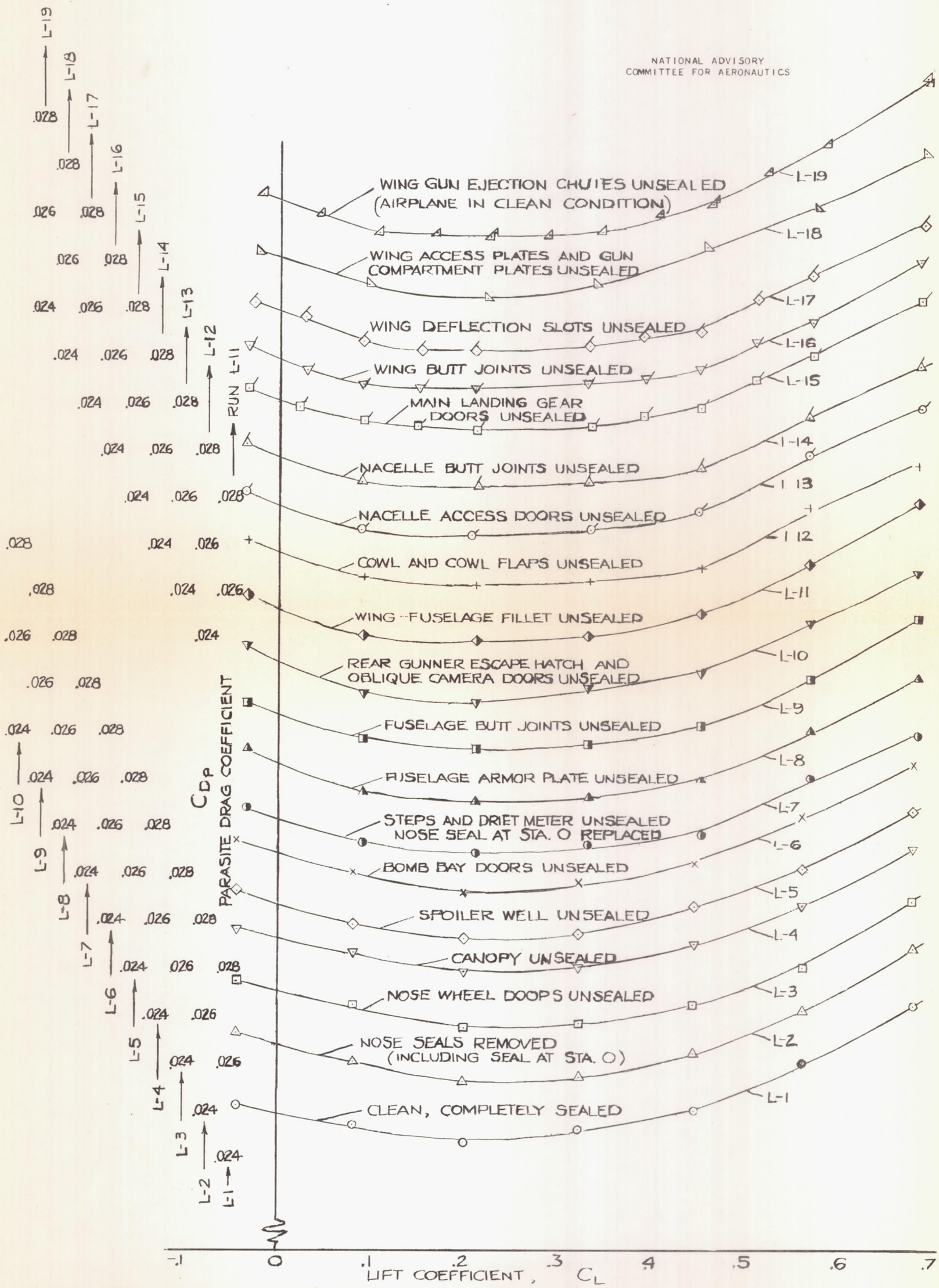

FIGURE 24.- EFFECT OF SEALING ON PARASITE DRAG.

NATIONAL ADVISORY
COMMITTEE FOR AERONAUTICS

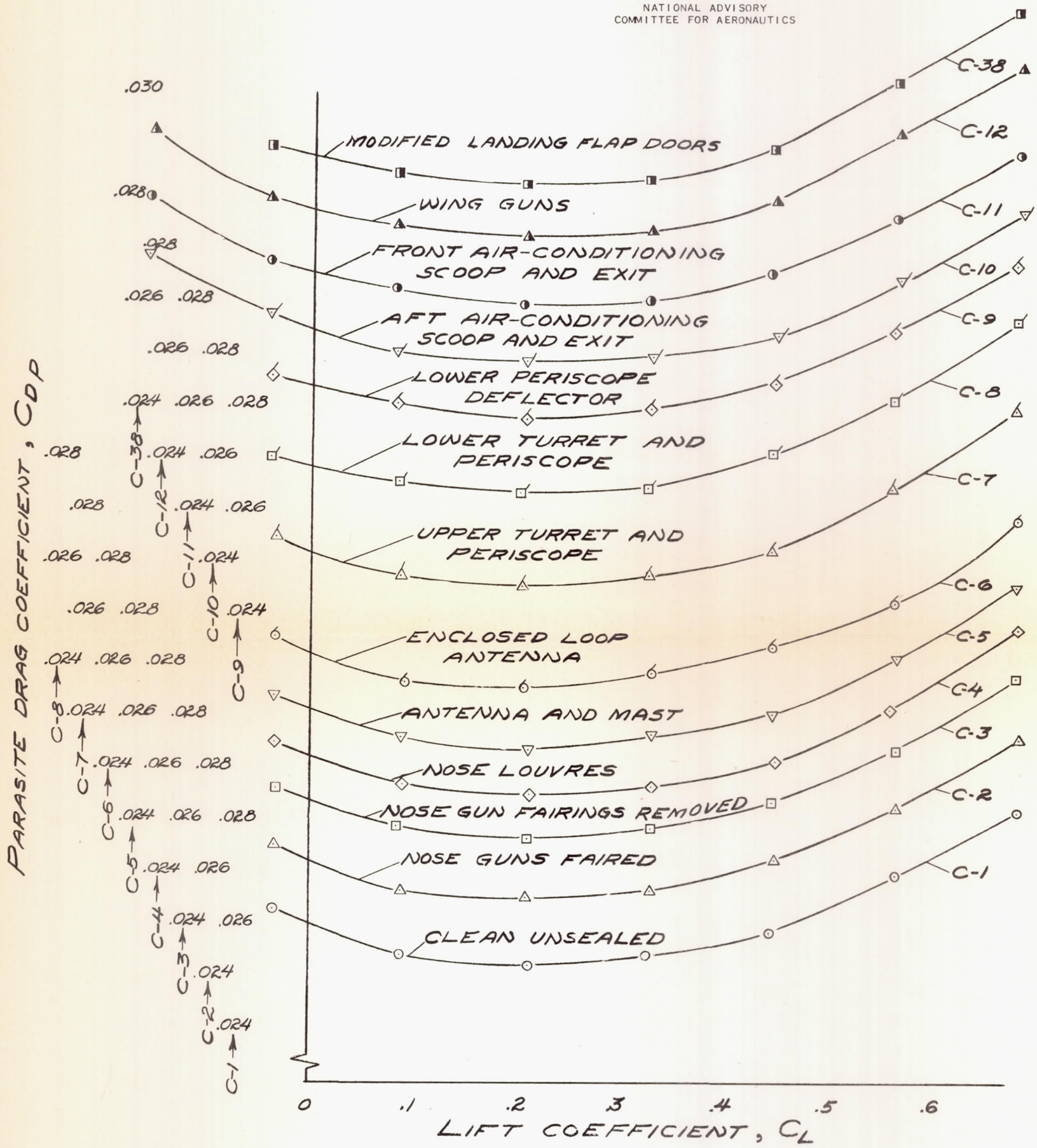

FIGURE 25.-EFFECT OF COMPONENT PROTUBERANCES ON PARASITE DRAG.

NATIONAL ADVISORY
COMMITTEE FOR AERONAUTICS

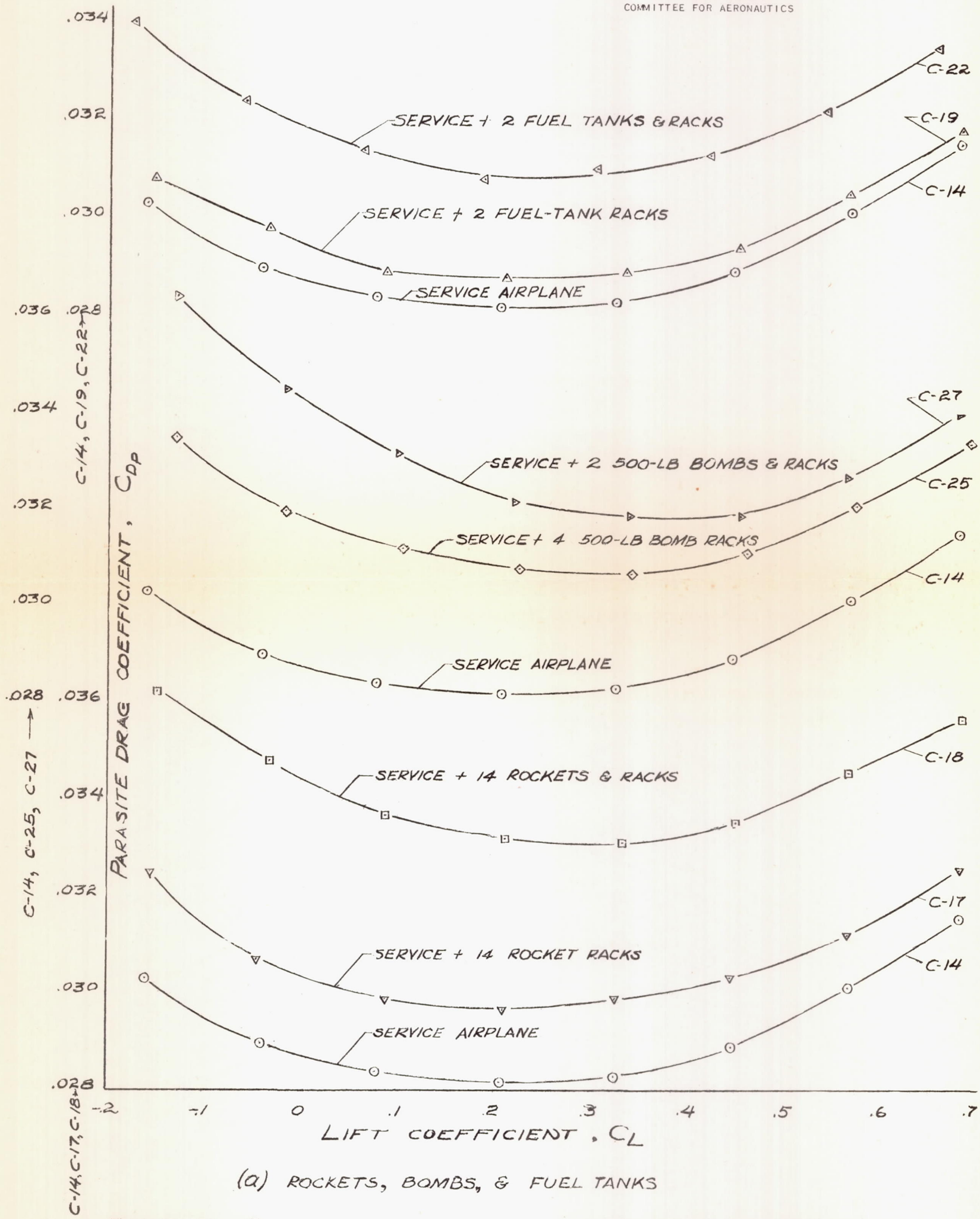

(a) ROCKETS, BOMBS, & FUEL TANKS

FIGURE 26.- EFFECT OF ADJUNCT PROTUBERANCES ON THE PARASITE DRAG.

NATIONAL ADVISORY
COMMITTEE FOR AERONAUTICS

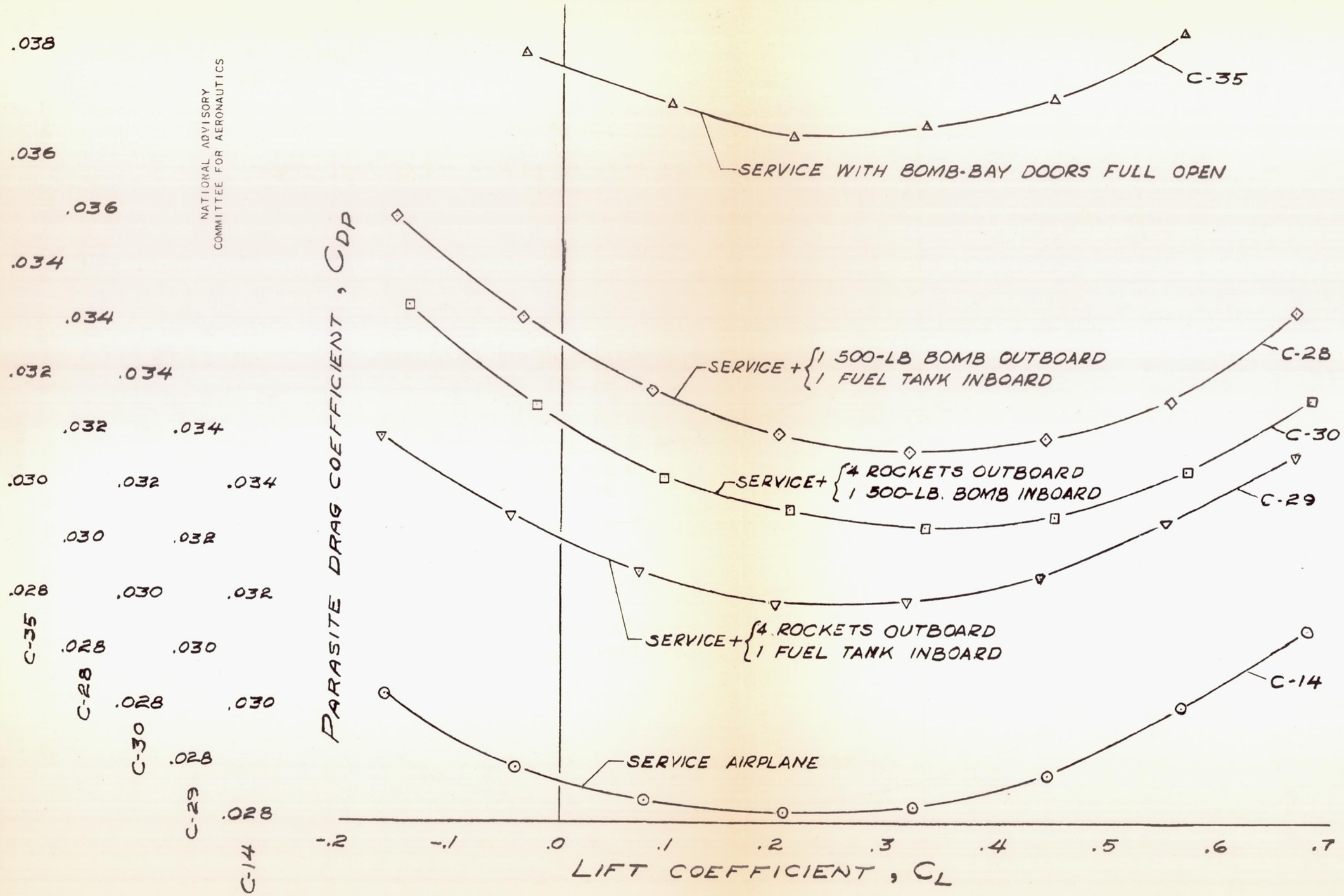

(b) COMBINATIONS OF ROCKETS, BOMBS, AND FUEL TANKS

FIGURE 26.- CONCLUDED

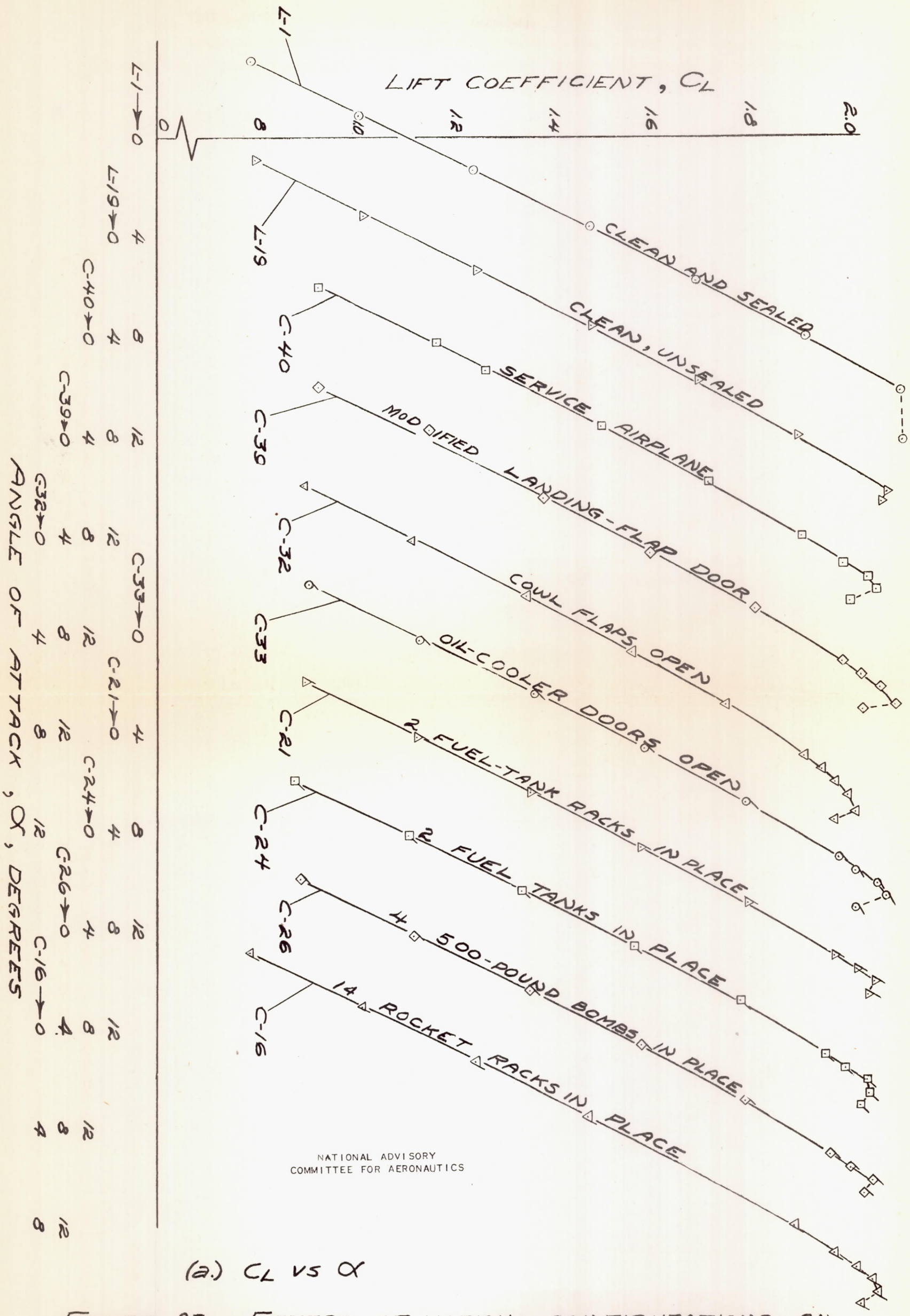

(a.) C_L vs α

FIGURE 27.-EFFECT OF VARIOUS CONFIGURATIONS ON AERODYNAMIC CHARACTERISTICS WITH FLAPS DEFLECTED 52°.

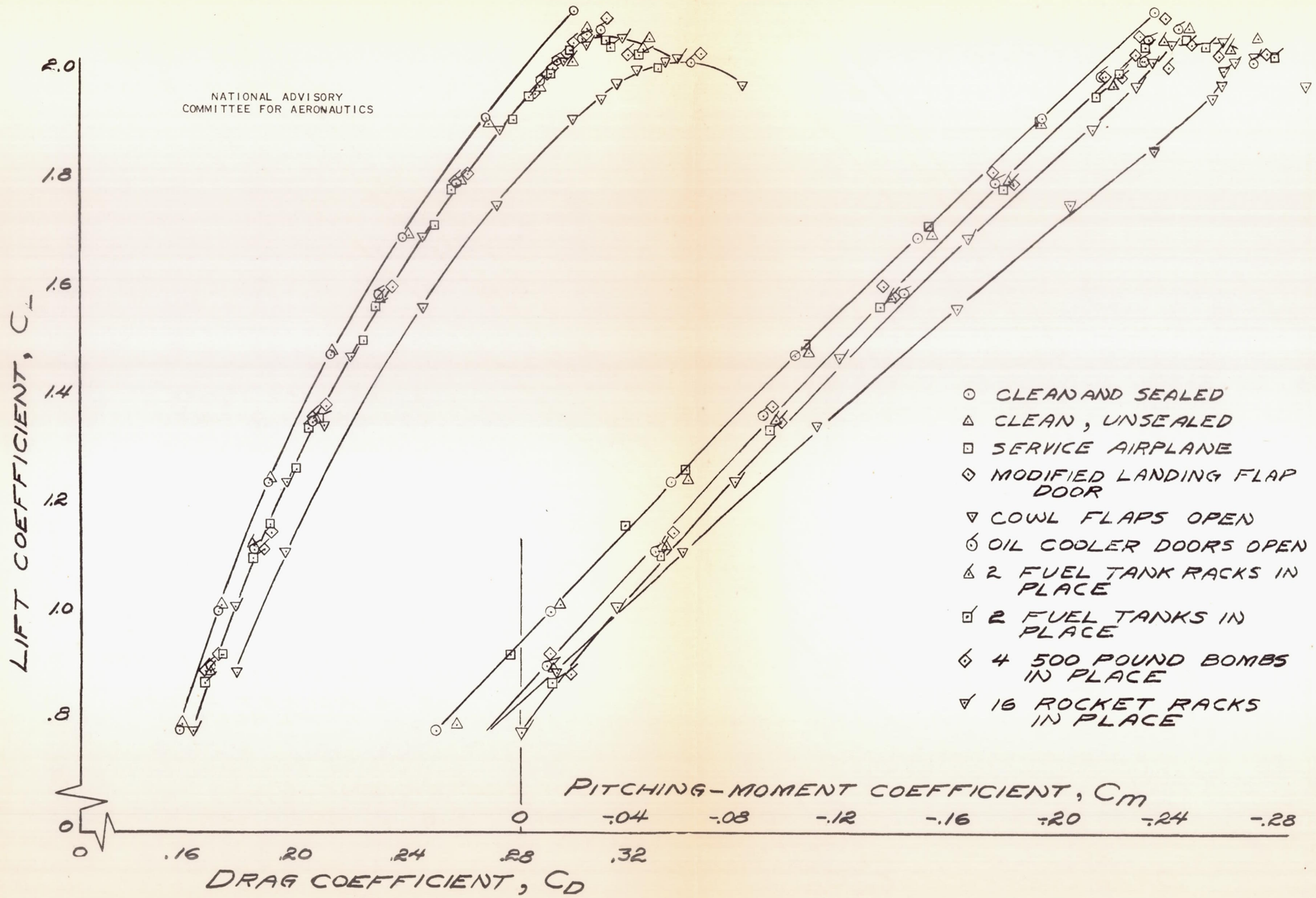

(b.) C_L vs C_D and C_m

FIGURE 27.- CONCLUDED.

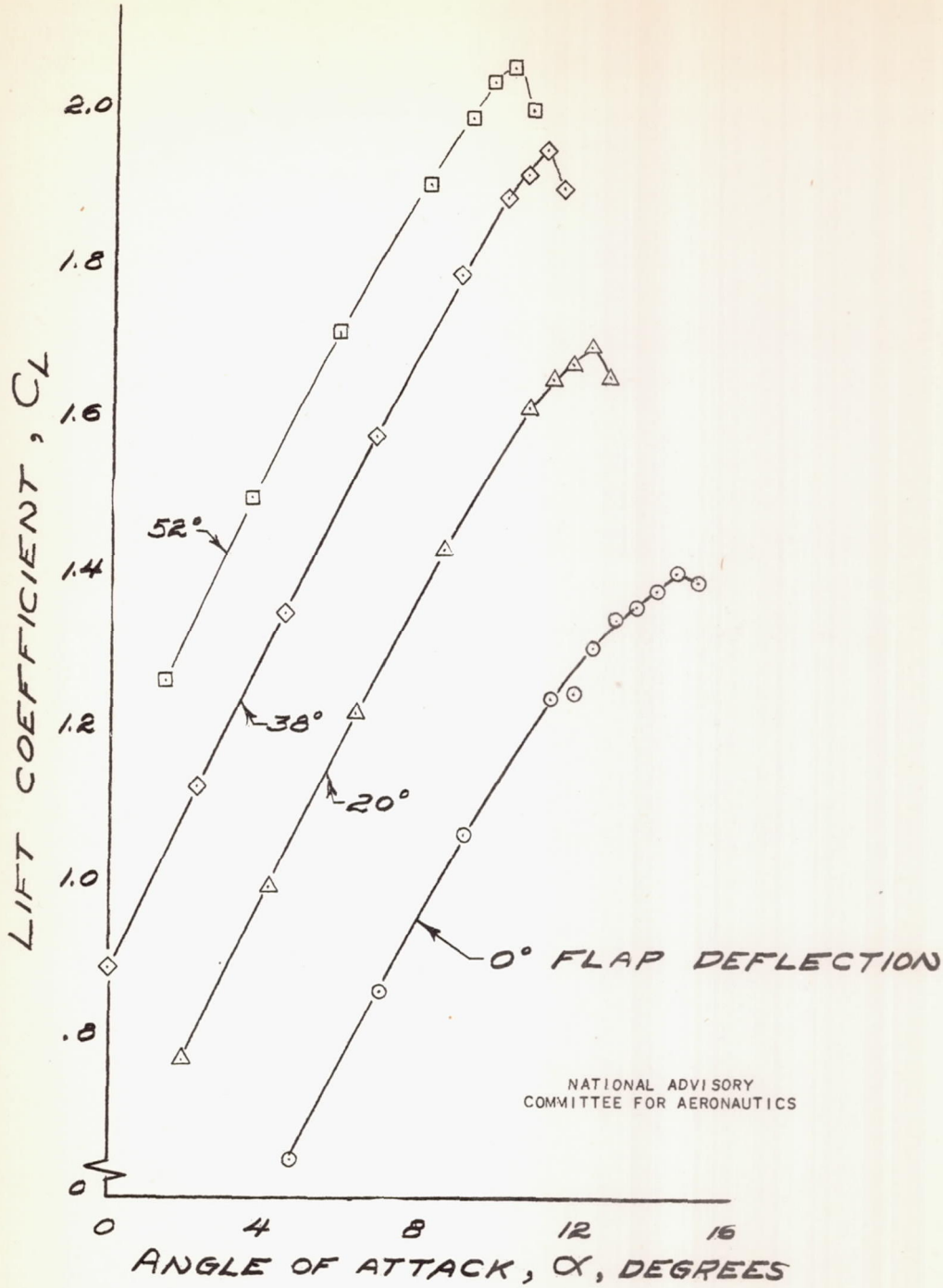

(a) C_L vs α

FIGURE 28.- EFFECT OF LANDING-FLAP DEFLECTION ON THE AERODYNAMIC CHARACTERISTICS OF THE SERVICE AIRPLANE.

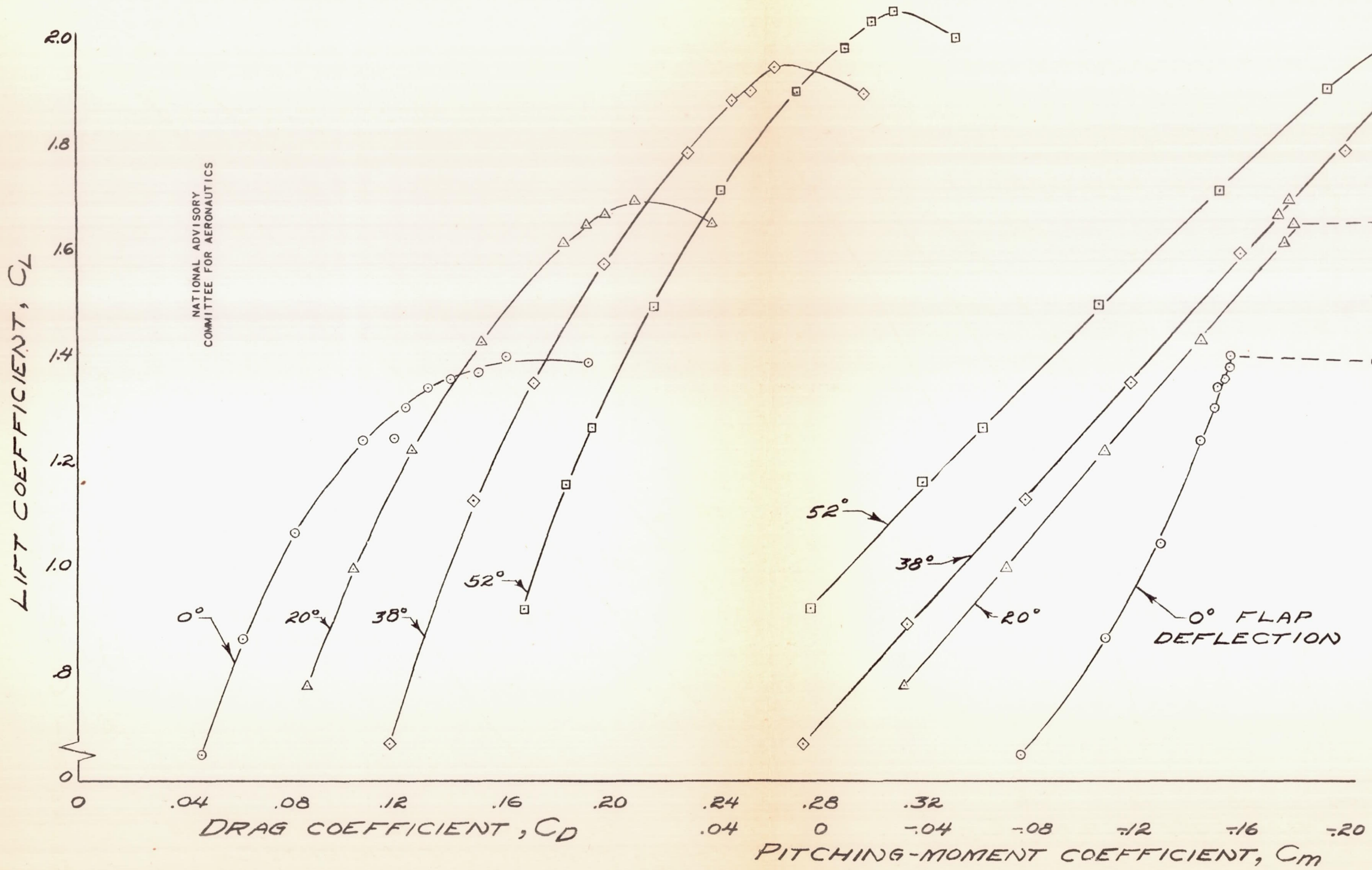

NATIONAL ADVISORY COMMITTEE FOR AERONAUTICS

FIGURE 28.- CONCLUDED.

(b) C_L VS C_D AND C_m

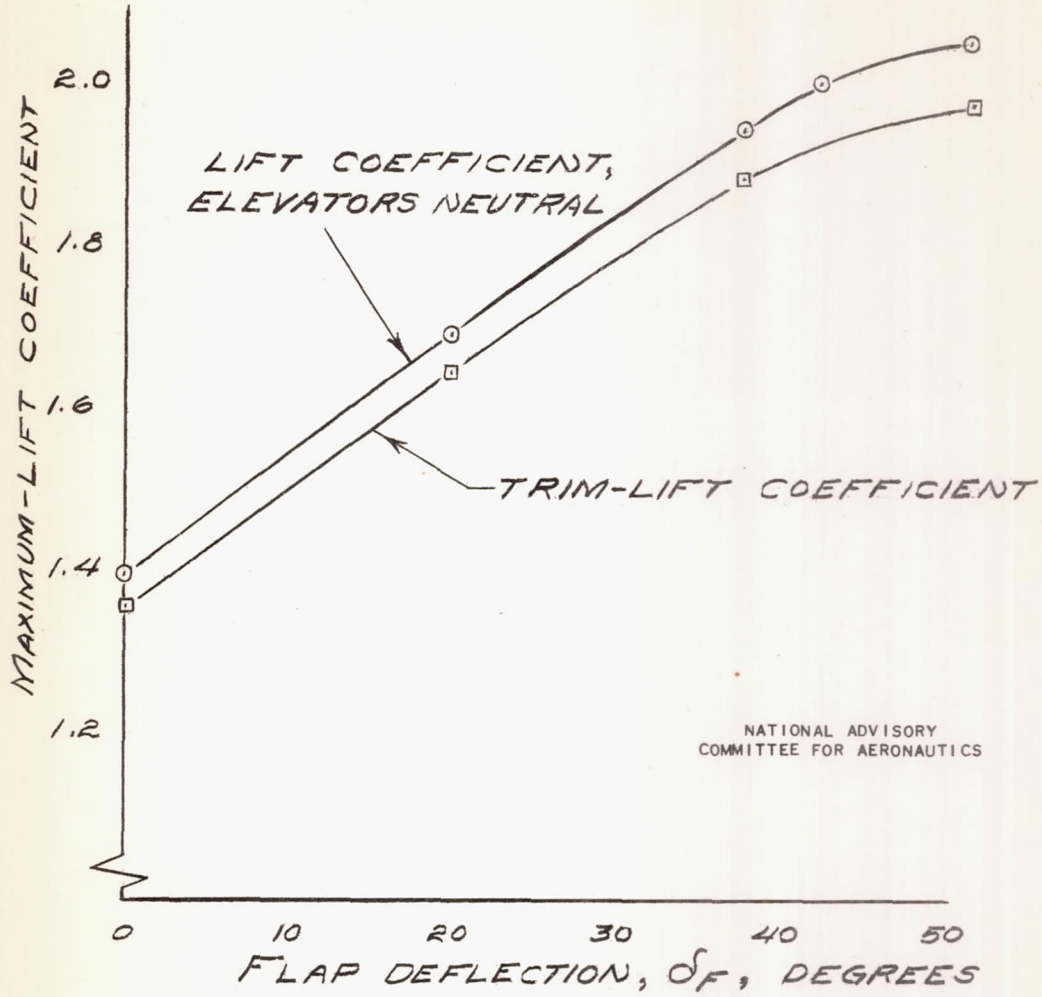

FIGURE 29.- VARIATION OF MAXIMUM-LIFT COEFFICIENT WITH FLAP ANGLE. SERVICE AIRPLANE.

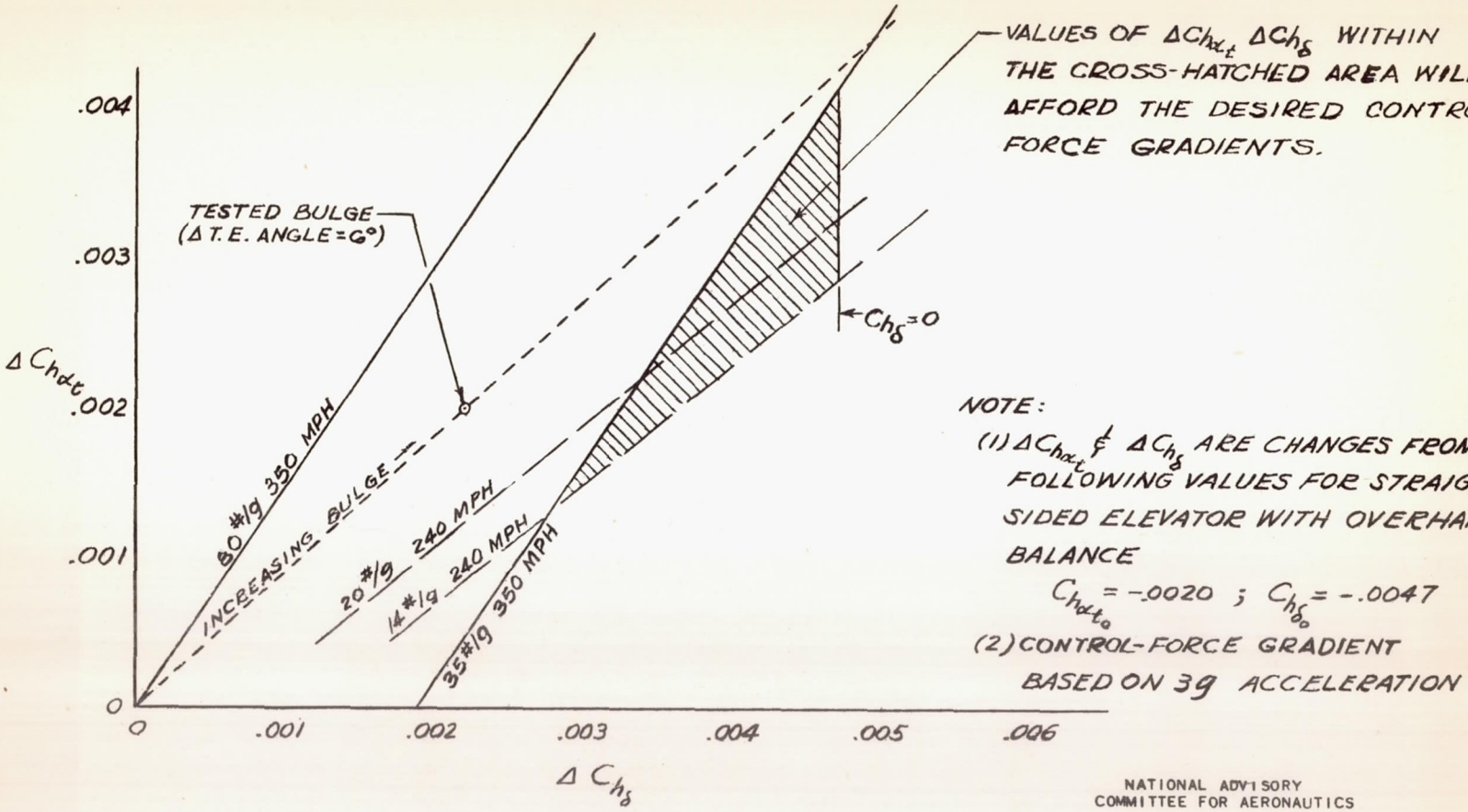

FIGURE 30.— GRAPHICAL ESTIMATION OF ELEVATOR HINGE-MOMENT PARAMETERS REQUIRED FOR SATISFACTORY CONTROL-FORCE GRADIENT IN STEADY TURNING FLIGHT.